



THE UNIVERSITY OF  
**WAIKATO**  
*Te Whare Wānanga o Waikato*

Research Commons

<http://waikato.researchgateway.ac.nz/>

## Research Commons at the University of Waikato

### Copyright Statement:

The digital copy of this thesis is protected by the Copyright Act 1994 (New Zealand).

The thesis may be consulted by you, provided you comply with the provisions of the Act and the following conditions of use:

- Any use you make of these documents or images must be for research or private study purposes only, and you may not make them available to any other person.
- Authors control the copyright of their thesis. You will recognise the author's right to be identified as the author of the thesis, and due acknowledgement will be made to the author where appropriate.
- You will obtain the author's permission before publishing any material from the thesis.

**SUBMERGED THIN PLATE WEIRS WITH UNEQUAL  
UPSTREAM AND DOWNSTREAM BEDS**

A thesis submitted in fulfilment  
of the requirements for the degree

of

**Master of Philosophy**

at

**The University of Waikato**

by

**GUINEVERE NALDER**

---

The University of Waikato

2006

## Abstract

This thesis describes a short study to examine the behaviour of submerged flow over a thin plate weir with differing upstream and downstream bed levels i.e. an unequal bed weir as opposed to an equal bed weir where the upstream and downstream beds are at the same level.

As submerged weir flow is a function of downstream conditions, it was thought that a lower downstream bed would make submerged flow over the weir easier, This is turn suggested that;

- The shape of the upstream head ( $H_u$ ) vs downstream head ( $H_d$ ) graph would change, being initially more steep in the unequal bed case.
- The Froude Number of the approaching flow would be lower for the unequal bed weir than for an equal bed weir at the same submergence.
- Using one of the existing submerged flow formula would lead to an erroneous calculated value.

A series of measurements was done on two model weirs of different sizes subject to successive levels of submergence. Analysis of the readings of upstream and downstream heads indicated that the difference in bed levels was significant and the three effects above were noted.

The work also suggested a new form of equation to calculate flow over a submerged weir. This was looked at briefly.

## Table of Contents

Abstract		ii
Table of Contents		iii
List of Figures		vii
List of Tables		xi
List of Symbols		xii
Chapter 1	Introduction	
	1.1 Thin Plate Weirs	1
	1.2 Modular and Submerged Flow	1
	1.3 Submerged weirs with Differing Upstream and Downstream Bed Levels	2
	1.4 The Scope of This Study	2
	1.5 Thesis Overview	3
Chapter 2	Background	
	2.1 Specification for Thin Plate Weirs	4
	2.2 Modular Flow	4
	2.3 Equations for Modular Flow	5
	2.4 Submerged Flow	6
	2.4.1 Stages of Submergence	6
	2.4.2 Deeply Submerged Flow	7
	2.5 Equations for Calculating Discharges Over Submerged Weirs	9
	2.5.1 Submerged Orifice	10
	2.5.2 Opposing Modular Flows	10
	2.5.3 Empirical	11
	2.5.4 Choice of Formulas	11
	2.6 Discharge Over Equal and Unequal Bed Weirs	12
	2.6.1 Notation	12
	2.6.2 Anticipated Effect of Unequal Beds	12
	2.6.3 $H_u$ vs $H_d$ Plot	12
	2.6.4 Approach Froude Number	14
	2.6.5 Calculation of Discharge	15

2.7	Laboratory Study	15
2.7.1	Equal Bed Formulas	15
2.7.2	Effects of Unequal Beds	15
Chapter 3	Laboratory Study	
3.1	Introduction	17
3.2	The University of Canterbury Study	17
3.2.1	Equipment	17
3.2.2	Model Weir	18
3.2.3	Measurements	18
3.2.4	Model Study	18
3.3	Waikato Institute of Technology Study	19
3.3.1	Scale Models	19
3.3.2	Equipment	20
3.3.3	Model Weir	20
3.3.4	Measurement	21
3.3.5	Model Study	21
3.4	Standing Wave	22
Chapter 4	Comparison of Values Calculated by Equal Bed Formula	
4.1	Introduction	24
4.2	Standing Wave Data Points	24
4.3	University of Canterbury Study Results	24
4.4	Waikato Institute of Technology Study Results	32
4.5	Choice of Discharge Equation	41

Chapter 5	Effect of Unequal Beds	
5.1	Choice of Models	42
5.2	Shape of $H_u$ vs $H_d$ Plot	43
	5.2.1 University of Canterbury Study Results	43
	5.2.2 Waikato Institute of Technology Study Results	43
5.3	Approach Froude Number	
	5.3.1 University of Canterbury Study Data	58
	5.3.2 Waikato Institute of Technology Study Data	
5.4	Calculation of Discharge with Conventional Formulas	67
	5.4.1 Method of Comparison	67
	5.4.2 Waikato Institute of Technology Study Data	67
Chapter 6	Possible New Discharge Formula for Flow Over a Submerged Thin Plate Weir	
6.1	Existing Equations	72
6.2	$H_u$ vs $H_d$ Graph: General Shape	73
	6.2.1 Introduction	73
	6.2.2 The University of Canterbury Study Data	74
	6.2.3 Waikato Institute of Technology Study Data	75
6.3	$H_u$ vs $H_d$ Dimensioned Expression	75
	6.3.1 Non-Dimensional Factors	75
	6.3.2 University of Canterbury Study Data	76
	6.3.3 Waikato Institute of Technology Study Data	78
6.4	Coefficient and Constant	
	6.4.1 Introduction	82
	6.4.2 Constant	82
	6.4.3 Coefficient	84
6.5	Summary	86

Chapter 7	Summary and Further Possible Work	
7.1	Unequal Bed Effect $L$	87
7.2	Further Work on Unequal Bed Effect $L$	87
7.3	Alternative Discharge Equation	87
References		89

## List of Figures

Figure 2.1	Standard Thin Plate Weir Cross-Section	4
Figure 2.2	Modular Flow Over a Thin Plate Weir	5
Figure 2.4.1	Types of Submerged Flow Over a Thin Plate Weir	7
Figure 2.4.2	Flow Over a Deeply Submerged Weir	8
Figure 2.5	Submerged Flow Over a Thin Plate Weir	9
Figure 2.6.3(a)	Typical $H_u$ vs $H_d$ , Values for Submerged Weir	13
Figure 2.6.3(b)	Expected $H_u$ vs $H_d$ , Shape for Equal and Unequal Bed Levels	14
Figure 4.3-1	Model C7, Discharge $0.01 \text{ m}^3 / \text{s}$ , Discharge vs Submergence	28
Figure 4.3-2	Model C7, Discharge $0.0145 \text{ m}^3 / \text{s}$ , Discharge vs Submergence	28
Figure 4.3-3	Model C7, Discharge $0.0198 \text{ m}^3 / \text{s}$ , Discharge vs Submergence	29
Figure 4.3-4	Model C7, Discharge $0.025 \text{ m}^3 / \text{s}$ , Discharge vs Submergence	29
Figure 4.3-5	Model C8, Discharge $0.0098 \text{ m}^3 / \text{s}$ , Discharge vs Submergence	30
Figure 4.3-6	Model C8, Discharge $0.0151 \text{ m}^3 / \text{s}$ , Discharge vs Submergence	30
Figure 4.3-7	Model C8, Discharge $0.0206 \text{ m}^3 / \text{s}$ , Discharge vs Submergence	31
Figure 4.3-8	Model C8, Discharge $0.025 \text{ m}^3 / \text{s}$ , Discharge vs Submergence	31
Figure 4.4.1	Model W1, Discharge $0.0048 \text{ m}^3 / \text{s}$ , Discharge vs Submergence	38
Figure 4.4.1	Model W3, Discharge $0.0071 \text{ m}^3 / \text{s}$ , Discharge vs Submergence	38
Figure 4.4-3	Model W6,(Falling Branch) Discharge $0.0071 \text{ m}^3 / \text{s}$ , Discharge vs Submergence	39
Figure 4.4-4	Model W11,(Falling Branch) Discharge $0.0048 \text{ m}^3 / \text{s}$ , Discharge vs Submergence	39
Figure 4.4-5	Model W11,(Rising Branch) Discharge $0.0225 \text{ m}^3 / \text{s}$ , Discharge vs Submergence	40
Figure 4.4-6	Model W17,(Rising Branch) Discharge $0.0073 \text{ m}^3 / \text{s}$ , Discharge vs Submergence	40

Figure 5.2.1-1	Comparison Shapes with Discharge 10 l/s	46
Figure 5.2.1-2	Comparison Shapes with Discharge 15 l/s	46
Figure 5.2.1-3	Comparison Shapes with Discharge 20 l/s	47
Figure 5.2.1-4	Comparison Shapes with Discharge 25 l/s	47
Figure 5.2.2-1	$H_u$ vs $H_d$ for W11 and W16 (Falling Branch), Discharge 0.0046 m <sup>3</sup> /s	54
Figure 5.2.2-2	$H_u$ vs $H_d$ for W17 and W23(Falling Branch), Discharge 0.0048 m <sup>3</sup> /s	54
Figure 5.2.2-3	$H_u$ vs $H_d$ for W11 and W16 (Falling Branch), Discharge 0.0074 m <sup>3</sup> /s	55
Figure 5.2.2-4	$H_u$ vs $H_d$ for W17 and W23 (Falling Branch), Discharge 0.0125 m <sup>3</sup> /s	55
Figure 5.2.2-5	$H_u$ vs $H_d$ for W17 and W23 (Falling Branch), Discharge 0.0046 m <sup>3</sup> /s	56
Figure 5.2.2-6	$H_u$ vs $H_d$ for W17 and W23 (Rising Branch), Discharge 0.0231 m <sup>3</sup> /s	56
Figure 5.2.2-7	$H_u$ vs $H_d$ for W11 and W16 (Rising Branch), Discharge 0.0287 m <sup>3</sup> /s	57
Figure 5.3.1-1	Approach Froude Numbers for Models C1 and C7 Discharge 0.0095 m <sup>3</sup> /s	60
Figure 5.3.1-2	Approach Froude Numbers for Models C1 and C7 Discharge 0.0145 m <sup>3</sup> /s	60
Figure 5.3.1-3	Approach Froude Numbers for Models C1 and C7 Discharge 0.0193 m <sup>3</sup> /s	61

Figure 5.3.2-1	Approach Froude Numbers for Models W11 and W16 Discharge 0.0048 m <sup>3</sup> /s	64
Figure 5.3.2-2	Approach Froude Numbers for Models W1 and W23 Discharge 0.0047 m <sup>3</sup> /s	64
Figure 5.3.2-3	Approach Froude Numbers for Models W11 and W16 Discharge 0.0075 m <sup>3</sup> /s	65
Figure 5.3.2-4	Approach Froude Numbers for Models W17 and W23 Discharge 0.0125 m <sup>3</sup> /s	65
Figure 5.3.2-5	Approach Froude Numbers for Models W17 and W23 Discharge 0.0178 m <sup>3</sup> /s	66
Figure 5.3.2-6	Approach Froude Numbers for Models W17 and W23 Discharge 0.0231/4 m <sup>3</sup> /s	66
Figure 5.3.2-7	Approach Froude Numbers for Models W17 and W23 Discharge 0.029 m <sup>3</sup> /s	67
Figure 6.2.2	Plot of $H_u$ vs $\text{Exp}(H_d^2)$ for Model C1, Discharge 15 l/s	74
Figure 6.2.3	Plot of $H_u$ vs $\text{Exp}(H_d^2)$ for Model W1, Discharge 0.0258 m <sup>3</sup> /s	75
Figure 6.3.2	Plot of $H_u$ vs $\text{Exp}(H_d/P_d)^2$ for Model C5, Discharge 15 l/s	76
Figure 6.3.3	$H_u$ vs $\text{Exp}((H_d/P_d)^2)$ for Model w20, Discharge 0.208 m <sup>3</sup> /s	78

## List of Tables

Table 3.2.4 Models for University of Canterbury Study	19
Table 3.3.5 Models for Waikato Institute of Technology Model Study	23
Table 4.3.1 Comparison of Calculated Discharges for Submerged Weirs with Equal Beds (C7)	25
Table 4.3.1 Comparison of Calculated Discharges for Submerged Weirs with Equal Beds (C8)	26
Table 4.4 Actual Height WINTEC Weir Models	32
Table 4.4.1 Comparison of Calculated Discharges for WINTEC Model W1	39
Table 4.4.2 Comparison of Calculated Discharges for WINTEC Model W3	40
Table 4.4.3 Comparison of Calculated Discharges for WINTEC Model W6	41
Table 4.4.4 Comparison of Calculated Discharges for WINTEC Model W11	42
Table 4.4.5 Comparison of Calculated Discharges for WINTEC Model W17	43
Table 5.1 Choice of WINTEC Models	42
Table 5.2.1-1 Comparison Shapes with Discharge 10 l/s	44
Table 5.2.1-2 Comparison Shapes with Discharge 15 l/s	44
Table 5.2.1-3 Comparison Shapes with Discharge 20 l/s	45
Table 5.2.1-4 Comparison Shapes with Discharge 25 l/s	45
Table 5.2.2-1 Comparison Shapes, WINTEC Models, Approx. Scaled Discharge 0.0047 m <sup>3</sup> /s	48
Table 5.2.2-2 Comparison Shapes, WINTEC Models Approx. Scaled Discharge 0.0074 m <sup>3</sup> /s	49
Table 5.2.2-3 Comparison Shapes, WINTEC Models Approx. Scaled Discharge 0.0125 m <sup>3</sup> /s	50
Table 5.2.2-4 Comparison Shapes, WINTEC Models Approx. Scaled Discharge 0.0178 m <sup>3</sup> /s	51
Table 5.2.2-5 Comparison Shapes, WINTEC Approx. Scaled Discharge 0.0231 m <sup>3</sup> /s	52

Table 5.2.2-6	Comparison Shapes, WINTEC Models, Approx. Scaled Discharge 0.0287 m <sup>3</sup> /s	53
Table 5.3.1	Froude Numbers for University of Canterbury Data	59
Table 5.3.2-1(a)	Approach Froude Numbers WINTEC Data	62
Table 5.3.2-1(b)	Approach Froude Numbers WINTEC Data	63
Table 5.4.2-1	Comparison Errors, Approx Scaled Discharge 0.0047 m <sup>3</sup> /s	68
Table 5.4.2-2	Comparison Errors, Approx Scaled Discharge 0.0074 m <sup>3</sup> /s	69
Table 5.4.2-3	Comparison Errors, Approx Scaled Discharge 0.0125 m <sup>3</sup> /s	69
Table 5.4.2-4	Comparison Errors, Approx Scaled Discharge 0.0178 m <sup>3</sup> /s	70
Table 5.4.2-5	Comparison Errors, Approx Scaled Discharge 0.0231 m <sup>3</sup> /s	70
Table 5.4.2-6	Comparison Errors, Approx Scaled Discharge 0.0287 m <sup>3</sup> /s	71
Table 6.3.2	Proposed Basic Discharge Equation for University of Canterbury Models	77
Table 6.3.3-1	Proposed Basic Discharge Equation for WINTEC Models W2 – W9	79
Table 6.3.3-2	Proposed Basic Discharge Equation for WINTEC Models W10 – W19	80
Table 6.3.3-3	Proposed Basic Discharge Equation for WINTEC Models W20 – W23	81
Table 6.4.2	Constant as Function of H <sub>o</sub>	83
Table 6.4.3-1	Coefficient as Function of L	84
Table 6.4.3-2	Coefficient as Function of H <sub>o</sub>	85

## List of Symbols

- $H_u$  Upstream head measure relative to weir crest
- $H_d$  Downstream head measure relative to weir crest
- $\beta$  Submergence measured as  $\beta = \frac{H_d}{H_u}$
- $H_o$  Value of  $H_u$  for a modular flow with the same discharge as the submerged flow
- $P_u$  Weir crest height measured from upstream bed
- $P_d$  Weir crest height measured from downstream bed
- $\mathcal{L}$  Bed levels factor measured as  $\mathcal{L} = \frac{P_u}{P_d}$

## Chapter 1 Introduction

### 1.1 Thin Plate Weirs

Thin plate weirs are one of the simplest structures used for measuring discharge in open channels and continue to be used despite the development of more sophisticated structures such as Parshall flumes.

BS 3680 the British Standard for measuring open channel discharge includes a section (Part 4A) for thin plate weirs. This specifies the design of the weir in cl.9.2.

Flow over a thin plate weir can take one of two forms – modular flow and submerged flow. Which occurs usually depends on the downstream water level. This thesis describes a study of a particular aspect of submerged flow.

### 1.2 Modular and Submerged Flow

Modular Flow is the name given to the normal discharge over a thin plate weir i.e. a nappe of water springing off the crest with an aerated space between it and the tailwater. Under these conditions the nappe plunges into the tailwater. If the tailwater is sufficiently shallow, the nappe will impinge on the bed with possible erosion.

In contrast to modular flow, submerged flow occurs when the aerated space fills with water and the downstream water level rises above the crest of the weir. This usually occurs when heavy discharge on a downstream constriction causes the tailwater level to rise. When the tailwater is sufficiently high it can, in turn, force the headwater level up. **Submergence** is defined as the ratio of downstream and upstream heads ( $H_d/H_u$ ) and is designated by  $\beta$ .

B.S. 3680 Part 4A lists applicable formulas for both modular and submerged flow (see Chapter 2).

### 1.3 Submerged Weirs with Differing Upstream and Downstream Bed Levels

The literature on the flow over submerged thin plate weirs is not as substantial as that on aspects of modular flow. However, all the published literature shows a common feature - **the assumption that upstream and downstream beds are at the same level.** (*Equal bed weir*). In practice, weirs which become submerged have usually been in place for a long time and it is to be expected that the impact of modular flow would result in some downstream erosion. (*Unequal bed weir*). The weir where the author was first faced with calibrating a submerging weir had been in operation for over a century. (It was on a tributary of the Forth River.) Leveling showed that although the average upstream bed level was 0.371 m below datum at the end of the crest the average bed level 4 m downstream of the weir was 0.423 m below datum.

As submerged flow is controlled by downstream conditions, it is to be expected that submerged flow over a weir with differing upstream and downstream bed levels would differ from submerged flow where bed levels are the same. Consequently, an expression for discharge over a submerged weir which was developed assuming equal upstream and downstream beds (a conventional formula) can be expected to give only approximately correct estimates for flow over a weir with unequal beds.

### 1.4 The Scope of This Study

The research described in this thesis was not designed to be an exhaustive study of the phenomena of submerged weirs with unequal beds. Its purpose was to establish whether an effect actually existed and whether it was sufficiently large to warrant concern. It was not considered necessary to perform a sophisticated set of experiments and in fact only simple equipment was readily available.

Two sets of experiments were carried out.; a short run with a full size weir and a more substantial set of readings done with a half size weir. A range of discharges

and models were used where a model is the weir with a given pair of bed levels. For each model/discharge combination, readings were taken for upstream and downstream heads as the weirs were steadily submerged by raising tailwater.

The data were examined to estimate the effects of the differing levels on the shape of the graph of upstream head vs downstream head and the Froude Number for the approaching flow. A comparison was also made of the discharges predicted by a conventional formula for equally and unequally bedded weirs. Subsequently, the work lead to a brief consideration of a possible new formula for calculating flow over a submerged weir.

## **1.5 Thesis Overview**

Chapter 2 reviews the background of modular and submerged flow and discusses the expected effects of differing upstream and downstream bed levels. Chapter 3 describes the laboratory study and Chapter 4 covers the resulting comparison of discharge values estimated from three existing equations for submerged weir flow.

The expected effects of unequal bed levels on discharge are discussed in Chapter 5 and Chapter 6 introduces a possible new form of a discharge equation for submerged flow over a thin plate weir. Chapter 7 summarises the work in this study and suggest further avenues of investigation.

## Chapter 2 - Background

### 2.1 Specification for Thin Plate Weirs

B.S. 3680 Part 4A defines a standard thin plate weir. As modular flow is highly dependent on the shape of the crest the Standard specifies a cross-section for the plate. This is shown in Figure 2.1; a horizontal crest of 1-2 mm and a downstream chamfer at  $45^\circ$  to the horizontal.

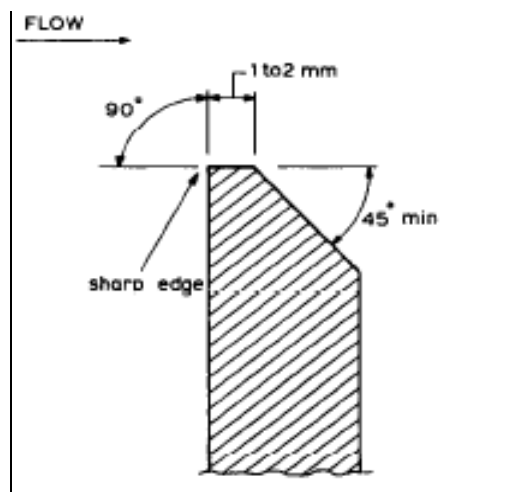
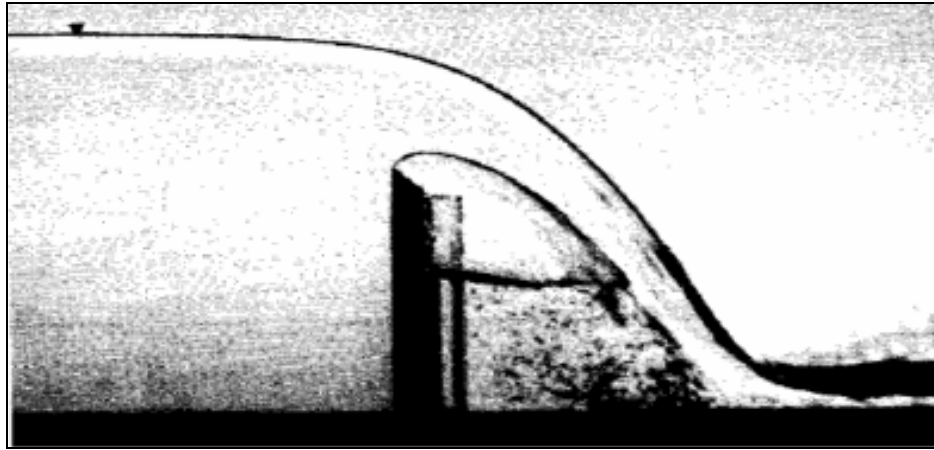


Figure 2.1 Standard Thin Plate Weir Cross -Section

### 2.2 Modular Flow

As has been mentioned, 'Modular Flow' is the name given to the normal discharge over a thin plate weir i.e. a nappe of water springing off the crest with an aerated space between it and the tailwater. Under these conditions the nappe plunges into the tailwater. Figure 2.2 shows a typical laboratory situation.



**Figure 2.2 Modular Flow Over a Thin Plate Weir**

### **2.3 Equations for Modular Flow**

The simplest equation for calculating modular discharge over a thin plate weir is

$$Q = C_d L H_u^{\frac{3}{2}}$$

where  $C_d$  is an empirically derived coefficient of discharge,  
 $L$  is length of weir,  
 $H_u$  upstream head measured relative to the weir crest.

Later researchers have expanded on this basic formula providing equations with

- Expressions for  $C_d$
- Allowance for velocity head upstream
- Corrections to give effective head and width

BS 3680 Part 4A (1981) lists these equations along with further details and references.

The work described in this thesis required a modular flow equation. The one chosen was that developed by Kindsvater and Carter (1959)

$$Q = \left( 0.602 + \frac{H_u}{P} \right) * \left( \frac{2}{3} \right) * \sqrt{2g} * (b - 0.9) * (H_u + 0.001)$$

where again

$Q$  = discharge in m<sup>3</sup>/s

$H_u$  = upstream head measured from crest level

$b$  = bed width

## 2.4 Submerged Flow

As has been mentioned, submerged flow occurs when the aerated space fills with water and the downstream water level rises above the crest of the weir. The rising tailwater leads to a clearly delineated succession of surface and subsurface effects.

### 2.4.1 Stages of Submergence:

Initially some aeration remains in the nappe and the flow over the weir reaches the channel bed. A hydraulic jump is formed downstream of the weir – *Limited Jump*.

With increasing submergence, the jump approaches the weir face and at the limit of this condition, the nappe is submerged but the flow still impinges on the channel bed – *Impinging Flow*

With further submergence the flow lifts off the bed but still plunges over the weir – hence *Plunging Flow* – and the turbulent face of the hydraulic jump gradually dissipates.

When the hydraulic jump disappears, the flow ceases to plunge into the tailwater, but flows almost horizontally. The downstream surface is now marked by undulations often in the form of a standing wave - *Surface Wave*.

With increasing discharge the surface smoothes and the flow forms a jet. Four of these forms can be seen in Figure 2.4.1.

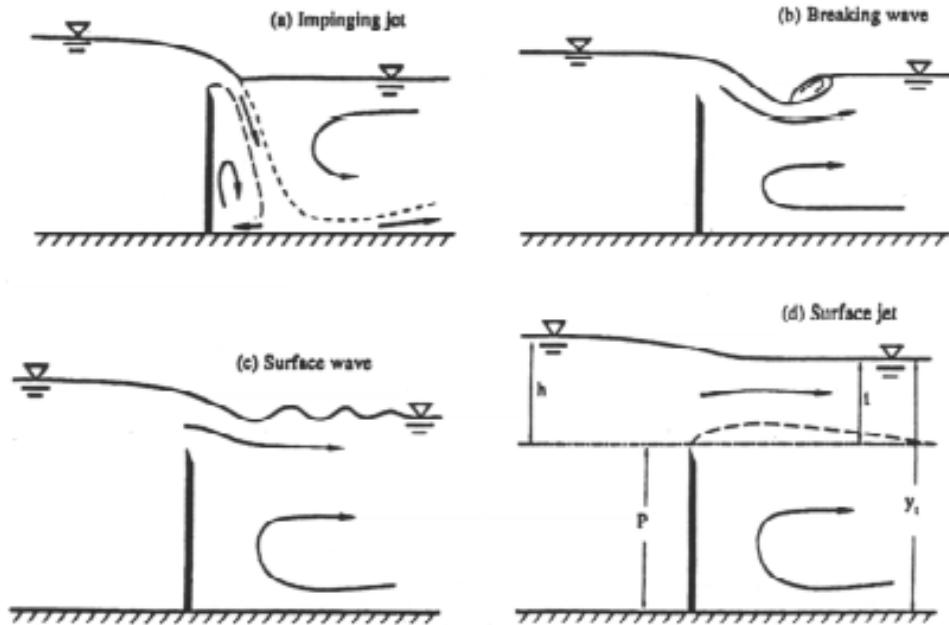


**Figure 2.4.1 Types of Submerged Flow Over a Thin Plate Weir**

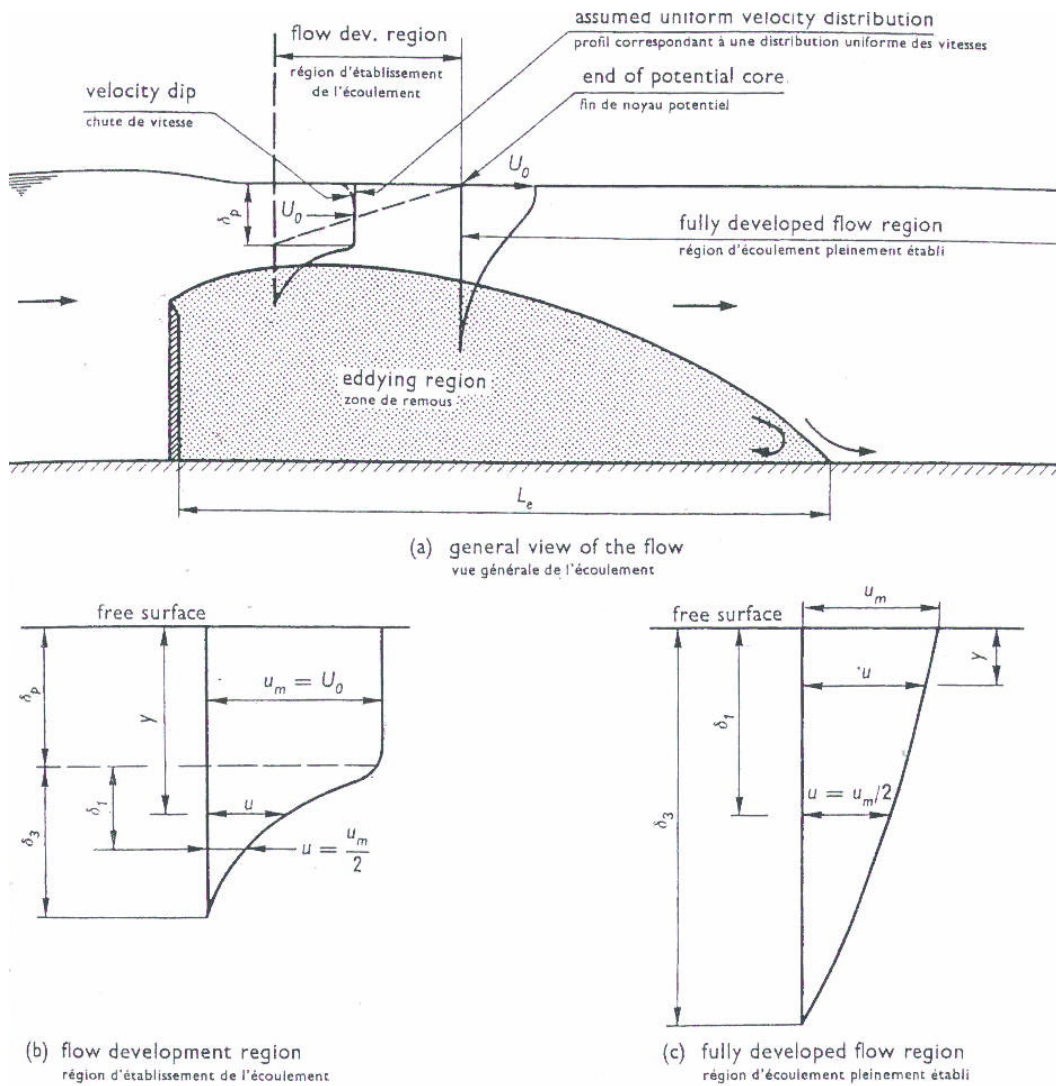
(From, Wu & Rajaratnam, (1996))

The same pattern is repeated in reverse as the tailwater lowers. However, it has been noted that there is a hysteresis effect and the transition from surface wave to impinging flow occurs at lower values of submergence. (Wu & Rajaratnam, 1996) This effect was noticed in the study reported in this thesis and corresponded in part to a delay in re-establishing the aerated space under the nappe.

## 2.4.2 Deeply Submerged Flow

In the extreme case of deep submergence, a small dip is formed immediately downstream of the weir and the main flow behaves like a surface jet. While it might be expected that at very deep submergence the upstream and

downstream water levels would be equal (i.e.  $\beta = 1$ ), it is possible for the downstream water level to exceed the upstream water level (i.e.  $\beta \neq 1$ ). Vertical spreading of the jet can lift the water surface. This was noticed in the model study. (see Chapter 3).



Definition sketches.

Fig. 5.

Schémas de principe.

### Figure 2.4.2 Flow Over a Deeply Submerged Weir

(From Rajaratnam and Muralidhar (1969))

Rajaratnam and Muralidhar (1969) examined the highly submerged case. Figure 2.4.2 is based on their Figure 5. They found that the turbulence formed a distinct region with a boundary approximating the underside of the nappe. Actual discharge was by means of the flow over the 'top' of the turbulent zone. Near the weir a vertical cross-section of the flow shows a horizontal flow section ('potential core') and a logarithmic section which corresponds to the boundary of the turbulent zone. Downstream where the turbulence has tapered off ('fully developed section') the flow has the usual logarithmic velocity distribution.

## 2.5 Equations for Calculating Discharges Over Submerged Weirs

In contrast to the modular flow case, there are few equations for calculating discharge over a submerged thin plate weir. A review of the literature indicates that derivations follow 3 approaches. ( see Figure 2.5).

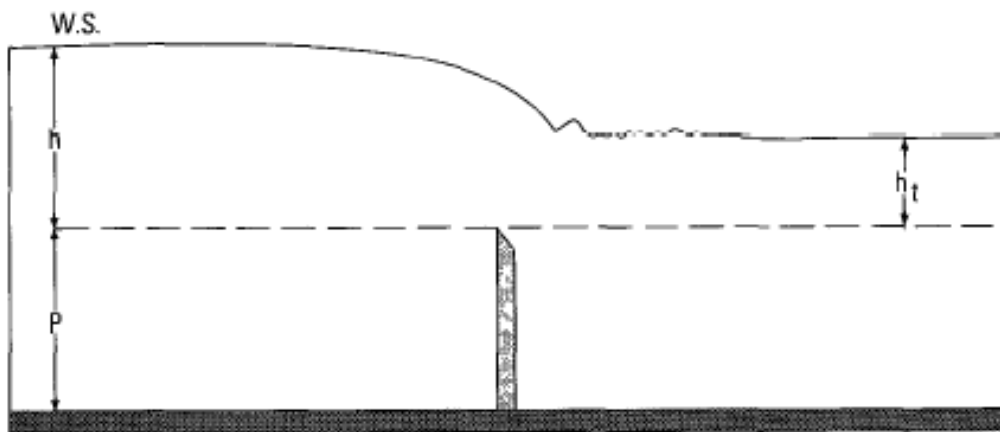


**Figure 2.5 Flow Over a Submerged Thin Plate Weir**

### 2.5.1. Submerged Orifice:

In this approach, the discharge is regarded as a combination of a submerged orifice acting under a head of  $H_u - H_d$  and a modular flow with head  $H_u - H_d$ . The most recent equation based on this approach is that of Abou-Seida and Quraishi (1976) i.e.

$$Q = \frac{2}{3} C_d b \sqrt{2g} H_u^{3/2} \left[ (1 - \beta)^{1/2} (1 + 0.5\beta) \right] \quad (1)$$

where ,

$H_u$  is upstream head measured relative to the weir crest,

$H_d$  is downstream head measure relative to the weir crest,

$\beta$  is submergence  $H_d/H_u$ , and

$C_d$  is the discharge coefficient.

### 2.5.2. Opposing Modular Flows:

In his 1947 paper Villemonte put forward this approach as an easier alternative to the submerged orifice approach. Here submerged discharge is treated as the resultant of two opposing modular flows, one downstream under a head of  $H_u$  and one upstream under a head of  $H_d$ . Villemonte's own equation (Villemonte, 1947) has gained wide acceptance and is quoted in BS 3680 Part 4A. The equation is

$$Q = (1 - \beta^{1.5})^{0.385} Q_m \quad (2)$$

where,  $Q_m$  is modular discharge corresponding to the head  $H_u$

### 2.5.3. Empirical:

Here measurements are made on laboratory models (usually) or actual weirs and an equation is derived from the data. Most of the early work on submerged thin plate weirs (e.g. Francis, Bazin) used this approach. More recently, Borghei *et.al.* (2003) developed equations for flow over oblique weirs including one for submerged flow i.e.

$$Q = \left[ \left( \left( 0.008 \frac{L}{B} + 0.985 \right) + \left( 0.161 \frac{L}{B} - 0.479 \right) \right) * \left( \frac{H_d}{H_u} \right)^3 \right]^2 * Q_m \quad (3)$$

where,

L is the length of the weir, and

B is the width of the channel.

When this is simplified for a normal weir by setting  $(L/B) = 1$ , the equation becomes

$$Q = \left[ 0.993 - 0.318\beta^3 \right]^2 Q_m \quad (4)$$

where  $\beta$  is submergence  $H_d/H_u$ .

As this equation will be referred to later it has (with Professor Borghei's permission) been defined as the 'Modified BVGJ'.

### 2.5.4 Choice of Formulas

If the unequal upstream and downstream beds have an effect then it is expected that estimating flow using an equal bed formula would lead to a value which was incorrect. Hence it was necessary to establish which of these formulas was the most accurate. The details of this comparison are shown in Chapter 4. After analysis it was decided to use the Modified BVGJ for some models and the Villemonte formula for the remainder. In both cases, modular flow was calculated using the Kindsvater and Carter formula.

## 2.6 Discharge Over an Unequal Bed Weir

### 2.6.1 Notation

As there is no recognized terminology for a weir with differing upstream downstream bed levels, this work uses the following definitions. A thin plate weir with different upstream and downstream bed levels is called an **unequal bed weir**; when the levels are the same it is an **equal bed weir**. The difference in bed levels is described by the **bed levels factor**  $\mathbf{L}$  where  $\mathbf{L}$  is the ratio of the crest height above upstream bed to crest height above downstream bed i.e.

$$\mathbf{L} = P_u/P_d$$

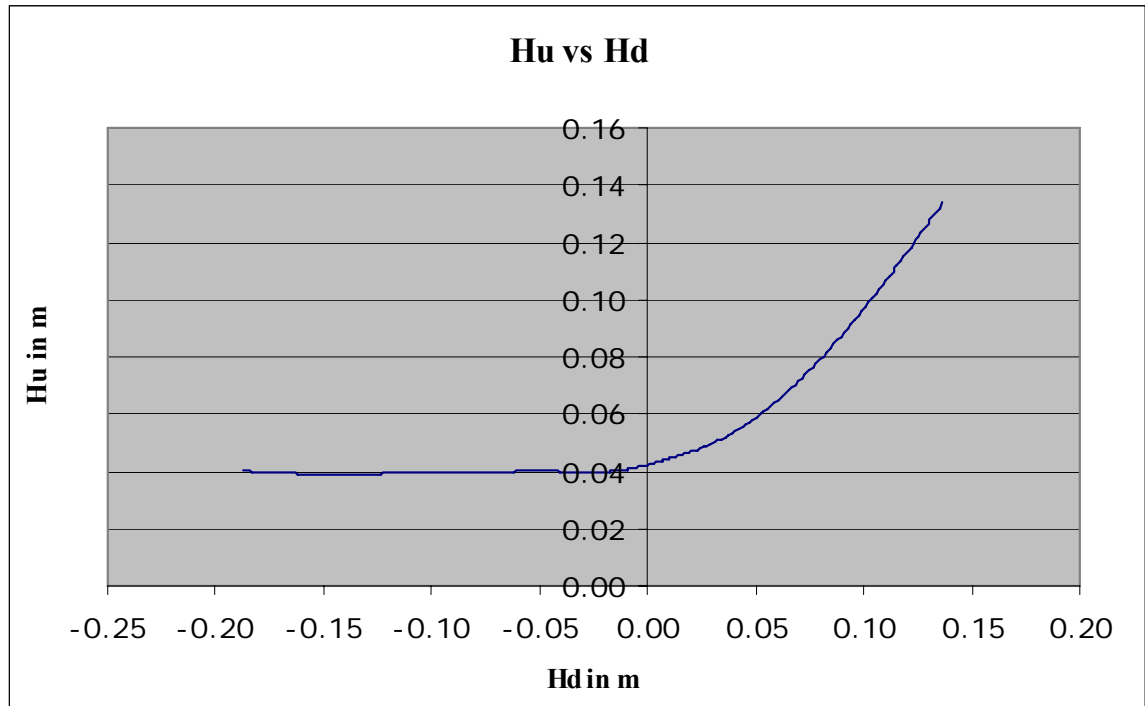
### 2.6.2 Anticipated Effect of Unequal Beds

Figure 2.4.2 shows that the main regions just downstream of a submerged thin plate weir and the turbulent zone and the overlying jet. When the downstream bed is lower, it is expected that the turbulent zone will physically move downwards. It may enlarge slightly as more potential energy is being transformed into kinetic energy. This effect is expected to be minor compared with the physical movement

The effect on the turbulent zone will make it easier for the rising downstream water level to influence the upstream water level, forcing it up. Consequently initially a given  $H_d$  would correspond to a higher  $H_u$  in the unequal bed case than in the equal bed case. This in turn would lead to the following effects.

### 2.6.3 $H_u$ vs $H_d$ Plot

Plotting  $H_u$  against  $H_d$  for a submerging weir is expected to lead to a plot of the form of Figure 2.6.3(a). Initially because  $H_d$  is negative (i.e downstream water level below the crest) the graph is a horizontal line. This may tilt up slightly as  $H_d$  approaches the origin and the rising downstream level is already influencing the upstream water level.



**Figure 2.6.3(a) Typical  $H_u$  vs  $H_d$  Values for Submerged Weir at Fixed Discharge.**

With submergence, both the upstream and downstream water levels rise. Initially the graph has a shallow slope as the downstream head's influence is restricted to the potential core region (Figure 2.4.2). As  $H_d$  increases this core becomes thicker and the slope of the graph becomes steeper. Eventually the graph approaches the asymptote corresponding to  $H_u = H_d$  i.e.  $\beta = 1$  although it has been noted that a  $\beta \geq 1$  is possible.

For the unequal bed case with the same discharge and upstream weir height, after the delayed onset, the initial rise is expected to be steeper than for the equal bed case as the potential core for the unequal bed is already thicker. The graph will steepen but the relative increase in slope will be less than for the equal bed case leading to high submergence graph slope which is smaller than that of the equal bed case. Hence the two  $H_u$  vs  $H_d$  plots can be expected to cross at high submergence (Figure 2.6.3(b)). This crossing point has been called **equal-unequal intersection**.

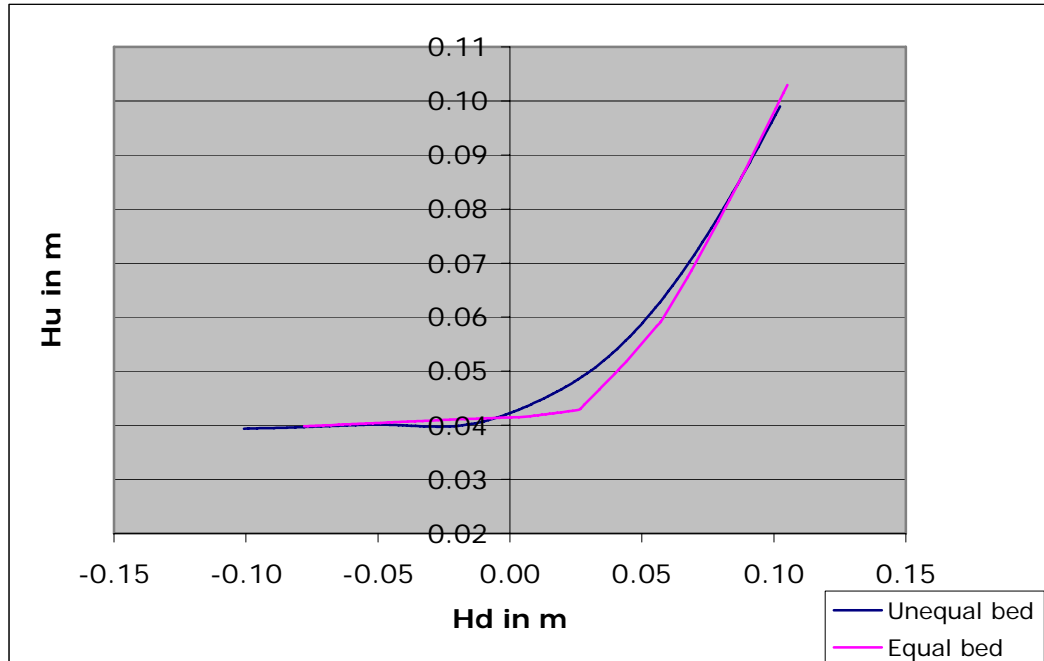


**Figure 2.6.3(b) Expected  $H_u$  vs  $H_d$  Shape for Equal and Unequal Bed Levels**

#### 2.6.4. Approach Froude Number

As Froude Number is defined as

$$Fr = \frac{q}{H\sqrt{gH}}$$

the value of the approach Froude number will depend on the upstream head as in this formula  $H$  is upstream depth. Hence for a given  $H_d$  up to the equal-unequal intersection the unequal bed case would show a lower  $Fr$  value than the equal bed case. When  $H_d$  is above the intersection the Froude number for the unequal case would be slightly higher.

Below the equal-unequal intersection the slope of the curve for the unequal bed will be higher than that of the equal bed case. Consequently for a given submergence the unequal bed would have a lower  $H_u$  and thus a higher Fr value than the equal bed case.

### **2.6.5 Calculation of Discharge**

The formulas for discharge over a submerged weir are all functions of the upstream head  $H_u$  and the submergence  $\beta$  ( usually as  $[1- \beta]$ ).. Inherent in these equations is an assumed relationship between  $H_u$  and  $\beta$  described by Figure 2.6.3(a)

For the unequal case, below the equal-unequal intersection, a given  $H_d$  has a lower  $\beta$  and a higher  $H_u$ , than for the equal bed case. Consequently applying a conventional formula would be expected to overestimate the discharge. Conversely, for  $H_d$  above the equal-unequal intersection the conventional formula would underestimate.

## **2.7 Laboratory Study**

### **2.7.1 Equal Bed Formulas**

As comparisons were to be made between the equal and unequal situations, it was necessary to establish which of the three equal bed formulas described above was the most accurate. Initially it was expected that the presence of the  $(1-\beta)$  factor would render the Villemonte equation and the Abou-Seida and Quraishi equation inaccurate at high submergences and thus not convenient for this study. The three formulas were compared by running equal bed models in both sets of experiments.

### **2.7.2 Effects of Unequal Beds**

The laboratory study resulted in a large amount of data with fine gradations of  $L$  values. To establish initially whether an unequal bed effect exists comparisons were done between models with extreme values of  $L$  i.e. 4 models with  $L = 1$  compared with models with  $L = 0.33, 0.52,$  and  $0.6$ .

**$H_u$  vs  $H_d$ :** Pairs of curves were plotted and examined for differences in steepness and intersection at high submergences

**Approach Froude Number:** Approach Froude Numbers were calculated for each pair of data sets and plotted as a function of submergence  $\beta$ . It was decided to use  $\beta$  as an independent variable as it leads to a dimensionless plot.

**Discharge:** For each data set, the discharges were calculated with the chosen equal bed formula and compared with the actual discharge. The errors for each of the two model data sets were tabulated and briefly compared. Lack of time did not permit a detailed statistical analysis.

## **Chapter 3 LABORATORY STUDY**

### **3.1 Introduction**

As the University of Waikato does not possess a suitable flume, the laboratory study had to be carried out at two other institutions.

One section was a short programme of experiments on a full scale weir at the Hydraulics Laboratory, Department of Civil Engineering, The University of Canterbury, Christchurch, New Zealand. The other was a much longer model study done in the Hydraulics Laboratory, School of Engineering and Built Environment, Waikato Institute of Technology (W.I.N.T.E.C.) in Hamilton, New Zealand.

### **3.2 The University of Canterbury Study**

#### **3.2.1 Equipment**

This study used the large tilting flume - 12 m long, 0.6 m wide and 0.46m deep – although it was kept level for this experiment. Water was pumped from sump to a 12m high constant head water tower. This tower has a weir system and the surplus water returns to the sump. The inflow was controlled by an electro-pneumatically controlled butterfly valve controlled by a Shimaden F21 programmable controller and monitored by a Krohn magnetic flow meter.

Outflow is controlled by brass sluice gate, raised and lowered by gears. The sluice can be closed systematically tooth by tooth on a ratchet pawl system.

### **3.2.2 Model Weir**

The test weir was made of 6 mm Perspex sheet, glued to the front of a base cut from Perspex block. The dimensions were 0.6 m wide, 0.12 m high and the crest had the standard BS3680 Part 4A cross-section – 2 mm horizontal and downstream face chamfer of 45 degrees.

The base was screwed into the floor of the flume and the weir waterproofed by lengths of Blu Tack laid where the weir touched the flume walls, both upstream and downstream. Aeration was provided by *narrow* tubing placed against the weir face and secured to the flume wall by Blu Tack.

The upstream and downstream beds were modelled by painted plywood inserts 0.6 m wide and 1.8 m long. These were held down by threaded brass rods through aluminium strips across the width of the flume.

### **3.2.3 Measurements**

Nominal discharge was obtained by entering the required value into the controller. Initially the model was run in the modular state and the values of the discharge calculated by the Kindsvater and Carter equation using the initial upstream head as a check.

Water levels were measured by pointer gauges at each end of a carriage mounted on rails fixed to the sides of the flume. All levels were related to the crest of the weir.

### **3.2.4 Model Study**

There were 8 models. These consisted of 6 upstream bed inserts with 0,1,2,3,4,5,6 downstream bed inserts respectively and a second even bed case of 5 upstream and 5 downstream beds inserts. Details of these models can be seen in Table 3.2.4

Four nominal discharges were used; 10, 15, 20, and 25 litres per second.

For each setting/discharge combination, the model was initially run in the modular region to check the actual discharge. The model was then slowly submerged by closing the sluice gate tooth by tooth and allowing the water level to settle. The upstream and downstream water levels were measured and note taken of the type of flow. This was particularly important when the standing wave developed.

<b>Model No.</b>	<b>No. u/s beds</b>	<b>No. d/s beds</b>	<b>P<sub>u</sub></b>	<b>P<sub>d</sub></b>	<b>L (= P<sub>u</sub>/P<sub>d</sub>)</b>
C1	6	0	0.067	0.2016	0.33
C2	6	1	0.067	0.1798	0.37
C3	6	2	0.067	0.1556	0.43
C4	6	3	0.067	0.1326	0.51
C5	6	4	0.067	0.1078	0.62
C6	6	5	0.067	0.0868	0.77
C7	6	6	0.067	0.067	1.00
C8	5	5	0.0852	0.0852	1.00

**Table 3.2.4 Models for University of Canterbury Study**

### **3.3 Waikato Institute of Technology Study**

#### **3.3.1 Scale Models**

In designing a scale model, one of the goals is to ensure that the prototype and the model have the same dimensionless numbers. For open channel flow this means particularly Froude number (Fr.) and Reynolds' number (Re.) Unfortunately as the engineer generally uses water in both model and prototype, it is impossible to 'model' viscosity. In turn this means that the engineer cannot simultaneously retain both Fr and Re similitude

The usual compromise is to design the model to retain the Froude number and run the model at sufficiently high  $Re$  to nullify the viscosity effect i.e. completely turbulent. To ensure  $Fr$  similitude in this modelling the following relationships apply:

$$\begin{aligned}\text{Length prototype} &= 2 \times \text{length model} \\ \text{Discharge prototype} &= 2^{2.5} \times \text{discharge model}\end{aligned}$$

In practise, prototype discharge was obtained by inserting the prototype head into the discharge equation.

### **3.3.2 Equipment**

This part of the study used the smaller Armfield flume in the Hydraulics Laboratory, School of Engineering and Building Construction, Waikato Institute of Technology. The flume was 3 m long, 0.1 m wide with glass walls 0.031 m deep. Like the Canterbury flume the Armfield can be tilted, but for this experiment was set level. Water was held in a supply tank and pumped by a Worthington-Simpson Centrifugal pump. Discharge was controlled by a butterfly valve and monitored by the Armfield flow meter supplied with the flume. The valve had to be set by hand and so required a practiced hand to set it accurately

Outflow was controlled by a tilting weir raised by a crank handle. In studies of this type, this method of outflow control (*i.e.* an overshot gate) is preferable to a lowered sluice as the water level settles more quickly.

### **3.3.3. Model Weir**

The weir itself was a narrower version of that used at the University of Canterbury 0.13 m high and 0.1 m wide. It was slotted into the floor of the flume. The beds were modelled by lengths of Perspex 12 mm thick, 0.9 m upstream length and 1.2 m downstream length. The bed inserts were held down by threaded aluminium rods through a cross bar – one upstream and one downstream. Again water proofing

was by copious strips of Blu-Tack, and a short length of tubing was Blu-Tacked to the face of the weir to provide aeration.

### **3.3.4 Measurement**

Discharge was monitored by flow meter, but these readings were checked by initially running the model under modular conditions and calculating the discharge using the Kindsvater and Carter Equation. This also acted as a check on scale effects. As the flume was only 0.1 m wide, there was the possibility that the water level would have been artificially high leading to an overestimation by the Kindsvater and Carter equation.

It was decided that even if this occurred, there would be an internal consistency of behaviour and that meaningful results could still be obtained. When the measurements were made, it was found that there was good agreement between the Kindsvater and Carter equation and the flow meter for discharges of 1,2,3,4, and 5 litres per second. The only major inconsistency came with the lowest discharge (0.5 litre per sec), although being at the lower end of the flow meter scale, there may be some error in the flow meter as well. For this model, the discharge as calculated by the Kindsvater and Carter equation was used.

Water and bed levels were measured by a single moveable point gauge. As this gauge was above the author's eye level, she was fortunate to have the assistance of Mr Bryan Fowles, the Laboratory Technician for the department. His skill in placing and reading pointer gauges quickly and efficiently (as well as in setting the valve) meant that 23 models, each with 6 different discharges could be run in a reasonable period of time.

### **3.3.5 Study**

The same procedure was followed as in the University of Canterbury study; for each combination of upstream and downstream beds and discharge, the model was systematically submerged and measurements taken of upstream and downstream

water levels. In this study measurements were taken with both rising and falling submergences, making possible an estimate of possible hysteresis effects

The models were run with nominal discharges of 0.5,1,2,3,4, and 5 litre per sec. However, for the highest discharge it was often not possible to get to the heavily submerged phase, due to insufficient freeboard in the flume.

The models consisted of 2 to 6 upstream Perspex slabs each with the appropriate combination of downstream bed. These combination resulted in values of  $L$  ranging from 0.52 to approximately 1 with 6 even bed cases. – See Table 3.3.5

### **3.4 Standing Wave**

As has been discussed previously (Section 2.4.1) with both the increasing and decreasing submergence, the flow goes through a standing wave. As this wave can be quite marked, a water level reading taken on the wave is often misleading as the pointer gauge may touch the surface anywhere between crest and trough. If the experimenter is particularly lucky, it may touch on the mid-level. Also the standing wave does not develop in exactly the same place with changing discharge or models

Readings taken at the standing wave were flagged in the recording of the results. Later the validity of the reading was checked with plots of  $H_u$  vs  $H_d$ . (Section 4.2)

<b>Model No</b>	<b>No. u/s bed inserts</b>	<b>No. d/s bed inserts</b>	<b>P<sub>u</sub> scaled</b>	<b>P<sub>d</sub> scaled</b>	<b>L (= P<sub>u</sub>/P<sub>d</sub>)</b>
1	2	2	0.255	0.248.8	1.02
2	2	1	0.255	0.275	0.93
3	3	3	0.2318	0.2236	1.04
4	3	2	0.2306	0.2486	0.93
5	3	1	0.2308	0.2748	0.84
6	4	4	0.2058	0.1974	1.04
7	4	3	0.2062	0.2238	0.92
8	4	2	0.2058	0.2498	0.82
9	4	1	0.2064	0.2752	0.75
10	4	0	0.2064	0.303	0.68
11	5	5	0.181	0.1716	1.05
12	5	4	0.181	0.1978	0.92
13	5	3	0.1814	0.2248	0.81
14	5	2	0.1814	0.250.2	0.73
15	5	1	0.1814	0.2756	0.66
16	5	0	0.1812	0.303	0.60
17	6	6	0.157	0.1468	1.07
18	6	5	0.1564	0.1724	0.91
19	6	4	0.1564	0.1986	0.79
20	6	3	0.1568	0.2246	0.70
21	6	2	0.1566	0.2502	0.63
22	6	1	0.1568	0.2756	0.57
23	6	0	0.1568	0.3032	0.52

**Table 3.3.5. Models for Waikato Institute of Technology Model Study**

## **Chapter 4 Comparison of Values Calculated by Equal Bed Formulas**

### **4.1 Introduction**

The first step in the analysis was to compare the three formulas for discharge over a submerged thin plate weir which was described in Chapter 1. As the Modified BVGJ formula does not contain the  $(1-\beta)$  factor it was initially thought that this would be more accurate than the other two especially at high submergences.

However, Borghei *et.al* developed their equations using weirs ranging in height 0.460 m to 0.511m and Abou-Seid and Quraishi used two weirs of heights 0.151m and 0.113m. BS 3680 Part 4a gives the practical limit for weir height for use of the Kindsvater and Carter equation as 0.10 m. As this study used weirs ranging in height from 0.067 m to 0.125 m it was necessary to compare the formulas by running the models with equal beds.

### **4.2 Standing Wave Data Points**

In each model run, readings were taken when the standing wave was reached. A data consistency check was done by plotting  $H_u$  against  $H_d$  and noting if the standing wave point was obviously off the curve. When this occurred the  $H_u$  value was retained and the  $H_d$  value adjusted to bring the point onto a smooth curve. This was done for all runs.

### **4.3 University of Canterbury Study Results**

The calculated results for the two equal bed models are shown in Table 4.3-1 and Table 4.3-2. These tables show  $Q_{mi}$  the pre-submergence discharge calculated using the Kindsvater and Carter equation and the discharges calculated using each of the three submerged discharge equation as submergence increases.  $Q_{abs}/q$  represents the discharge calculated by the Abou-Seida and Quraishi formula,  $Q_{vkc}$  is the discharge calculated applying

the Villemonte correction to the Kindsvater and Carter modular flow equation, and  $Q_{bkc}$  is the discharge calculated using the Modified BVGJ formula applied to Kindsvater and Carter equation. The percentage errors are the differences between the initial modular flow value and the calculated discharge expressed as a percentage of the initial modular flow.

Gauge Discharge	Model	C7						
	(Hd/Hu)	Q <sub>mi</sub>	Q abs/q Discharge	Q abs/q % Error	Q <sub>vkc</sub> Discharge	Q <sub>vkc</sub> % Error	Q <sub>bkc</sub> Discharge	Q <sub>bkc</sub> % Error
10 l/s	0.1359	0.0100	0.0097	2.6	0.0098	2.3	0.0098	1.9
	0.6179	0.0100	0.0083	17.0	0.0081	19.4	0.0088	12.3
	0.8907	0.0100	0.0062	37.5	0.0065	34.9	0.0078	22.1
	0.9697	0.0100	0.0045	54.6	0.0053	46.6	0.0087	13.0
	1.0088	0.0100					0.0096	3.5
	1.0207	0.0100					0.0115	14.6
	1.0208	0.0100					0.0138	38.0
15 l/s	0.2614	0.0146	0.0141	3.3	0.0138	5.1	0.0143	2.3
	0.6418	0.0146	0.0128	12.5	0.0123	15.8	0.0134	8.2
	0.8339	0.0146	0.0110	24.4	0.0110	24.5	0.0125	14.3
	0.9304	0.0146	0.0086	40.8	0.0093	36.4	0.0121	16.9
	0.9772	0.0146	0.0062	57.2	0.0075	48.5	0.0134	8.2
20 l/s	0.0915	0.0198	0.0194	1.9	0.0193	2.5	0.0192	2.8
	0.5783	0.0198	0.0176	11.2	0.0168	15.1	0.0182	7.9
	0.6994	0.0198	0.0174	12.1	0.0167	15.5	0.0184	7.3
	0.8616	0.0198	0.0141	28.8	0.0142	28.2	0.0165	16.9
	0.9102	0.0198	0.0125	37.1	0.0130	34.2	0.0161	18.5
	0.9798	0.0198	0.0086	56.6	0.0104	47.3	0.0194	2.3
25l/s	0.0734	0.0250	0.0248	0.9	0.0246	1.7	0.0244	2.4
	0.6078	0.0250	0.0218	12.7	0.0208	16.8	0.0226	9.5
	0.8268	0.0250	0.0191	23.7	0.0188	24.7	0.0213	14.8
	0.9073	0.0250	0.0155	38.2	0.0161	35.7	0.0198	20.9
	0.9516	0.0250	0.0141	43.6	0.0156	37.7	0.0222	11.3
	0.9857	0.0250	0.0089	64.4	0.0112	55.2	0.0234	6.6
	1.0000	0.0250	0.0000	100.0	0.0000	100.0	0.0286	14.4

**Table 4.3-1 Comparison of Calculated Discharges for Submerged Weirs with Equal Beds**

	Model	C8						
Gauge	(Hd/Hu)	Qmi	Q abs/q	Q abs/q	Qvkc	Qvkc	Qbkc	Qbkc
Discharge			Discharge	% Error	Discharge	% Error	Discharge	% Error
10 l/s	0.2130	0.0098	0.0102	3.8	0.0103	5.1	0.0105	7.2
	0.4690	0.0098	0.0100	2.1	0.0099	1.0	0.0106	8.1
	0.8498	0.0098	0.0073	25.2	0.0076	22.5	0.0087	11.1
	0.9481	0.0098	0.0061	37.9	0.0069	29.1	0.0097	0.8
	0.9916	0.0098	0.0032	67.7	0.0044	55.0	0.0111	13.3
	0.9976	0.0098	0.0022	77.9	0.0035	64.5	0.0139	42.3
15 l/s	0.6885	0.0151	0.0134	11.4	0.0133	12.2	0.0145	3.8
	0.8750	0.0151	0.0110	27.3	0.0115	23.7	0.0135	10.4
	0.9368	0.0151	0.0093	38.1	0.0105	30.7	0.0140	7.6
	0.9814	0.0151	0.0063	58.4	0.0080	46.9	0.0153	1.1
	0.9949	0.0151	0.0055	63.4	0.0082	45.8	0.0247	63.6
	1.0000	0.0151	0.0000	100.0	0.0000	100.0	0.0350	131.8
20 l/s	0.1611	0.0206	0.0199	3.3	0.0202	2.0	0.0204	1.2
	0.5000	0.0206	0.0187	9.0	0.0184	10.5	0.0198	3.8
	0.6967	0.0206	0.0177	14.0	0.0176	14.8	0.0192	6.6
	0.8098	0.0206	0.0161	21.8	0.0164	20.5	0.0184	10.7
	0.8543	0.0206	0.0153	25.8	0.0159	23.0	0.0182	11.4
	0.9404	0.0206	0.0128	37.8	0.0144	29.9	0.0195	5.2
	0.9723	0.0206	0.0111	46.0	0.0136	34.0	0.0228	10.6
	0.9917	0.0206	0.0073	64.6	0.0102	50.4	0.0258	25.2
	0.9923	0.0206	0.0080	61.3	0.0113	45.2	0.0293	42.2
25 l/s	0.1613	0.0250	0.0242	3.1	0.0246	1.8	0.0248	0.9
	0.6235	0.0250	0.0229	8.2	0.0226	9.6	0.0246	1.5
	0.8231	0.0250	0.0203	18.7	0.0208	16.8	0.0235	6.1
	0.9308	0.0250	0.0155	37.9	0.0172	31.0	0.0225	9.9
	0.9459	0.0250	0.0160	35.8	0.0183	26.8	0.0254	1.5
	0.9578	0.0250	0.0158	36.6	0.0186	25.8	0.0275	9.8
	0.9827	0.0250	0.0152	39.0	0.0198	20.9	0.0386	54.5
	0.9903	0.0250	0.0134	46.6	0.0185	25.9	0.0442	76.8
	0.9966	0.0250	0.0091	63.7	0.0142	43.1	0.0502	101.0

Table 4.3-2 Comparison of Calculated Discharges for Submerged Weirs with Equal Beds

With the exception of the initial run with model C8 all of the formulas underestimate the discharge. However, the Modified BVGJ showed the smallest error of the three. The formulas showed the expected large errors as the submergence approached 1 i.e. the plot approached  $\beta = 1$  as an asymptote. Here the  $(1 - \beta)$  factor is dominant in the expression. In contrast, the submergence in the Modified BVGJ formula has to have the value 1.43 (i.e.  $\sqrt[3]{\frac{0.933}{0.318}}$ ) before the correction factor become zero. Also, the correction factor is a function of  $(1 - \beta^3)$  the decrease in value is much slower than for the other two.

The pattern can be seen in Figures 4.3-1,-2,-3,-4,-5,-6,-7,-8 where the data are for the three submerged flow calculations are plotted along with the horizontal line representing the actual (modular flow). The plots use the same notation as the Tables 4.3-1 and -2.

The Modified BVGJ formula shows an interesting shape, dipping to a minimum and then rising sharply. This represents discharges which are a function of  $(H / \sqrt{H_u})^3$ , whereas Abou-Seida and Quraishi and Villemonte expressions are a function of  $(H_d \sqrt{H_u})$ . Further analysis would require the expression connecting  $H_d$  and  $H_u$ . This study has included some work on this, (Chapter 6) but a definitive expression has not yet been developed.

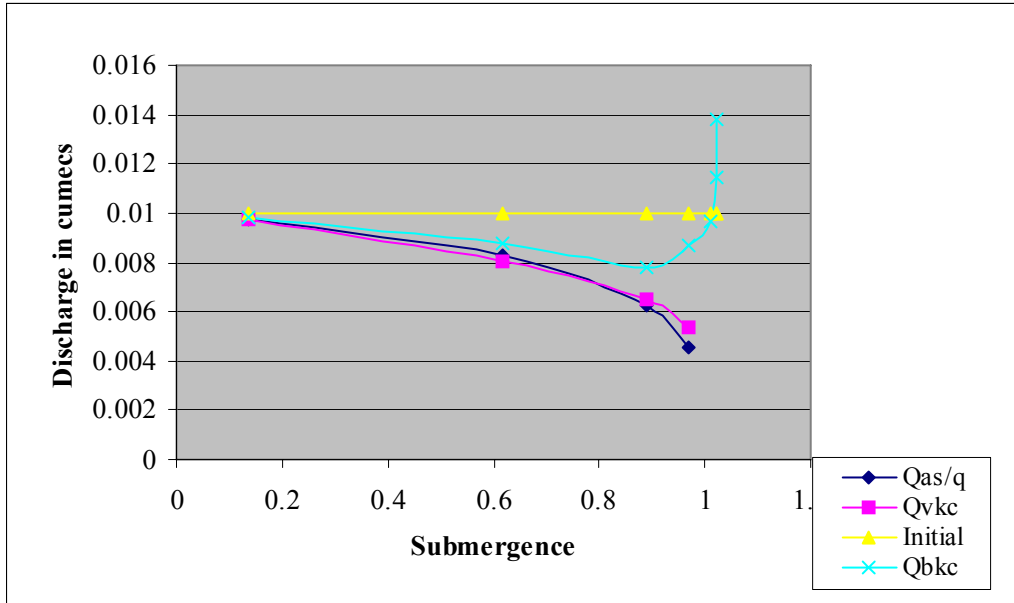


Figure 4.3-1 Model C7, Discharge 0.01 m<sup>3</sup>/s, Discharge vs Submergence  $\beta$

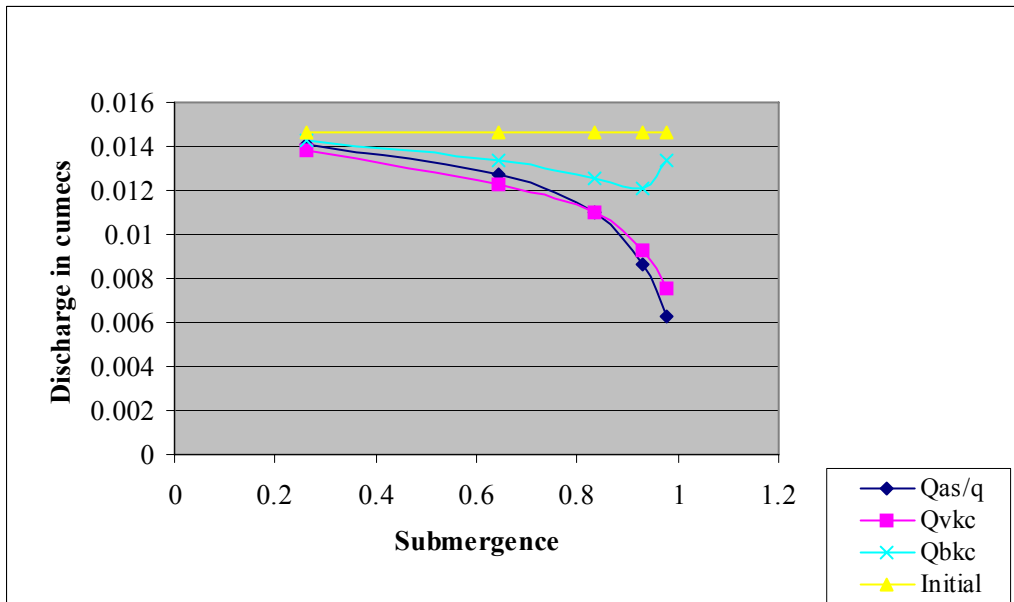


Figure 4.3-2 Model C7, Discharge 0.0145 m<sup>3</sup>/s, Discharge vs Submergence  $\beta$

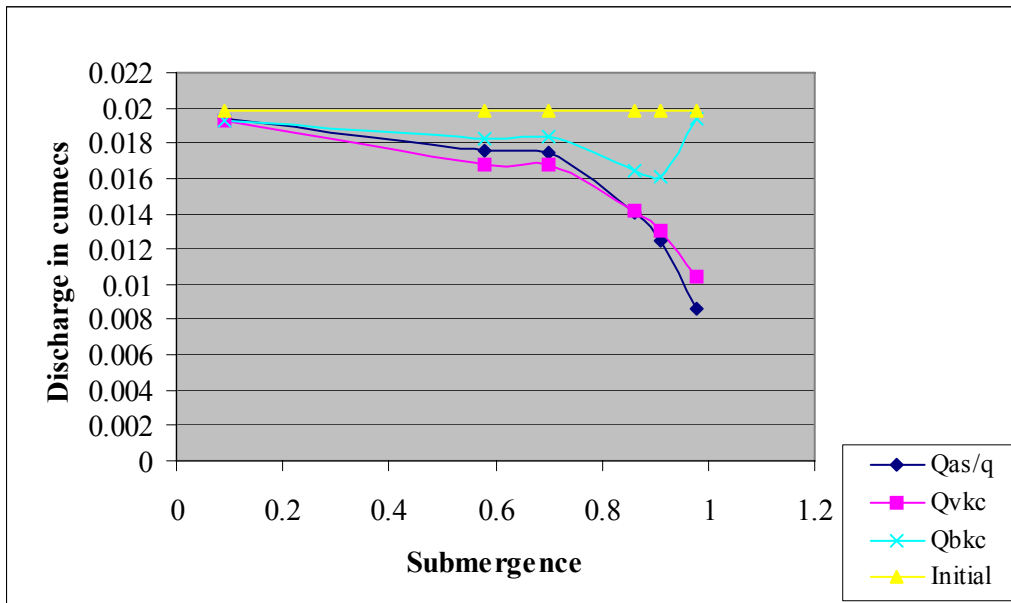


Figure 4.3-3 Model C7, Discharge 0.0198 m<sup>3</sup>/s, Discharge vs Submergence  $\beta$

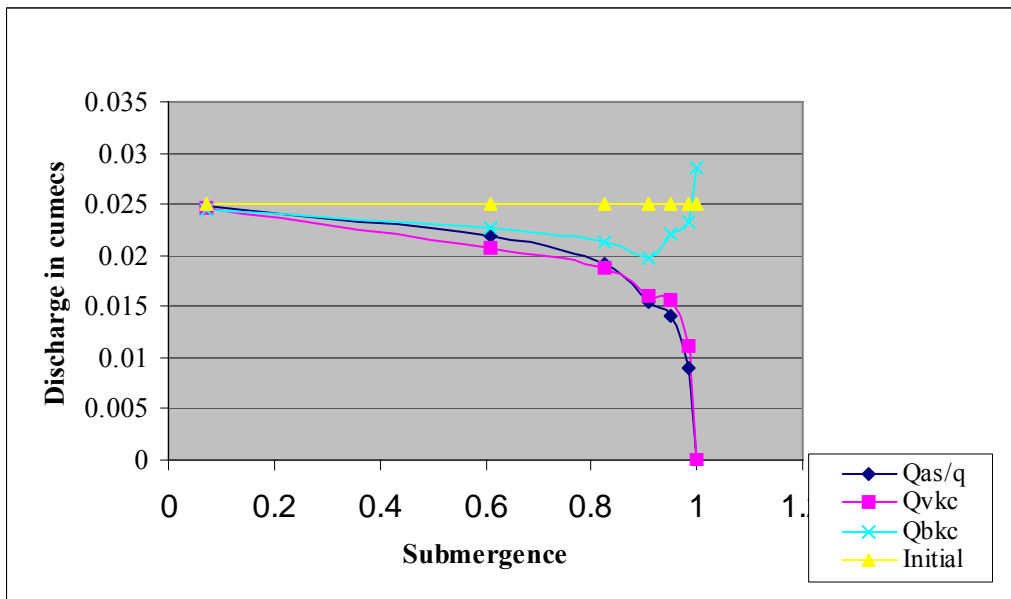


Figure 4.3-4 Model C7, Discharge 0.025 m<sup>3</sup>/s, Discharge vs Submergence  $\beta$

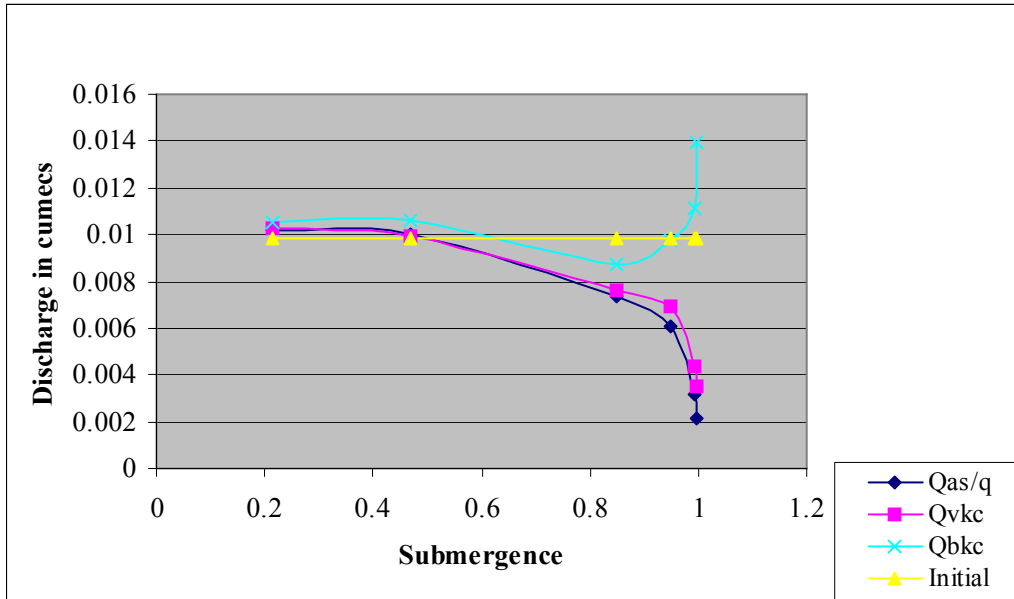


Figure 4.3-5 Model C8, Discharge 0.0098 m<sup>3</sup>/s, Discharge vs Submergence  $\beta$

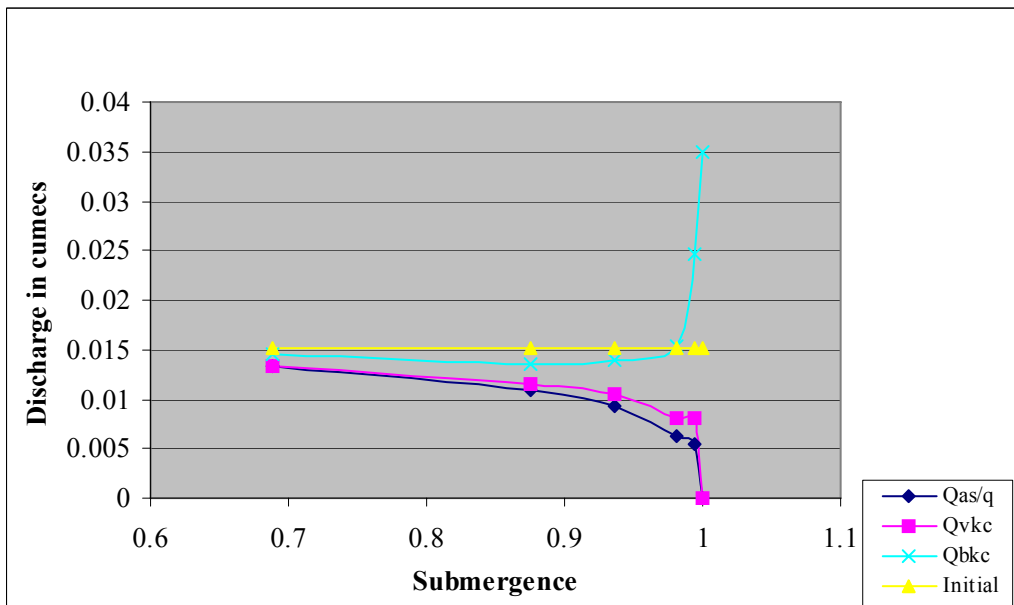


Figure 4.3-6 Model C8, Discharge 0.0151 m<sup>3</sup>/s, Discharge vs Submergence  $\beta$

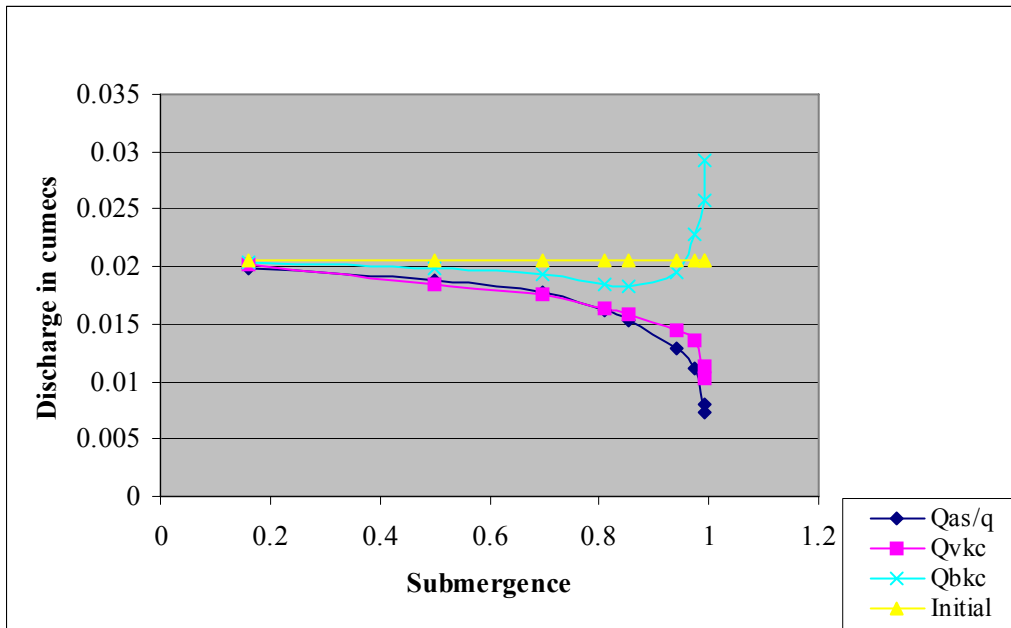


Figure 4.3-7 Model C8, Discharge 0.0206 m<sup>3</sup>/s, Discharge vs Submergence  $\beta$

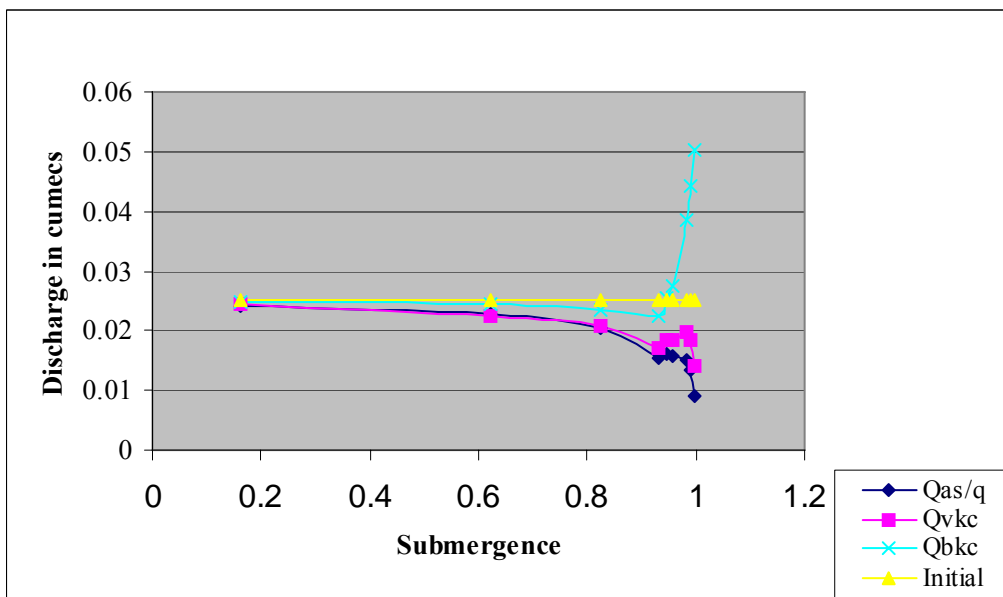


Figure 4.3-7 Model C8, Discharge 0.025 m<sup>3</sup>/s, Discharge vs Submergence  $\beta$

#### 4.4 Waikato Institute of Technology Study Results

The results of this study are shown in Tables 4.4 -1,-2,-3,-4, and-5. In contrast to the University of Canterbury study, the WINTEC measurements showed that the Villemonte correction applied to Kindsvater and Carter's modular flow equation gave a more accurate estimate for models W1, W3, W6 and the lower discharges (0.5 l/s– 3 l/s) of model W11. For the higher discharges of model W11 and model W17, Modified BVGJ gave a more accurate calculation. Figures 4.4-1,-2,-3,-4,-5, and -6 show typical plots of the calculations done for Models W1, W3, and W6. Figures 4.4-4 and -5 are plots for the lower and higher calculated discharges of model W11 while Figure 4.4 – 6 shows a typical plot for plot for model W17.

This contrast can be understood by referring to the actual heights of the weirs. Although the WINTEC models were run as half size models, the actual heights were:

Model	Height m
1	0.125
3	0.114
6	0.101
11	0.890
17	0.077

**Table 4.4 Actual Height WINTEC Weir Models**

The heights for model 11 and 17 are in the same range as the heights for the Canterbury models – C7 = 0.067m and C8 = 0.085m.

BS 3680 Part 4a quotes for Kindsvater and Carter's equation. a practical lower limit of weir height of 0.100 and an upper limit of  $H_u/P_u$  of 2.5. In general, models 1,3, and 6 come within these limits. Villemonte's paper does not quote the heights of the weirs used to develop his correction. However, his Figure 3 gives a range of  $(P_u/H_u)$  values along with the corresponding free flow head. If it is assumed that the highest values of  $(P_u/H_u)$  would correspond to  $H_u$  close to that specified for the

Model W1								
Gauge Discharge	(Hd/Hu)	Qmi	Q abs/q D'charge	Q abs/q % Error	Qvkc D'charge	Qvkc % Error	Qbkc D'charge	Qbkc % Error
0.5 l/s r	0.4379	0.0048	0.0052	7.8	0.0050	3.3	0.0053	10.0
	0.8543	0.0048	0.0047	1.2	0.0047	1.2	0.0055	13.7
	0.9893	0.0048	0.0022	53.6	0.0029	39.7	0.0067	39.0
0.5 l/s f	0.9893	0.0048	0.0022	53.6	0.0029	39.7	0.0067	39.0
	0.8680	0.0048	0.0046	4.1	0.0046	3.3	0.0054	12.6
	0.4337	0.0048	0.0053	9.6	0.0050	5.0	0.0054	11.8
1 l/s r	0.2288	0.0097	0.0103	6.9	0.0100	3.4	0.0102	5.8
	0.8041	0.0097	0.0107	10.3	0.0103	7.1	0.0116	19.9
	0.9471	0.0097	0.0081	16.3	0.0088	9.0	0.0123	26.8
	0.9818	0.0097	0.0065	33.2	0.0079	18.7	0.0151	56.0
1 l/s f	0.9818	0.0097	0.0065	33.2	0.0079	18.7	0.0151	56.0
	0.9423	0.0097	0.0085	11.8	0.0092	5.0	0.0125	29.5
	0.8238	0.0097	0.0102	5.8	0.0100	3.5	0.0113	16.9
	0.5618	0.0097	0.0108	11.7	0.0102	5.4	0.0110	14.2
	0.2434	0.0097	0.0102	5.5	0.0099	1.9	0.0101	4.6
2 l/s r	0.3205	0.0157	0.0164	4.4	0.0156	0.4	0.0163	3.8
	0.8051	0.0157	0.0154	1.9	0.0149	5.1	0.0167	6.3
	0.8902	0.0157	0.0152	3.4	0.0153	2.4	0.0183	16.8
	0.9457	0.0157	0.0138	12.0	0.0149	5.1	0.0206	31.4
2 l/s f	0.9457	0.0157	0.0138	12.0	0.0149	5.1	0.0206	31.4
	0.8831	0.0157	0.0157	0.1	0.0158	0.6	0.0187	19.2
	0.8226	0.0157	0.0147	6.1	0.0144	8.5	0.0162	3.3
	0.2520	0.0157	0.0162	2.9	0.0155	1.2	0.0159	1.6
3 l/s r	0.2302	0.0200	0.0209	4.3	0.0200	0.2	0.0205	2.5
	0.5493	0.0200	0.0207	3.4	0.0194	2.9	0.0210	5.0
	0.8539	0.0200	0.0197	1.6	0.0194	2.9	0.0223	11.7
	0.9194	0.0200	0.0183	8.4	0.0190	5.0	0.0240	20.2
3 l/s f	0.9194	0.0200	0.0183	8.4	0.0190	5.0	0.0240	20.2
	0.8416	0.0200	0.0205	2.7	0.0201	0.6	0.0230	14.8
	0.5740	0.0200	0.0207	3.6	0.0194	2.8	0.0211	5.4
	0.3085	0.0200	0.0207	3.4	0.0197	1.5	0.0205	2.5
	0.0234	0.0200	0.0197	1.6	0.0193	3.3	0.0191	4.6
4 l/s r	0.2681	0.0260	0.0270	3.9	0.0258	0.8	0.0266	2.3
	0.5330	0.0260	0.0266	2.5	0.0250	4.0	0.0269	3.6
	0.7455	0.0260	0.0247	5.1	0.0235	9.8	0.0259	0.4
	0.8411	0.0260	0.0236	9.2	0.0231	11.1	0.0264	1.3
	0.8657	0.0260	0.0264	1.4	0.0261	0.4	0.0304	16.8
4 l/s f	0.8657	0.0260	0.0264	1.4	0.0261	0.4	0.0304	16.8
	0.8271	0.0260	0.0246	5.2	0.0240	7.8	0.0271	4.3
	0.6947	0.0260	0.0256	1.5	0.0241	7.1	0.0265	1.8
	0.4872	0.0260	0.0267	2.7	0.0250	3.7	0.0269	3.4
	0.2336	0.0260	0.0265	1.8	0.0254	2.5	0.0260	0.1
5 l/s r	0.0884	0.0310	0.0310	0.0	0.0302	2.7	0.0300	3.1
	0.3330	0.0310	0.0317	2.1	0.0300	3.3	0.0313	1.1
	0.5589	0.0310	0.0313	0.8	0.0292	5.7	0.0317	2.1
	0.7914	0.0310	0.0308	0.5	0.0296	4.5	0.0330	6.4
	0.8637	0.0310	0.0301	3.0	0.0297	4.1	0.0345	11.2
5 l/s f	0.8637	0.0310	0.0301	3.0	0.0297	4.1	0.0345	11.2
	0.8007	0.0310	0.0301	2.9	0.0290	6.6	0.0324	4.5
	0.5662	0.0310	0.0305	1.8	0.0285	8.1	0.0309	0.4
	0.2503	0.0310	0.0317	2.3	0.0303	2.2	0.0312	0.5
	0.0177	0.0310	0.0307	0.9	0.0299	3.4	0.0295	4.7

Table 4.4-1 Comparison of Calculated Discharges For WINTEC Model W1

Model W3									
Gauge Discharge	(Hd/Hu)	Qmi	Q abs/q D'charge	Q abs/q % Error	Qvkc D'charge	Qvkc % Error	Qbkc D'charge	Qbkc % Error	
0.5 l/s r	0.6555	0.0045	0.0049	9.4	0.0047	4.6	0.0051	14.2	
	0.9409	0.0045	0.0038	16.3	0.0041	9.4	0.0055	22.9	
0.5 l/s f	0.9409	0.0045	0.0038	16.3	0.0041	9.4	0.0055	22.9	
	0.6607	0.0045	0.0050	11.3	0.0048	6.5	0.0052	16.3	
	0.0515	0.0045	0.0047	5.2	0.0047	5.1	0.0047	4.1	
1.0 l/s r	0.2048	0.0071	0.0077	7.9	0.0075	5.1	0.0076	7.0	
	0.5991	0.0071	0.0081	14.7	0.0077	8.7	0.0084	18.1	
	0.8828	0.0071	0.0072	1.3	0.0073	2.5	0.0086	21.3	
	0.9791	0.0071	0.0046	35.5	0.0055	22.6	0.0101	41.8	
1.0 l/s f	0.9791	0.0071	0.0046	35.5	0.0055	22.6	0.0101	41.8	
	0.8915	0.0071	0.0069	2.5	0.0070	0.7	0.0084	19.0	
	0.5763	0.0071	0.0083	16.9	0.0079	10.7	0.0085	20.0	
	0.1096	0.0071	0.0074	4.4	0.0073	2.8	0.0073	2.7	
2.0 l/s r	0.0632	0.0124	0.0129	4.3	0.0127	2.5	0.0126	1.7	
	0.4777	0.0124	0.0130	4.6	0.0122	1.2	0.0131	5.9	
	0.6978	0.0124	0.0133	7.0	0.0126	1.4	0.0138	11.2	
	0.8714	0.0124	0.0123	1.1	0.0123	1.2	0.0143	15.5	
	0.9424	0.0124	0.0112	10.1	0.0120	3.3	0.0164	31.9	
2.0 l/s f	0.9424	0.0124	0.0112	10.1	0.0120	3.3	0.0164	31.9	
	0.8870	0.0124	0.0116	6.8	0.0117	5.8	0.0139	12.1	
	0.4434	0.0124	0.0131	5.3	0.0124	0.4	0.0132	6.2	
	0.0646	0.0124	0.0125	0.9	0.0123	0.8	0.0122	1.6	
3.0 l/s r	0.1277	0.0172	0.0178	3.3	0.0173	0.6	0.0173	0.8	
	0.4211	0.0172	0.0185	7.5	0.0175	1.5	0.0186	7.9	
	0.5334	0.0172	0.0197	14.4	0.0185	7.4	0.0199	16.0	
	0.7370	0.0172	0.0195	13.2	0.0185	7.6	0.0204	18.6	
	0.8792	0.0172	0.0176	2.5	0.0177	2.6	0.0208	21.0	
	0.9407	0.0172	0.0157	8.6	0.0168	2.3	0.0228	32.4	
	0.9407	0.0172	0.0157	8.6	0.0168	2.3	0.0228	32.4	
	0.8723	0.0172	0.0181	5.4	0.0181	5.1	0.0212	23.0	
3.0 l/s f	0.7573	0.0172	0.0190	10.6	0.0182	5.5	0.0201	16.7	
	0.3794	0.0172	0.0183	6.7	0.0174	1.1	0.0183	6.6	
	0.0519	0.0172	0.0176	2.4	0.0173	0.5	0.0171	0.5	
4.0 l/s r	0.5036	0.0214	0.0240	12.2	0.0225	5.3	0.0242	13.2	
	0.7863	0.0214	0.0240	12.1	0.0230	7.5	0.0256	19.7	
	0.8919	0.0214	0.0217	1.2	0.0219	2.2	0.0262	22.5	
	0.9323	0.0214	0.0210	1.8	0.0221	3.5	0.0291	35.9	
4.0 l/s f	0.9323	0.0214	0.0210	1.8	0.0221	3.5	0.0291	35.9	
	0.8903	0.0214	0.0219	2.2	0.0220	3.0	0.0264	23.2	
	0.7886	0.0214	0.0243	13.5	0.0233	9.0	0.0260	21.4	
	0.5180	0.0214	0.0235	9.9	0.0221	3.1	0.0238	11.1	
	0.2442	0.0214	0.0232	8.6	0.0223	4.0	0.0228	6.8	
	0.0229	0.0214	0.0225	5.2	0.0221	3.2	0.0218	1.9	
5.0 l/s r	0.0836	0.0273	0.0283	3.8	0.0276	1.1	0.0275	0.6	
	0.2833	0.0273	0.0291	6.6	0.0277	1.6	0.0287	5.1	
	0.4863	0.0273	0.0297	8.9	0.0279	2.0	0.0299	9.5	
	0.6494	0.0273	0.0293	7.2	0.0275	0.6	0.0300	9.8	
	0.7857	0.0273	0.0279	2.3	0.0267	2.0	0.0298	9.1	
	0.8597	0.0273	0.0273	0.1	0.0270	1.2	0.0312	14.2	
	0.8597	0.0273	0.0273	0.1	0.0270	1.2	0.0312	14.2	
5.0 l/s f	0.6315	0.0273	0.0295	8.1	0.0277	1.3	0.0301	10.4	
	0.4698	0.0273	0.0295	8.2	0.0277	1.5	0.0297	8.6	
	0.2545	0.0273	0.0291	6.4	0.0278	1.7	0.0286	4.6	

Table 4.4-2 Comparison of Calculated Discharges For WINTEC Model W3

Model W6								
Gauge Discharge	Hd/Hu	Qmi	Q abs/q D'charge	Q abs/q % Error	Qvkc D'charge	Qvkc % Error	Qbkc D'charge	Qbkc % Error
0.5 l/s r	0.5847	0.0045	0.0049	8.8	0.0045	0.0	0.0049	8.5
	0.9204	0.0045	0.0039	13.1	0.0040	11.8	0.0050	11.9
0.5 l/s f	0.9234	0.0045	0.0039	13.4	0.0040	11.8	0.0051	12.7
	0.5987	0.0045	0.0049	8.0	0.0045	0.7	0.0049	7.9
1 l/s r	0.6347	0.0070	0.0079	12.3	0.0072	2.7	0.0078	12.0
	0.9170	0.0070	0.0062	11.5	0.0062	11.0	0.0078	11.9
1 l/s f	0.9821	0.0070	0.0044	37.6	0.0051	26.6	0.0099	41.8
	0.9821	0.0070	0.0044	37.6	0.0051	26.6	0.0099	41.8
	0.8975	0.0070	0.0068	2.4	0.0067	3.7	0.0082	16.5
	0.6575	0.0070	0.0077	9.7	0.0070	0.5	0.0077	9.7
	0.2560	0.0070	0.0076	7.9	0.0071	0.7	0.0073	3.6
2 l/s r	0.1977	0.0121	0.0131	8.4	0.0122	1.2	0.0124	2.8
	0.5607	0.0121	0.0132	8.8	0.0120	1.2	0.0129	6.9
	0.8914	0.0121	0.0121	0.4	0.0119	2.0	0.0142	17.4
	0.9591	0.0121	0.0101	16.7	0.0108	10.7	0.0161	33.2
2 l/s f	0.9591	0.0121	0.0101	16.7	0.0108	10.7	0.0161	33.2
	0.8995	0.0121	0.0118	2.2	0.0116	3.9	0.0141	16.7
	0.7582	0.0121	0.0132	8.7	0.0121	0.2	0.0134	10.9
	0.5420	0.0121	0.0133	9.7	0.0120	0.4	0.0130	7.6
	0.2083	0.0121	0.0132	8.9	0.0123	1.5	0.0125	3.4
3 l/s r	0.0345	0.0162	0.0178	9.7	0.0168	3.9	0.0166	2.7
	0.3669	0.0162	0.0183	13.2	0.0168	3.5	0.0176	8.9
	0.6192	0.0162	0.0181	11.7	0.0164	1.1	0.0178	10.1
	0.7641	0.0162	0.0183	12.9	0.0168	4.0	0.0187	15.1
	0.8841	0.0162	0.0167	2.9	0.0161	0.4	0.0191	18.2
	0.9347	0.0162	0.0160	1.3	0.0163	0.7	0.0216	33.3
3 l/s f	0.9674	0.0162	0.0141	12.7	0.0155	4.5	0.0247	52.2
	0.9674	0.0162	0.0141	12.7	0.0155	4.5	0.0247	52.2
	0.9335	0.0162	0.0163	0.9	0.0166	2.7	0.0219	35.4
	0.8788	0.0162	0.0172	6.3	0.0166	2.5	0.0196	20.8
	0.7650	0.0162	0.0182	12.5	0.0168	3.6	0.0186	14.8
	0.5892	0.0162	0.0180	11.0	0.0163	0.4	0.0177	9.0
0.2714	0.0162	0.0185	14.1	0.0171	5.2	0.0176	8.6	
4 l/s r	0.1210	0.0210	0.0229	9.2	0.0215	2.2	0.0215	2.4
	0.3962	0.0210	0.0232	10.6	0.0211	0.6	0.0223	6.4
	0.6217	0.0210	0.0230	9.4	0.0208	1.1	0.0226	7.7
	0.7768	0.0210	0.0220	4.6	0.0203	3.5	0.0225	7.2
	0.8462	0.0210	0.0228	8.3	0.0215	2.4	0.0246	17.1
	0.9142	0.0210	0.0212	1.0	0.0211	0.3	0.0263	25.3
	0.9449	0.0210	0.0208	1.0	0.0215	2.4	0.0297	41.2
4 l/s f	0.9449	0.0210	0.0208	1.0	0.0215	2.4	0.0297	41.2
	0.9214	0.0210	0.0206	1.9	0.0206	1.8	0.0262	24.8
	0.8645	0.0210	0.0219	4.2	0.0209	0.5	0.0242	15.5
	0.7728	0.0210	0.0223	6.3	0.0206	2.1	0.0228	8.7
	0.6705	0.0210	0.0226	7.5	0.0205	2.5	0.0224	6.7
	0.4708	0.0210	0.0231	10.0	0.0209	0.4	0.0224	6.6
0.1733	0.0210	0.0230	9.4	0.0214	1.8	0.0216	3.0	
5 l/s r	0.2331	0.0270	0.0285	5.5	0.0263	2.6	0.0269	0.3
	0.4730	0.0270	0.0289	6.9	0.0261	3.4	0.0279	3.4
	0.7278	0.0270	0.0265	1.9	0.0241	10.6	0.0266	1.6
	0.8226	0.0270	0.0258	4.3	0.0241	10.6	0.0272	0.9
	0.8691	0.0270	0.0267	1.1	0.0255	5.5	0.0298	10.2
5 l/s f	0.9207	0.0270	0.0251	6.9	0.0251	7.0	0.0319	18.0
	0.9207	0.0270	0.0251	6.9	0.0251	7.0	0.0319	18.0
	0.8792	0.0270	0.0256	5.2	0.0246	8.8	0.0290	7.5
	0.8413	0.0270	0.0246	9.0	0.0231	14.3	0.0264	2.3
	0.7421	0.0270	0.0257	5.0	0.0235	13.1	0.0259	4.2
	0.5949	0.0270	0.0271	0.4	0.0244	9.5	0.0266	1.6
	0.3045	0.0270	0.0285	5.4	0.0261	3.5	0.0271	0.3

Table 4.4-3 Comparison of Calculated Discharges For WINTEC Model W6

Model W11								
Gauge Discharge	(Hd/Hu)	Qmi	Q abs/q D'charge	Q abs/q % Error	Qvkc D'charge	Qvkc % Error	Qbkc D'charge	Qbkc % Error
0.5 l/s r	0.2034	0.0048	0.0053	11.0	0.00522	8.7	0.00531	10.6
	0.7721	0.0048	0.0047	2.3	0.0046	5.1	0.0051	5.3
	0.9735	0.0048	0.0029	39.8	0.0034	29.2	0.0058	20.4
	1.0121	0.0048		100.0		100.0	0.0083	72.5
0.5 l/s f	0.9780	0.0048	0.0027	43.4	0.0033	32.1	0.0059	22.4
	0.7793	0.0048	0.0048	0.7	0.0046	3.3	0.0052	7.4
	0.2587	0.0048	0.0050	4.6	0.0049	1.9	0.0050	4.9
1 l/s r	0.4823	0.0075	0.0076	1.7	0.0072	3.4	0.0078	3.6
	0.7988	0.0075	0.0073	2.9	0.0071	5.5	0.0079	5.6
	0.9551	0.0075	0.0054	27.4	0.0060	19.6	0.0088	16.9
	0.9962	0.0075	0.0023	68.9	0.0034	54.8	0.0114	52.2
1 l/s f	0.9962	0.0075	0.0023	68.9	0.0034	54.8	0.0114	52.2
	0.9554	0.0075	0.0055	26.8	0.0061	18.8	0.0089	18.3
	0.8165	0.0075	0.0071	5.7	0.0069	7.8	0.0078	3.8
	0.4822	0.0075	0.0076	0.9	0.0072	4.1	0.0077	2.8
2 l/s r	0.1954	0.0131	0.0131	0.3	0.0127	2.9	0.0129	1.3
	0.5689	0.0131	0.0128	2.0	0.0121	7.7	0.0131	0.0
	0.9098	0.0131	0.0113	14.0	0.0116	11.4	0.0144	9.6
	0.9653	0.0131	0.0095	27.8	0.0107	18.3	0.0168	27.9
2 l/s f	0.9864	0.0131	0.0076	41.9	0.0095	27.3	0.0202	54.2
	0.9864	0.0131	0.0076	41.9	0.0095	27.3	0.0202	54.2
	0.9646	0.0131	0.0097	26.0	0.0109	16.5	0.0170	29.9
	0.9141	0.0131	0.0111	15.1	0.0115	12.2	0.0144	9.7
3 l/s r	0.6028	0.0131	0.0125	4.4	0.0118	9.9	0.0128	2.1
	0.2038	0.0131	0.0129	1.9	0.0124	5.1	0.0127	3.4
	0.3664	0.0168	0.0182	8.3	0.0172	2.7	0.0181	8.0
	0.6391	0.0168	0.0176	4.6	0.0165	1.6	0.0180	7.3
3 l/s f	0.8853	0.0168	0.0167	0.7	0.0168	0.1	0.0199	18.6
	0.9435	0.0168	0.0151	10.0	0.0162	3.4	0.0222	32.4
	0.9759	0.0168	0.0123	26.9	0.0144	14.2	0.0252	50.2
	0.9759	0.0168	0.0123	26.9	0.0144	14.2	0.0252	50.2
4 l/s r	0.9483	0.0168	0.0146	13.1	0.0158	5.9	0.0222	31.9
	0.8822	0.0168	0.0172	2.1	0.0172	2.4	0.0204	21.2
	0.6694	0.0168	0.0170	1.2	0.0160	4.6	0.0175	4.4
	0.3858	0.0168	0.0178	6.2	0.0169	0.6	0.0178	6.2
4 l/s f	0.2091	0.0225	0.0227	1.1	0.0219	2.9	0.0223	1.0
	0.4627	0.0225	0.0229	2.0	0.0216	4.2	0.0230	2.4
	0.6898	0.0225	0.0219	2.5	0.0207	8.1	0.0227	0.7
	0.8987	0.0225	0.0196	13.0	0.0199	11.7	0.0241	7.1
5 l/s r	0.9385	0.0225	0.0191	15.0	0.0203	9.7	0.0273	21.2
	0.9385	0.0225	0.0191	15.0	0.0203	9.7	0.0273	21.2
	0.8948	0.0225	0.0201	10.5	0.0204	9.5	0.0245	9.0
	0.6973	0.0225	0.0215	4.3	0.0203	9.7	0.0223	1.0
5 l/s f	0.4720	0.0225	0.0226	0.4	0.0212	5.7	0.0227	1.0
	0.1962	0.0225	0.0227	0.8	0.0218	2.9	0.0222	1.3
	0.3545	0.0296	0.0285	3.6	0.0270	8.9	0.0283	4.4
	0.5652	0.0296	0.0282	4.7	0.0264	10.9	0.0286	3.5
5 l/s f	0.7736	0.0296	0.0251	15.1	0.0240	18.9	0.0266	10.0
	0.9355	0.0296	0.0240	19.1	0.0253	14.5	0.0336	13.5
	0.9355	0.0290	0.0240	17.4	0.0253	12.8	0.0336	15.8
	0.7874	0.0290	0.0245	15.6	0.0235	19.1	0.0261	9.9
	0.5669	0.0290	0.0285	1.9	0.0266	8.3	0.0288	0.6
	0.3501	0.0290	0.0283	2.5	0.0267	7.8	0.0280	3.3

Table 4.4-4 Comparison of Calculated Discharges For WINTEC Model W11

Model W17								
Gauge Discharge	(Hd/Hu)	Qmi	Q abs/q D'charge	Q abs/q % Error	Qvkc D'charge	Qvkc % Error	Qbkc D'charge	Qbkc % Error
0.5 l/s r	0.6154	0.0047	0.0048	2.1	0.0046	2.1	0.0050	6.5
	0.9481	0.0047	0.0032	31.8	0.0035	24.8	0.0049	5.3
	1.0084	0.0047					0.0071	51.2
	1.0210	0.0047					0.0102	117.3
0.5 l/s f	1.0210	0.0047					0.0102	117.3
	1.0134	0.0047					0.0071	51.0
	0.9395	0.0047	0.0035	25.0	0.0038	18.6	0.0052	9.8
	0.6442	0.0047	0.0047	0.7	0.0045	4.7	0.0049	4.0
1 l/s r	0.1717	0.0073	0.0075	3.1	0.0074	1.2	0.0075	2.3
	0.6723	0.0073	0.0070	4.4	0.0067	8.6	0.0073	0.0
	0.9112	0.0073	0.0059	19.7	0.0061	16.3	0.0076	3.9
	0.9883	0.0073	0.0033	54.8	0.0042	41.9	0.0095	30.0
1 l/s f	1.0106	0.0073					0.0126	72.6
	1.0106	0.0073					0.0126	72.6
	0.9840	0.0073	0.0039	46.9	0.0048	34.1	0.0096	32.1
	0.9089	0.0073	0.0059	19.2	0.0061	16.0	0.0076	3.7
2 l/s r	0.6715	0.0073	0.0070	4.7	0.0067	8.9	0.0073	0.3
	0.1662	0.0073	0.0072	2.0	0.0070	3.7	0.0071	2.7
	0.4027	0.0125	0.0124	1.1	0.0118	5.8	0.0125	0.2
	0.6545	0.0125	0.0120	4.3	0.0114	9.2	0.0124	0.8
2 l/s f	0.8336	0.0125	0.0115	8.4	0.0113	9.8	0.0128	2.4
	0.9450	0.0125	0.0094	25.0	0.0102	18.7	0.0140	12.2
	0.9784	0.0125	0.0079	37.0	0.0094	24.7	0.0171	36.6
	0.9982	0.0125	0.0029	76.7	0.0046	63.1	0.0207	65.9
3 l/s r	0.9982	0.0125	0.0029	76.7	0.0046	63.1	0.0207	65.9
	0.9786	0.0125	0.0080	36.2	0.0095	23.7	0.0174	38.9
	0.9453	0.0125	0.0094	24.5	0.0102	18.1	0.0141	13.2
	0.8474	0.0125	0.0111	11.4	0.0110	12.2	0.0126	0.5
3 l/s f	0.6544	0.0125	0.0119	5.1	0.0113	9.9	0.0123	1.6
	0.3053	0.0125	0.0123	1.7	0.0118	5.5	0.0123	1.7
	0.2105	0.0178	0.0174	2.3	0.0168	5.5	0.0171	3.7
	0.4993	0.0178	0.0173	2.9	0.0163	8.4	0.0175	1.5
4 l/s r	0.7628	0.0178	0.0156	12.4	0.0150	15.9	0.0166	6.9
	0.8814	0.0178	0.0146	18.0	0.0147	17.3	0.0174	2.3
	0.9330	0.0178	0.0143	19.7	0.0152	14.8	0.0200	12.1
	0.9696	0.0178	0.0123	31.0	0.0141	20.7	0.0230	29.1
4 l/s f	0.9831	0.0178	0.0113	36.3	0.0139	22.1	0.0273	53.4
	0.9831	0.0178	0.0113	36.3	0.0139	22.1	0.0273	53.4
	0.9706	0.0178	0.0122	31.5	0.0141	21.0	0.0231	29.8
	0.9411	0.0178	0.0135	24.3	0.0145	18.6	0.0196	10.4
5 l/s r	0.8763	0.0178	0.0150	15.6	0.0151	15.2	0.0177	0.4
	0.7416	0.0178	0.0162	9.0	0.0155	13.1	0.0171	4.1
	0.5045	0.0178	0.0173	2.5	0.0164	8.0	0.0176	1.1
	0.1805	0.0178	0.0174	2.1	0.0169	5.0	0.0171	3.7
5 l/s f	0.4330	0.0231	0.0225	2.6	0.0213	8.0	0.0226	2.1
	0.6687	0.0231	0.0213	7.6	0.0202	12.7	0.0220	4.6
	0.7863	0.0231	0.0220	4.9	0.0211	8.8	0.0233	1.1
	0.9125	0.0231	0.0176	23.8	0.0182	21.3	0.0226	2.0
6 l/s r	0.9440	0.0231	0.0177	23.6	0.0190	17.7	0.0261	13.1
	0.9665	0.0231	0.0167	27.7	0.0189	18.0	0.0300	29.7
	0.9665	0.0231	0.0167	27.7	0.0189	18.0	0.0300	29.7
	0.9492	0.0231	0.0169	26.6	0.0184	20.2	0.0260	12.3
6 l/s f	0.9138	0.0231	0.0176	23.7	0.0182	21.1	0.0227	1.5
	0.6783	0.0231	0.0211	8.6	0.0200	13.6	0.0218	5.5
	0.4359	0.0231	0.0222	3.8	0.0210	9.1	0.0224	3.2
	0.4297	0.0291	0.0274	5.8	0.0259	11.1	0.0275	5.4
7 l/s r	0.6288	0.0291	0.0274	5.9	0.0258	11.5	0.0281	3.6
	0.8141	0.0291	0.0237	18.6	0.0230	21.0	0.0258	11.2
	0.8976	0.0291	0.0218	25.2	0.0221	23.9	0.0268	8.0
	0.9171	0.0291	0.0238	18.3	0.0246	15.4	0.0310	6.4
7 l/s f	0.9451	0.0291	0.0233	19.8	0.0251	13.7	0.0347	19.2
	0.9451	0.0291	0.0233	19.8	0.0251	13.7	0.0347	19.2
	0.9177	0.0291	0.0240	17.6	0.0249	14.6	0.0313	7.6
	0.8094	0.0291	0.0240	17.6	0.0232	20.2	0.0261	10.4
8 l/s r	0.6261	0.0291	0.0279	4.1	0.0262	9.9	0.0286	1.9
	0.4297	0.0291	0.0274	5.8	0.0259	11.1	0.0275	5.4

Table 4.4-5 Comparison of Calculated Discharges For WINTEC Model W17

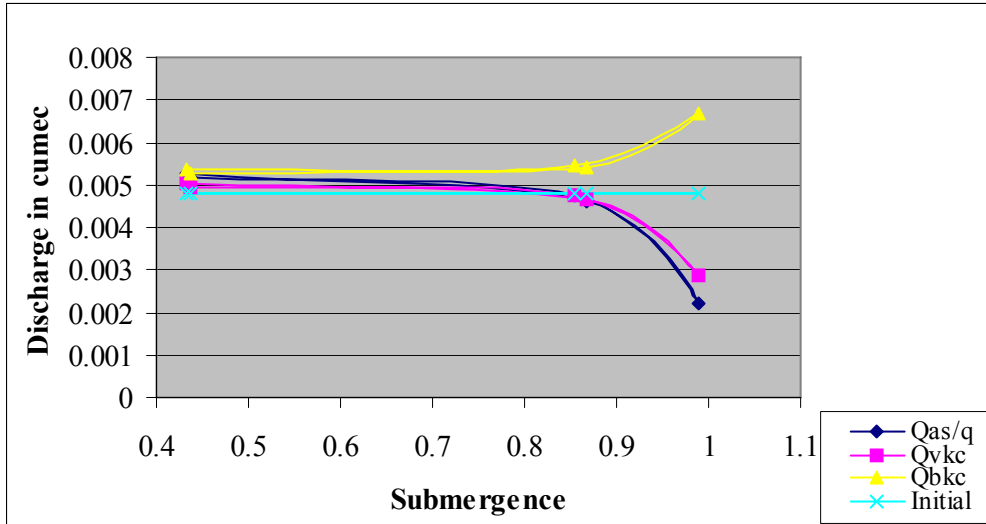


Figure 4.4-1 Model W1, Discharge 0.0048 m<sup>3</sup>/s, Discharge vs Submergence  $\beta$

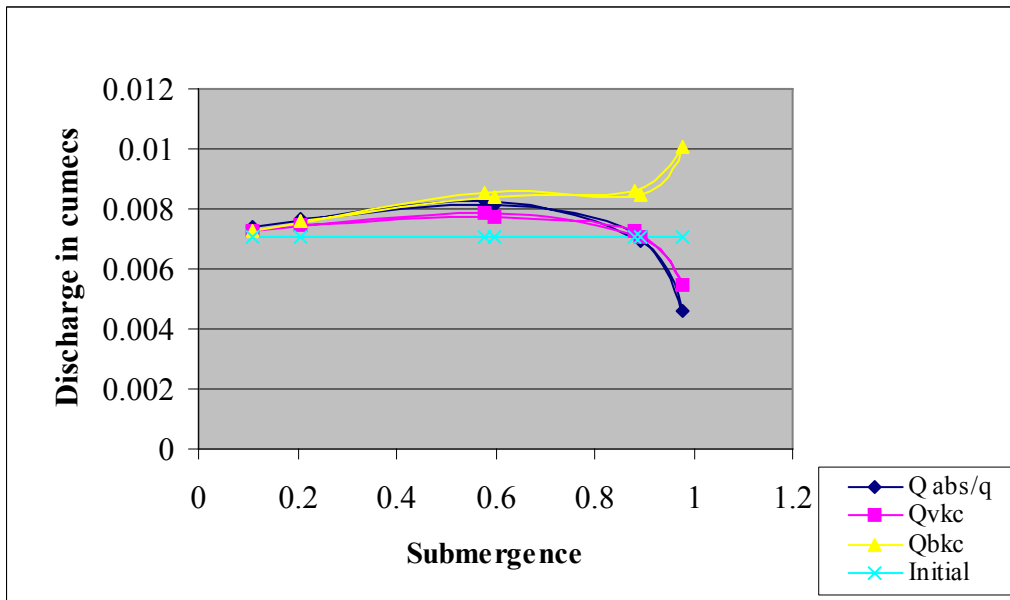
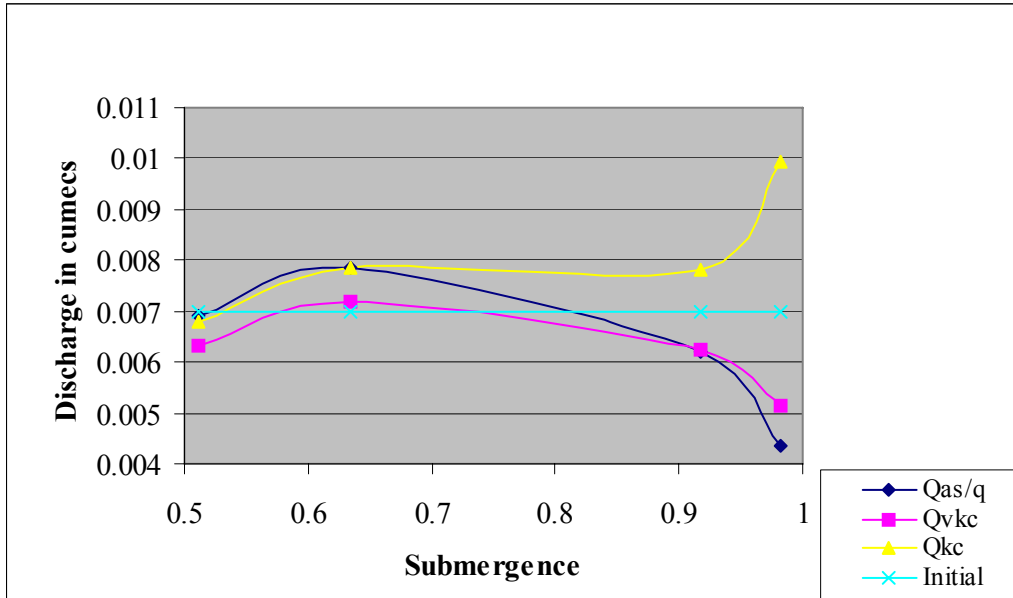
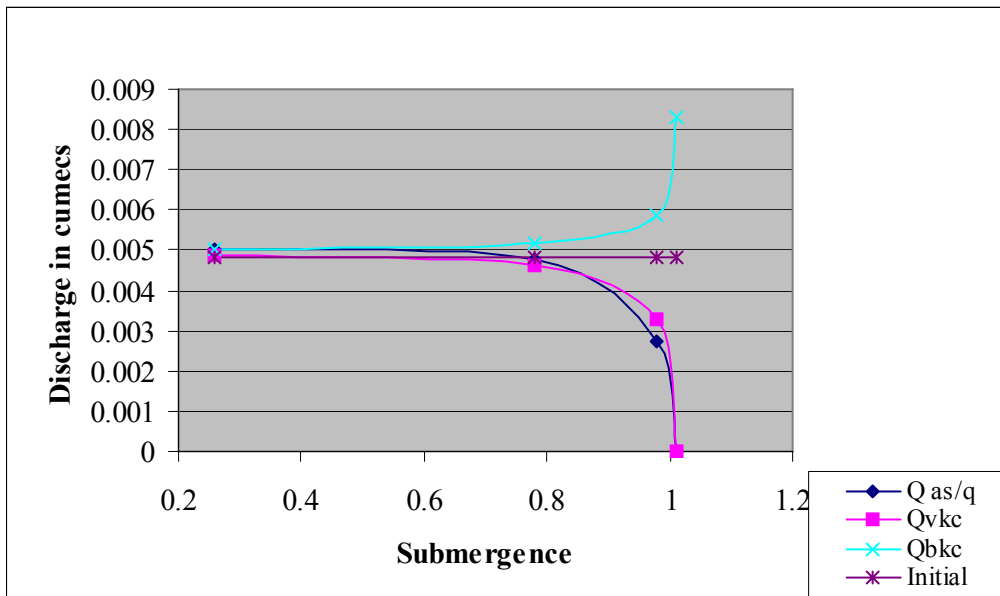


Figure 4.4-2 Model W3, Discharge 0.0071 m<sup>3</sup>/s, Discharge vs Submergence  $\beta$



**Figure 4.4-3 Model W6 (Falling Branch), Discharge 0.0071 m<sup>3</sup>/s,  
Discharge vs Submergence  $\beta$**



**Figure 4.4-4 Model W11 (Falling Branch), Discharge 0.0048 m<sup>3</sup>/s,  
Discharge vs Submergence  $\beta$**

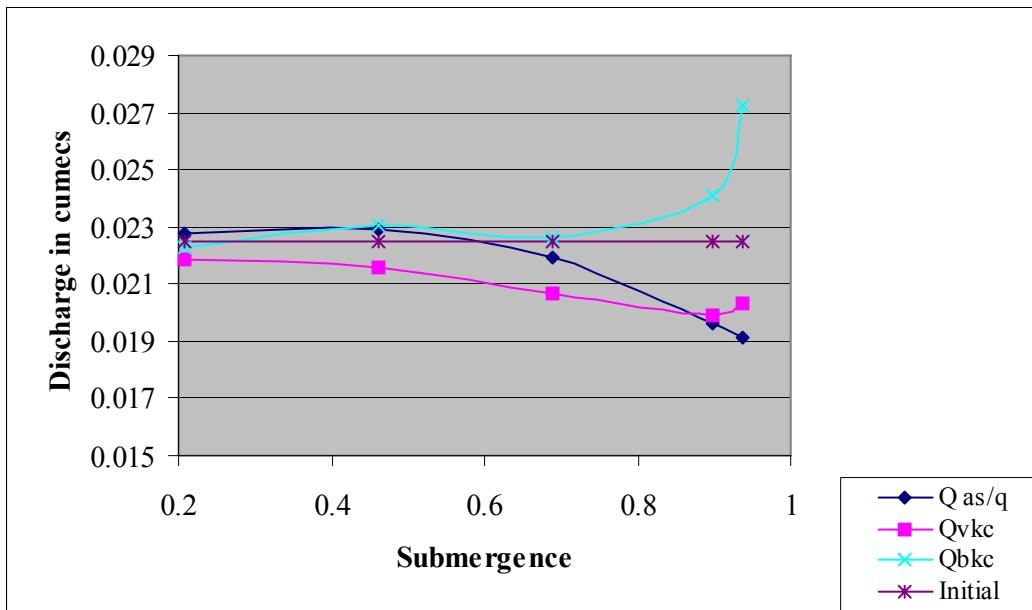


Figure 4.4-5 Model W11 (Rising Branch), Discharge 0.0225 m<sup>3</sup>/s,  
Discharge vs Submergence  $\beta$

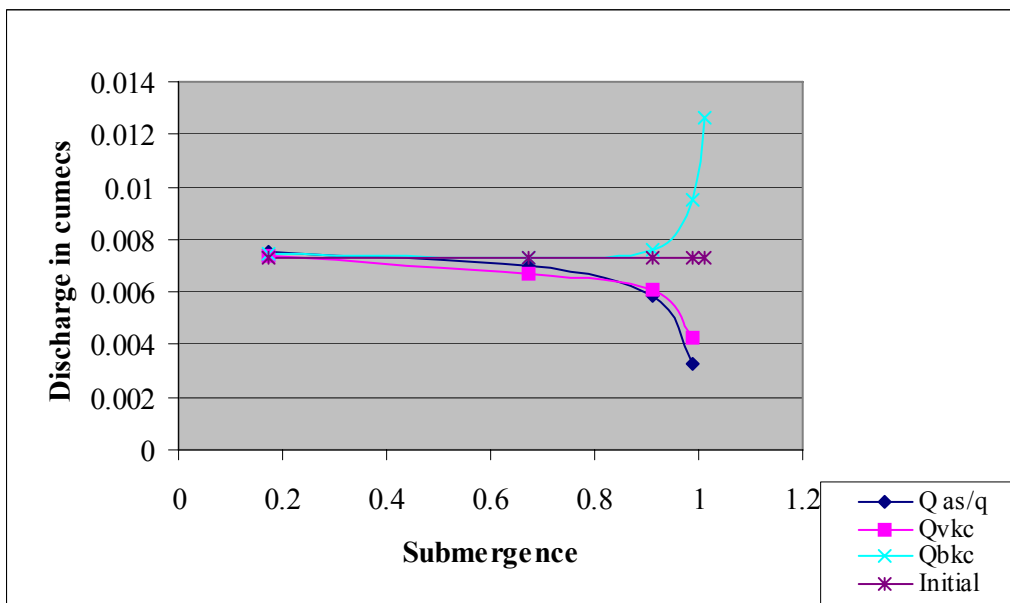


Figure 4.4-6 Model W17 (Rising Branch) Discharge 0.0073 m<sup>3</sup>/s,  
Discharge vs Submergence

free flow head, it is possible to estimate the height of the test weir. The four calculations lead to values ranging from 0.566 m to 0.596 m. As the study was done in a flume 0.914 m deep and readings were taken up to 95% submergence ( $\beta = 0.95$ ), the weir height was probably less than that calculated. As this work was done in Imperial units (a.k.a. American Customary) it is likely that the weir was designed in terms of feet, suggesting the height to have been about 0.300 m or 0.450 m as these correspond to 12 or 18 inches.

#### **4.5 Choice of Discharge Equation**

The comparison has indicated that the Modified BVGJ equation gives the better estimate of discharge for small weirs i.e. of height less than 100 mm. This is of interest as the formula was originally developed using weirs varying in upstream height from 406 to 511 mm. It also suggests that a submerged thin plate weir can be used to measure discharge in open channels where freeboard is limited and a small weir desirable.

For the comparison described in Section 5.4 Modified BVGJ is used for all weirs less than 0.1 m high and the Villemonte correction applied to Kindsvater and Carter is used for weirs greater than 0.1 m high.

## Chapter 5 Effects of Unequal Beds

### 5.1 Choice of Models

To investigate the possible effect of unequal beds it was decided to compare the extreme cases. For the Canterbury data this meant comparing model C1 with models C7 and for the WINTEC data models 17 and 23, and 11 and 16.

It was not always possible to get exactly the same discharge in each set of model runs, so comparisons were made based on which pairs had the closest discharges. This is particularly important for the WINTEC data where the discharge control valve had to be set by hand. The chosen comparisons are shown in Table 5.1

<b>Nominal Discharge</b> l/s	<b>Scaled Discharge(s)</b> m <sup>3</sup> /s	<b>Models</b>
0.5	0.0048	11, 16
	0.0044	17,23
1	0.0075/4	11, 16
2	0.0125/6	17, 23
3	0.0178	17, 23
4	0.0231/4	17, 23
5	0.029	11, 16

**Table 5.1 Choice of WINTEC Models**

## **5.2 Shape of $H_u$ vs $H_d$ Plot**

### **5.2.1 University of Canterbury Study Data**

The data for each of the four discharges are shown in Tables 5.2.1,-1,-2,-3, and- 4 and are plotted on Figures 5.2.1 -1, -2, and -3 for models C1 and C7 and discharges 10, 15 and 20 l/s. These show that the unequal bed does have a  $H_u$  vs  $H_d$  plot with a steeper initial section and the equal-unequal intersection can be seen. These data were plotted as line only as data points obscured the differences. The difference is clearest with the lowest flow. This is to be expected as high discharges can be expected to swamp the effect of the differing bed levels.

While model C7 had a discharge of 25 l/s calculations showed that the discharge for C1 was only 24 l/s. This is thought to have been due to a slipping valve. The difference is sufficient that a meaningful comparison cannot be made. However the plots are included as Figure 5.2.1-4 as they demonstrate the steeper initial rise of plot of the unequal bed weir.

### **5.2.2 Waikato Institute of Technology Study Data**

The WINTEC data are shown on Tables 5.2.2-1,-2,-3,-4,-5, and -6 and plotted on Figures 5.2.2-1 to -13. In general the expected pattern appears, although it is not obvious where the nominal discharge is 4 l/s. Here the difference in discharges is only 1.3% but this is sufficient to ensure that the equal/unequal intersection is not reached.

C1		C7	
H <sub>d</sub>	H <sub>u</sub>	H <sub>d</sub>	H <sub>u</sub>
-0.1868	0.0399	-0.0780	0.0398
-0.1384	0.0400	-0.0194	0.0412
-0.1142	0.0399	0.0056	0.0412
-0.0966	0.0404	0.0262	0.0424
-0.0908	0.0404	0.0440	0.0494
-0.0786	0.0400	0.0576	0.0594
-0.0662	0.0400	0.0684	0.0678
-0.0612	0.0400	0.0788	0.0772
-0.0002	0.0424	0.0884	0.0866
0.0420	0.0534	0.1148	0.1116
0.0666	0.0676	0.1396	0.1378
0.0776	0.0766	0.1612	0.1586
0.0872	0.0864	0.1792	0.1770
0.0960	0.0942	0.1954	0.1934
0.1076	0.1044	0.2112	0.2102
0.1142	0.1114		
0.1272	0.1250		
0.1364	0.1328		

**Table 5.2.1-1 Comparison Shapes with Discharge 10 l/s**

C1		C7	
H <sub>d</sub>	H <sub>u</sub>	H <sub>d</sub>	H <sub>u</sub>
-0.1824	0.0534	-0.0408	0.0528
-0.1510	0.0524	-0.0274	0.0524
-0.1408	0.0522	0.0138	0.0528
-0.1030	0.0526	0.0362	0.0564
-0.0348	0.0528	0.0522	0.0626
-0.0058	0.0524	0.0642	0.0690
0.0084	0.0524	0.0770	0.0788
0.0130	0.0532	0.0916	0.0906
0.0316	0.0572	0.1102	0.1092
0.0494	0.0630	0.1284	0.1268
0.0648	0.0714	0.1460	0.1460
0.0776	0.0820	0.1602	0.1580
0.0824	0.0846	0.1708	0.1680
0.0925	0.0926	0.1868	0.1824
0.0966	0.0962	0.1991	0.1952
0.1002	0.0994	0.2034	0.2000
0.1252	0.1242		
0.1452	0.1412		

**Table 5.2.1-2 Comparison Shapes with Discharge 15 l/s**

C1		C7	
H <sub>d</sub>	H <sub>u</sub>	H <sub>d</sub>	H <sub>u</sub>
-0.2768	0.0630	-0.0334	0.0640
-0.0780	0.0630	-0.0344	0.0640
-0.0734	0.0630	-0.0102	0.0638
-0.0558	0.0630	0.0058	0.0634
-0.0388	0.0628	0.0384	0.0664
-0.0224	0.0628	0.0498	0.0700
0.0024	0.0636	0.0660	0.0766
0.0201	0.0656	0.0730	0.0802
0.0272	0.0664	0.0972	0.0992
0.0562	0.0750	0.1170	0.1166
0.0682	0.0800	0.1282	0.1268
0.0730	0.0840	0.1364	0.1342
0.0914	0.0968	0.1550	0.1554
0.1166	0.1170	0.1786	0.1768
0.1272	0.1250	0.1960	0.1936
0.1420	0.1408	0.2110	0.2086
0.1546	0.1528		
0.1644	0.1619		
0.1764	0.1759		
0.2012	0.1992		

**Table 5.2.1-3 Comparison Shapes with Discharge 20 l/s**

C1		C7	
H <sub>d</sub>	H <sub>u</sub>	H <sub>d</sub>	H <sub>u</sub>
-0.3732	0.0722	-0.0256	0.0766
-0.0464	0.0722	-0.0256	0.0752
-0.0182	0.0724	0.0054	0.0736
0.0142	0.0722	0.0468	0.0770
0.0280	0.0762	0.0716	0.0850
0.0344	0.0760	0.0822	0.0906
0.0472	0.0810	0.0982	0.1032
0.0642	0.0850	0.1106	0.1122
0.0702	0.0872	0.1296	0.1296
0.0848	0.0960	0.1506	0.1500
0.0988	0.1056	0.1664	0.1652
0.1122	0.1152	0.1788	0.1770
0.1252	0.1244	0.1884	0.1866
0.1444	0.1446	0.1978	0.1960
0.1704	0.1699	0.2050	0.2018
0.1966	0.1946		

**Table 5.2.1-4 Comparison Shapes with Discharge 25 l/s**

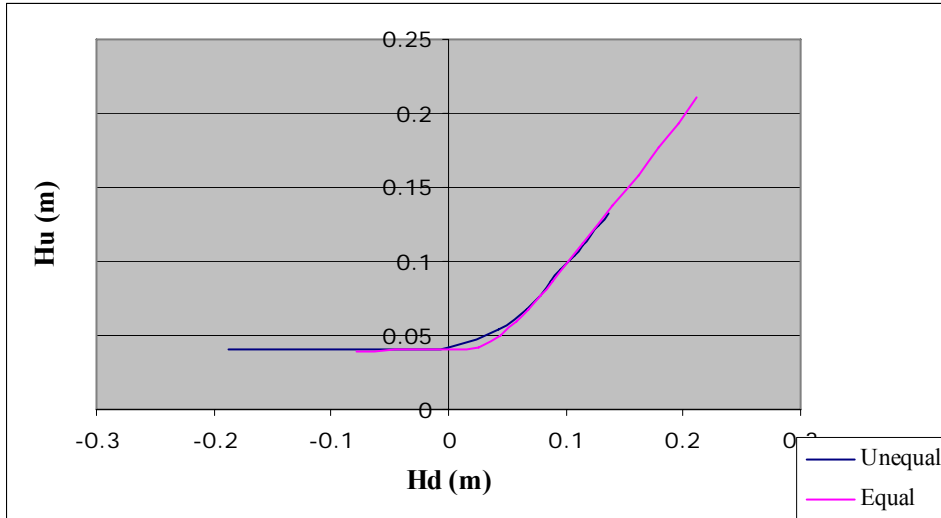


**Figure 5.2.1-1 Canterbury: Comparison Shapes with Discharge 10 l/s**

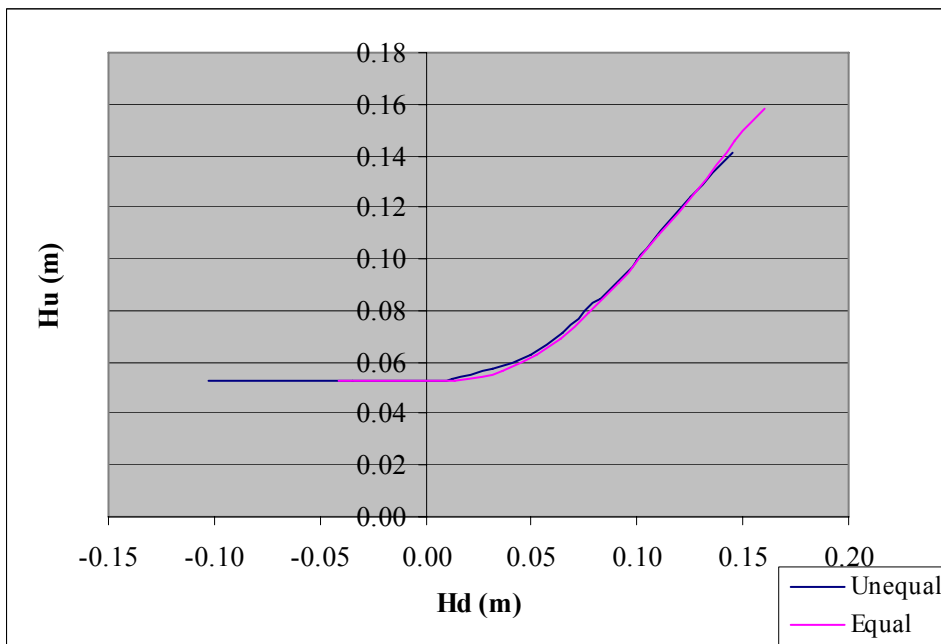


**Figure 5.2.1-2 Canterbury Comparison Shapes with Discharge 15 l/s**

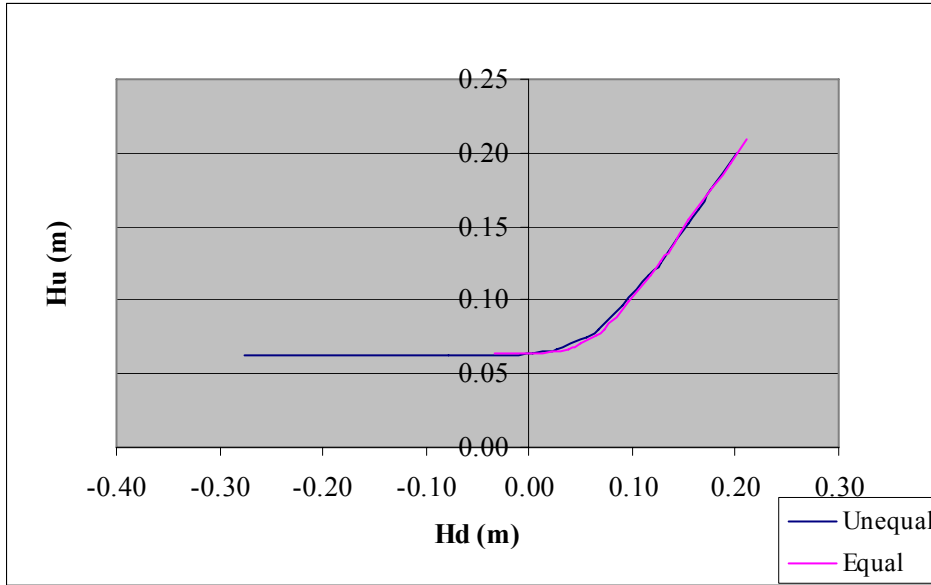


**Table 5.2.1-3 Canterbury Comparison Shapes with Discharge 20 l/s**

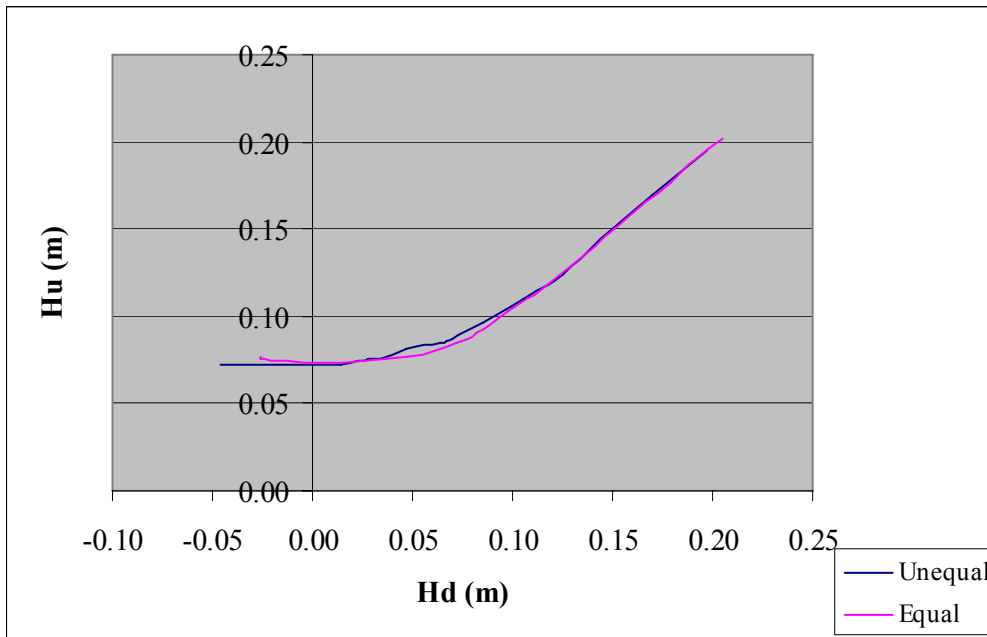


**Figure 5.2.1-4 Canterbury: Comparison Shapes with Discharge 25 l/s**

0.5 l/s (0.0048, 0.0047)				0.5 l/s (0.0047, 0.0048)			
W11		W16		W17		W23	
H <sub>d</sub> (m)	H <sub>u</sub> (m)	H <sub>d</sub> (m)	H <sub>u</sub> (m)	H <sub>d</sub> (m)	H <sub>u</sub> (m)	H <sub>d</sub> (m)	H <sub>u</sub> (m)
-0.1488	0.0546	-0.2820	0.0538	-0.1234	0.0534	-0.2854	0.0544
-0.1488	0.0548	-0.2820	0.0538	-0.1224	0.0462	-0.2854	0.0544
-0.1482	0.0546	-0.1836	0.0540	-0.1218	0.0462	-0.1746	0.0550
-0.1482	0.0546	-0.1310	0.0548	-0.1214	0.0540	-0.1206	0.0556
-0.0828	0.0548	-0.0810	0.0556	-0.0506	0.0550	-0.0732	0.0556
-0.0322	0.0570	-0.0338	0.0562	-0.0036	0.0566	-0.0264	0.0570
0.0120	0.0590	0.0110	0.0580	0.0384	0.0624	0.0178	0.0584
0.0542	0.0702	0.0258	0.0614	0.0804	0.0848	0.0580	0.0744
0.0956	0.0982	0.0704	0.0806	0.1194	0.1184	0.1012	0.1040
0.1340	0.1324	0.1108	0.1120	0.1556	0.1524	0.1324	0.1314
		0.1488	0.1464				
0.1340	0.1324			0.1556	0.1524	0.1324	0.1314
0.0978	0.1000	0.1488	0.1464	0.1210	0.1194	0.0966	0.1006
0.0558	0.0716	0.1138	0.1146	0.0808	0.0860	0.0524	0.0712
0.0148	0.0572	0.0716	0.0820	0.0402	0.0624	0.0126	0.0564
-0.0318	0.0548	0.0274	0.0610	-0.0048	0.0530	-0.0356	0.0542
-0.0808	0.0548	-0.0166	0.0524	-0.0524	0.0532	-0.0816	0.0534
-0.1476	0.0548	-0.0614	0.0530	-0.1234	0.0528	-0.1774	0.0534
-0.1482	0.0548			-0.1234	0.0526	-0.2834	0.0540
						-0.1630	0.0526
						-0.2824	0.0530
						-0.2822	0.0530

**Table 5.2.2-1 Comparison Shapes, Approx. Scaled Discharge 0.0047 m<sup>3</sup>/s**

W11		W16	
H <sub>d</sub> (m)	H <sub>u</sub> (m)	H <sub>d</sub> (m)	H <sub>u</sub> (m)
-0.1422	0.0730	-0.2818	0.0726
-0.1414	0.0722	-0.2814	0.0726
-0.1408	0.0722	-0.1666	0.0726
-0.0560	0.0730	-0.1130	0.0734
-0.0072	0.0742	-0.0678	0.0734
0.0382	0.0792	-0.0196	0.0750
0.0770	0.0964	0.0246	0.0770
0.1190	0.1246	0.0680	0.0926
0.1570	0.1576	0.1108	0.1202
		0.1500	0.1524
0.1570	0.1576	0.1864	0.1854
0.1200	0.1256		
0.0792	0.0970	0.1864	0.1854
0.0380	0.0788	0.1586	0.1598
-0.0540	0.0732	0.1194	0.1262
-0.1428	0.0728	0.0768	0.0970
-0.1428	0.0732	0.0322	0.0790
-0.1430	0.0732	-0.0120	0.0716
		-0.0470	0.0716
		-0.1450	0.0716
		-0.2810	0.0716
		-0.2810	0.0716

**Table 5.2.2-2 Comparison Shapes, WINTEC Models, Approx Discharge 0.0074 m<sup>3</sup>/s**

<b>2 l/s (0.0125, 0.0128)</b>			
<b>W17</b>		<b>W23</b>	
<b>H<sub>d</sub> (m)</b>	<b>H<sub>u</sub> (m)</b>	<b>H<sub>d</sub> (m)</b>	<b>H<sub>u</sub> (m)</b>
-0.1070	0.1016	-0.2688	0.1022
-0.1064	0.1010	-0.2688	0.1016
-0.1060	0.1010	-0.1414	0.1020
-0.1056	0.1008	-0.0986	0.1022
-0.0028	0.1010	-0.0554	0.1036
0.0422	0.1048	-0.0074	0.1040
0.0750	0.1146	0.0410	0.1096
0.1122	0.1346	0.0922	0.1286
0.1546	0.1636	0.1280	0.1486
0.1904	0.1946	0.1666	0.1776
0.2260	0.2264	0.2036	0.2086
		0.2376	0.2400
0.2260	0.2264	0.2698	0.2694
0.1924	0.1966		
0.1556	0.1646	0.2698	0.2694
0.1144	0.1350	0.2386	0.2406
0.0746	0.1140	0.2064	0.2112
0.0312	0.1022	0.1704	0.1800
-0.1014	0.0964	0.1286	0.1496
-0.1048	0.1022	0.0916	0.1286
-0.1048	0.1022	0.0466	0.1094
-0.1054	0.1026	-0.0054	0.1004
		-0.0464	0.0996
		-0.0946	0.0996
		-0.2680	0.0994
		-0.2680	0.0996
		-0.2678	0.0996

**Table 5.2.2-3 Comparison Shapes, WINTEC Models, Approx Discharge 0.0125m<sup>3</sup>/s**

<b>3l/s (0.0178)</b>			
<b>W17</b>		<b>W23</b>	
<b>H<sub>d</sub></b> <b>(m)</b>	<b>H<sub>u</sub></b> <b>(m)</b>	<b>H<sub>d</sub></b> <b>(m)</b>	<b>H<sub>u</sub></b> <b>(m)</b>
-0.0938	0.1270	-0.2544	0.1266
-0.0954	0.1266	-0.2544	0.1268
-0.0946	0.1266	-0.1060	0.1270
-0.0948	0.1266	-0.0740	0.1268
0.0264	0.1254	-0.0294	0.1268
0.0666	0.1334	0.0164	0.1286
0.1132	0.1484	0.0674	0.1394
0.1516	0.1720	0.0962	0.1506
0.1866	0.2000	0.1526	0.1798
0.2230	0.2300	0.1900	0.2076
0.2564	0.2608	0.2276	0.2378
		0.2612	0.2676
0.2564	0.2608		
0.2244	0.2312	0.2612	0.2676
0.1886	0.2004	0.2282	0.2384
0.1516	0.1730	0.1926	0.2096
0.1102	0.1486	0.1560	0.1806
0.0676	0.1340	0.0962	0.1506
0.0226	0.1252	0.0682	0.1392
-0.0934	0.1246	0.0196	0.1284
-0.0934	0.1246	-0.0234	0.1266
-0.0936	0.1242	-0.0694	0.1226
		-0.2550	0.1246
		-0.2548	0.1246
		-0.2548	0.1254

**Table 5.2.2-4 Comparison Shapes, WINTEC Models, Approx Discharge 0.0178 m<sup>3</sup>/s**

<b>4 l/s ( 0.0231 ,0.0234)</b>			
<b>W17</b>		<b>W23</b>	
<b>H<sub>d</sub> (m)</b>	<b>H<sub>u</sub> (m)</b>	<b>H<sub>d</sub> (m)</b>	<b>H<sub>u</sub> (m)</b>
-0.0824	0.1494	-0.2460	0.1502
-0.0816	0.1494	-0.2460	0.1502
-0.0818	0.1494	-0.2460	0.1502
-0.0818	0.1494	-0.0594	0.1494
-0.0816	0.1494	-0.0148	0.1506
0.0666	0.1538	0.0304	0.1526
0.1110	0.1660	0.1006	0.1664
0.1420	0.1806	0.1406	0.1840
0.1918	0.2102	0.1766	0.2084
0.2260	0.2394	0.2122	0.2352
0.2596	0.2686	0.2494	0.2658
0.2596	0.2686	0.2494	0.2658
0.2280	0.2402	0.2146	0.2366
0.1930	0.2112	0.175	0.2092
0.1506	0.1856	0.1366	0.1846
0.1126	0.1660	0.1000	0.1670
0.0666	0.1528	0.0444	0.1552
-0.0794	0.1482	-0.0134	0.1474
-0.0794	0.1484	-0.0588	0.1472
-0.0796	0.1474	-0.2434	0.1474
		-0.2434	0.147
		-0.2442	0.1468

**Table 5.2.2-5 Comparison Shapes, WINTEC Models, Approx Discharge 0.0231 m<sup>3</sup>/s**

<b>5 l/s (0.0287, 0.0287)</b>			
<b>W11</b>		<b>W16</b>	
<b>H<sub>d</sub></b> <b>(m)</b>	<b>H<sub>u</sub></b> <b>(m)</b>	<b>H<sub>d</sub></b> <b>(m)</b>	<b>H<sub>u</sub></b> <b>(m)</b>
-0.0978	0.1738	-0.2336	0.1740
-0.0978	0.1730	-0.2330	0.1730
-0.0968	0.1730	-0.0556	0.1730
-0.0968	0.1732	-0.0130	0.1746
0.0624	0.1760	0.0310	0.1762
0.1058	0.1836	0.0930	0.1898
0.1572	0.2032	0.1790	0.2258
0.2220	0.2518	0.2144	0.2498
0.2612	0.2792	0.2544	0.2770
0.2612	0.2792	0.2544	0.2770
0.2232	0.2526	0.2170	0.2522
0.1600	0.2032	0.1870	0.2260
0.1068	0.1850	0.1090	0.2048
0.0612	0.1748	0.0716	0.1890
-0.0950	0.1700	0.0420	0.1770
-0.0962	0.1710	0.0010	0.1700
-0.0962	0.1712	-0.0516	0.1716
		-0.2316	0.1722

**Table 5.2.2-6 Comparison Shapes, WINTEC Models, Approx Discharge 0.0287 m<sup>3</sup>/s**

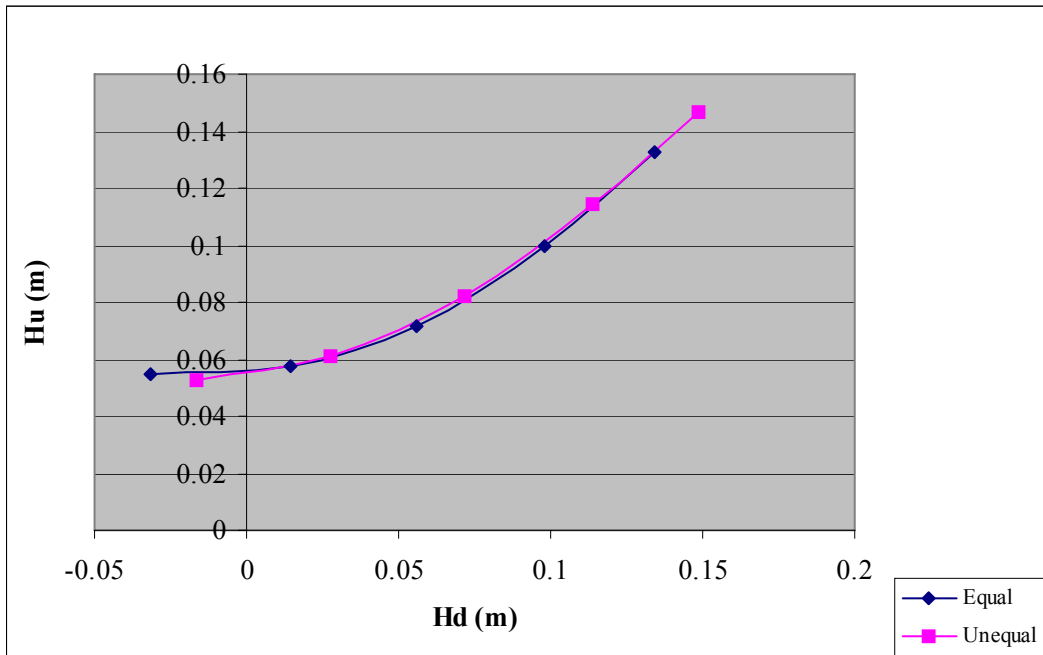


Figure 5.2.2-1  $H_u$  vs  $H_d$  for W11 and W16, (Falling Branch), Discharge  $0.0046 \text{ m}^3/\text{s}$

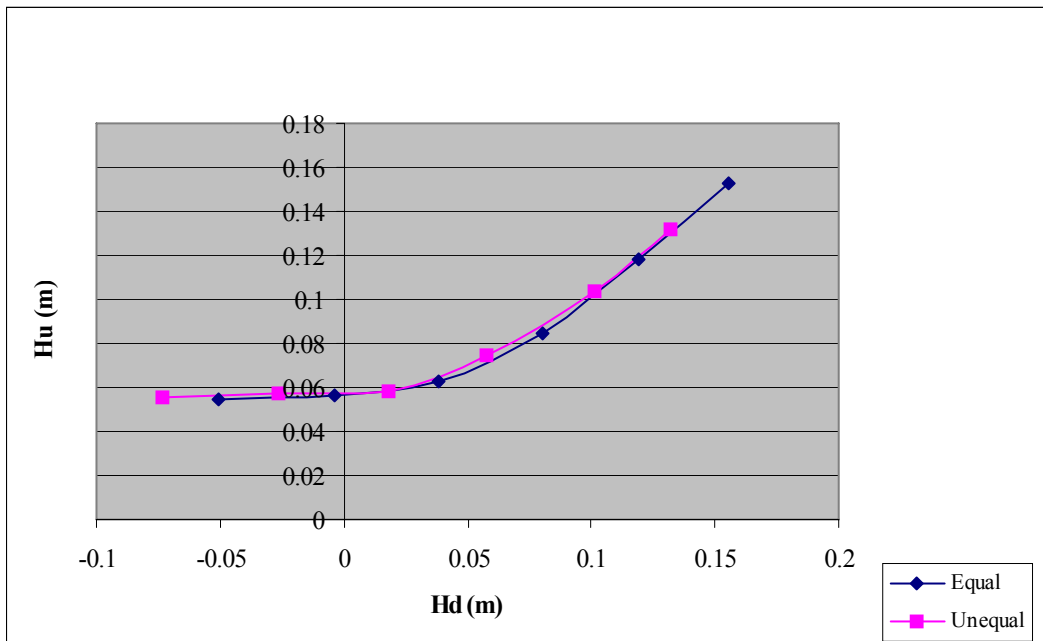


Figure 5.2.2-2  $H_u$  vs  $H_d$  for W17 and W23, (Rising Branch), Discharge  $0.0048 \text{ m}^3/\text{s}$

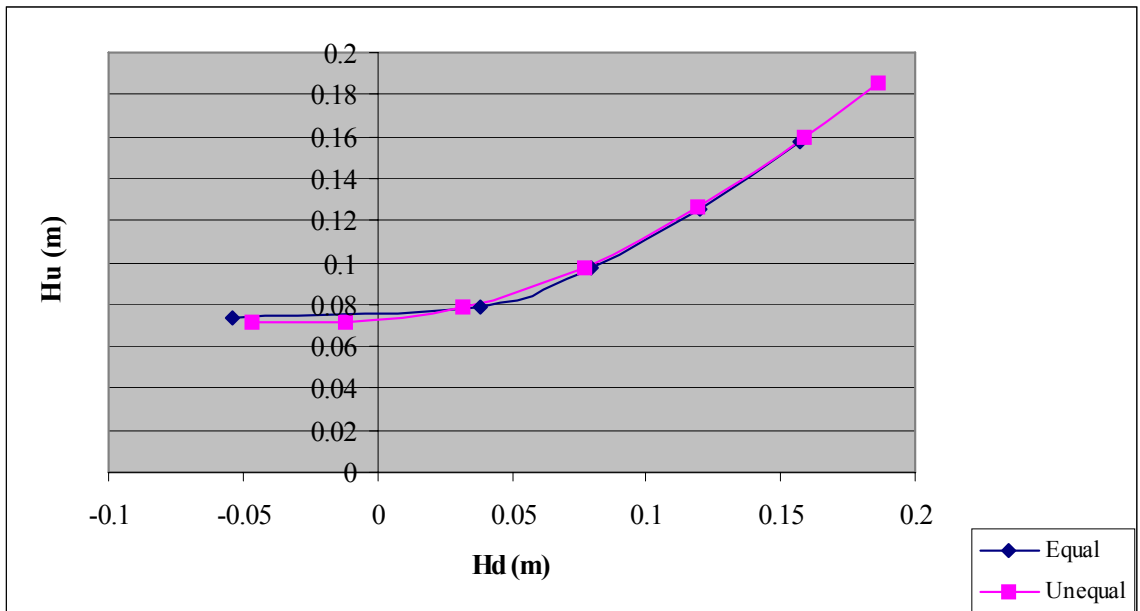


Figure 5.2.2-3  $H_u$  vs  $H_d$  for W11 and W16, (Falling Branch), Discharge  $0.0074 \text{ m}^3/\text{s}$

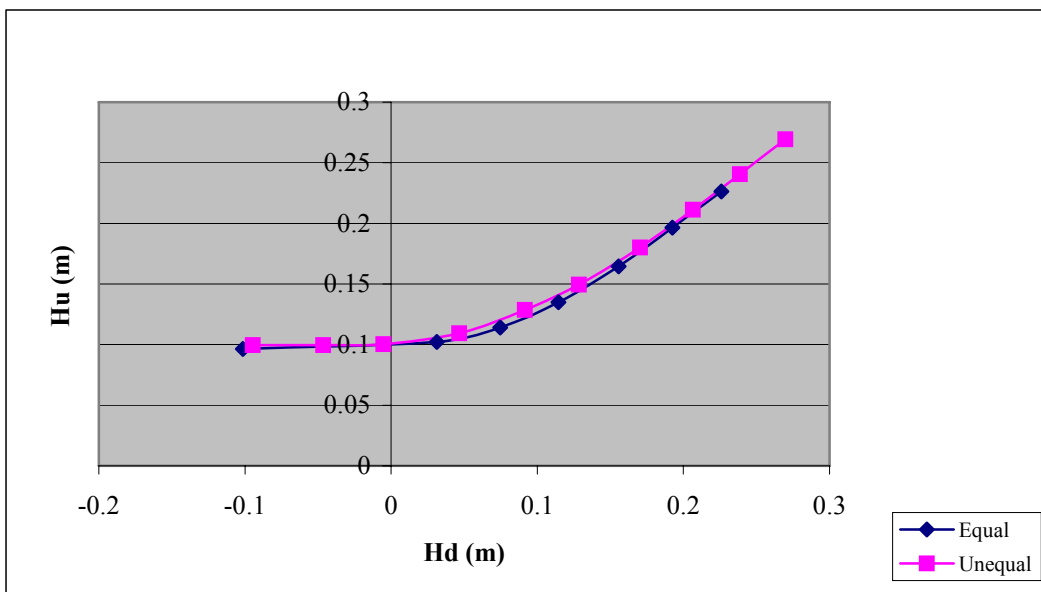


Figure 5.2.2-4  $H_u$  vs  $H_d$  for W17 and W23, (Falling Branch), Discharge  $0.0125 \text{ m}^3/\text{s}$

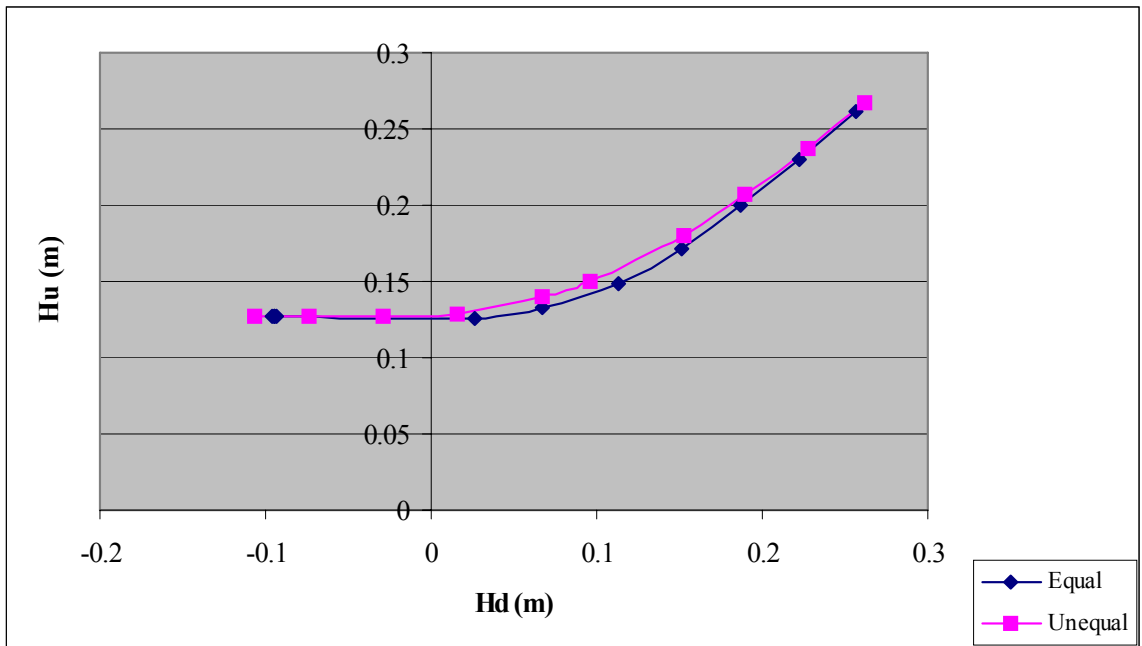


Figure 5.2.2-5  $H_u$  vs  $H_d$  for W17 and W23, (Rising Branch), Discharge  $0.0178 \text{ m}^3/\text{s}$

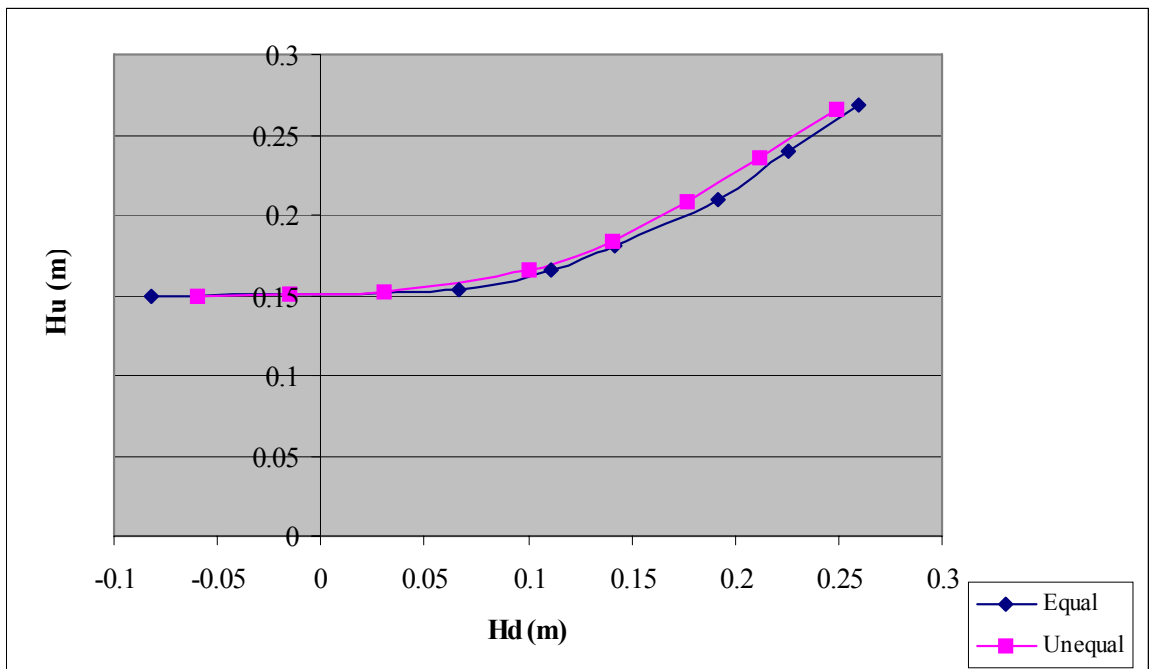


Figure 5.2.2-6  $H_u$  vs  $H_d$  for W17 and W23, (Rising Branch), Discharge  $0.0231 \text{ m}^3/\text{s}$

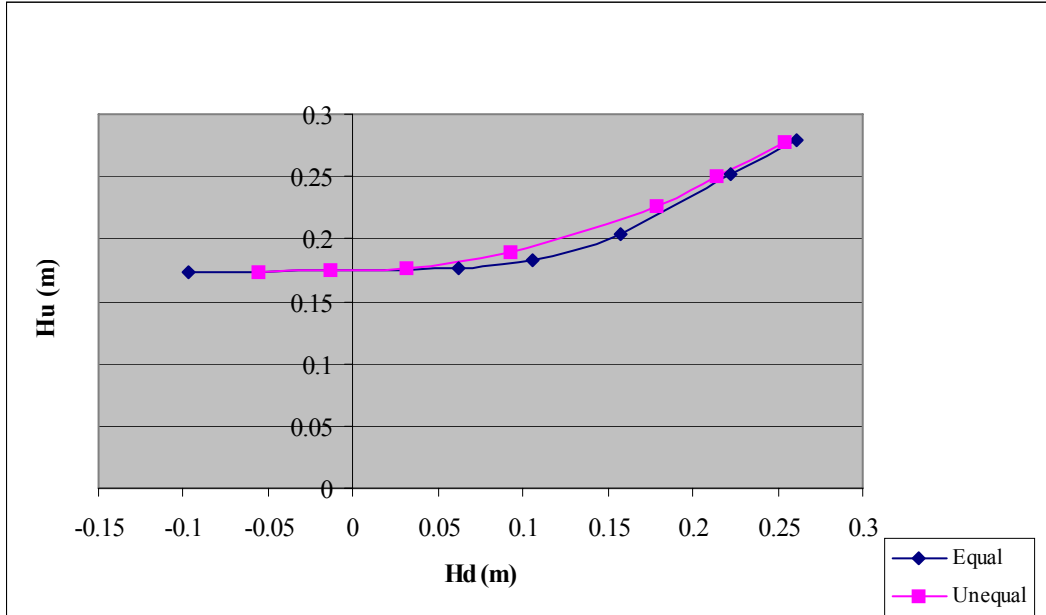


Figure 5.2.2-7  $H_u$  vs  $H_d$  for W11 and W16, (Rising Branch), Discharge  $0.0287 \text{ m}^3/\text{s}$

### **5.3 Approach Froude Number**

#### **5.3.1 University of Canterbury Data**

Table 5.3.1 lists the calculated Froude number with their corresponding values of downstream head and submergence for the first three discharges. Figures 5.3.1 -1,- 2, & -3 contain plots of the approach Froude number against submergence. The Froude Number is clearly lower in all cases. Plots of Froude number against downstream head are not included for reasons of space, but plots indicated that again Froude Number is lower for the unequal bed model than for the equal one.

#### **5.3.2 Waikato Institute of Technology Study Data**

Tables 5.3.2-1 (a) & (b) contain the equivalent data for the WINTEC. Plots of Froude Number vs Submergence are found on Figures 5.3.2-1 to 7. Again it is quite clear that the model with the unequal bed shows a lower approach Froude number. Some of the data relate to a  $\beta$  value greater than 1.0. this indicates that a spreading jet had been established. These data have been included for completeness

Discharge m <sup>3</sup> /s	C7			Discharge m <sup>3</sup> /s	C1		
	H <sub>d</sub>	β	Fr		H <sub>d</sub>	β	Fr
0.0094	0.0056	0.1359	0.1538	0.0095	0.0420	0.7865	0.1274
	0.0262	0.6179	0.1512				
	0.0440	0.8907	0.1375				
	0.0576	0.9697	0.1213				
0.0145	0.0138	0.2614	0.1974	0.0145	0.0084	0.1603	0.1935
	0.0362	0.6418	0.1887		0.0130	0.2444	0.1915
	0.0522	0.8339	0.1751		0.0316	0.5524	0.1824
	0.0642	0.9304	0.1627		0.0494	0.7841	0.1703
	0.0770	0.9772	0.1464		0.0648	0.9076	0.1550
					0.0824	0.9740	0.1352
			0.0925	0.9989	0.1252		
0.0198	0.0058	0.0915	0.2313	0.0193	0.0024	0.0377	0.2255
	0.0384	0.5783	0.2234		0.0201	0.3064	0.2204
	0.0512	0.7191	0.2117		0.0272	0.4096	0.2184
	0.0660	0.8616	0.1997		0.0562	0.7493	0.1989
	0.0730	0.9102	0.1924		0.0730	0.8690	0.1814
	0.0972	0.9798	0.1600		0.0914	0.9442	0.1605
			0.1166	0.9966	0.1348		

**Table 5.3.1 Froude Numbers for University of Canterbury Data**

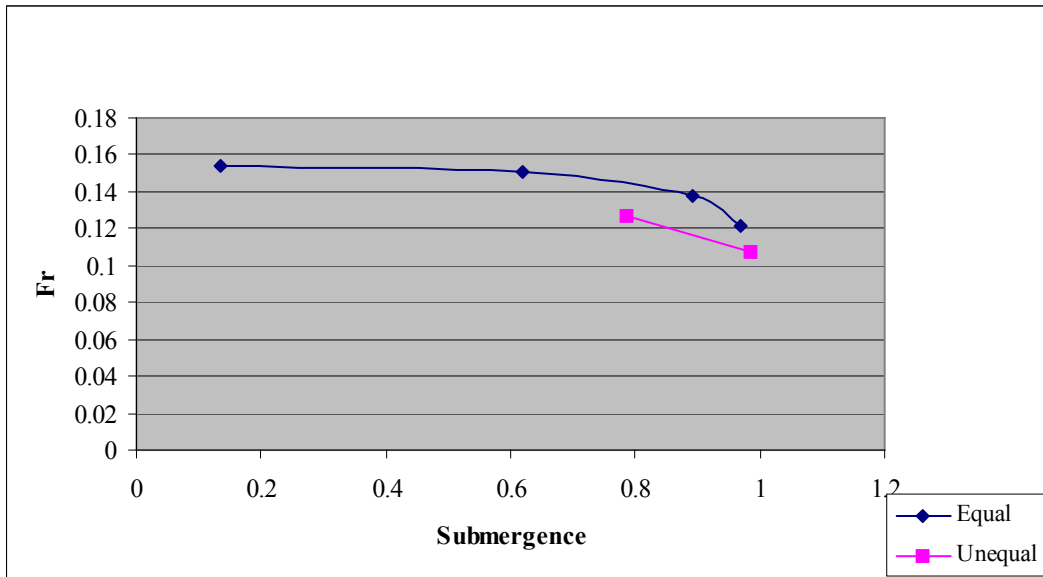


**Figure 5.3.1-1 Approach Froude Number for Models C1 and C7**  
**Discharge 0.0095 m<sup>3</sup>/s**

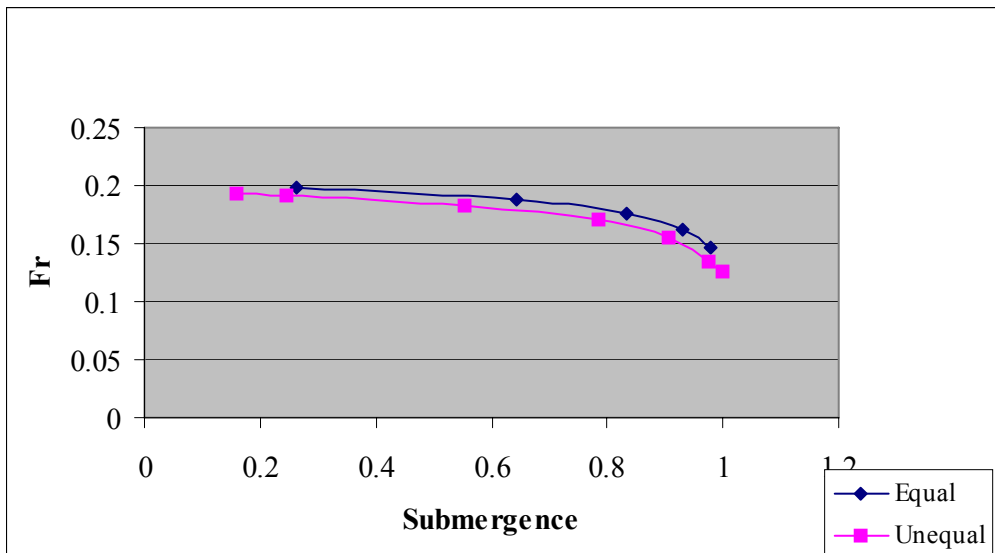


**Figure 5.3.1-2 Approach Froude Number for Models C1 and C7**  
**Discharge 0.0145 m<sup>3</sup>/s**

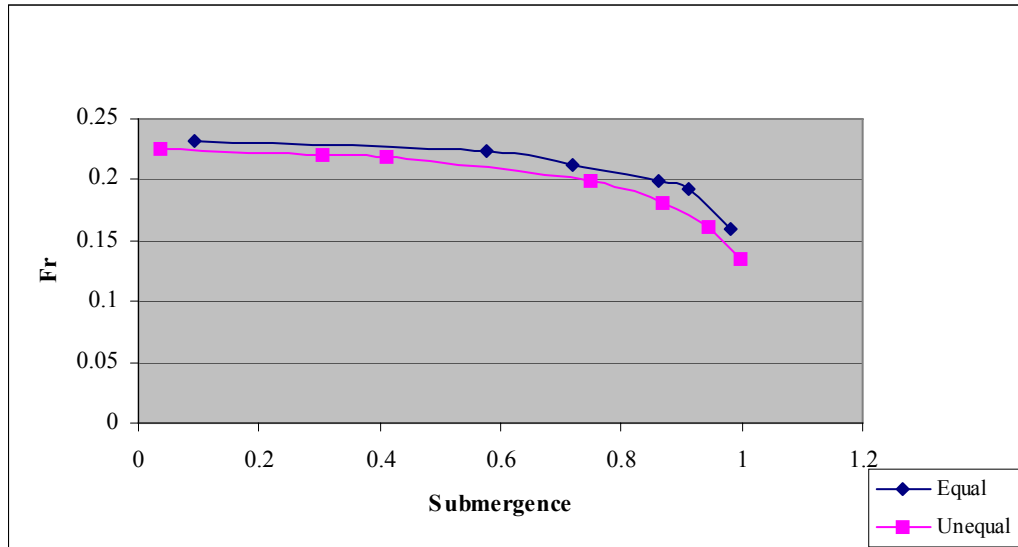


**Figure 5.3.1-3 Approach Froude Number for Models C1 and C7**  
**Discharge 0.0193 m<sup>3</sup>/s**

<b>Discharge</b> <b>m<sup>3</sup>/s</b>	<b>W11</b>			<b>W16</b>		
	<b>H<sub>d</sub></b>	<b>β</b>	<b>Fr</b>	<b>H<sub>d</sub></b>	<b>β</b>	<b>Fr</b>
0.0048	0.012	0.2034	0.0652	0.0110	0.1897	0.0641
	0.0542	0.7721	0.0609	0.0258	0.4202	0.0628
	0.0956	0.9735	0.0519	0.0704	0.8734	0.0560
	0.0978	0.9780	0.0514	0.1108	0.9893	0.0473
	0.0558	0.7793	0.0604	0.1488	1.0164	0.0400
	0.0148	0.2587	0.0659	0.1138	0.9930	0.0466
				0.0716	0.8732	0.0556
			0.0274	0.4492	0.0629	
0.0047	<b>W17</b>			<b>W23</b>		
	<b>H<sub>d</sub></b>	<b>β</b>	<b>Fr</b>	<b>H<sub>d</sub></b>	<b>β</b>	<b>Fr</b>
	0.0384	0.6154	0.0730	0.0178	0.3048	0.0768
	0.0804	0.9481	0.0631	0.0580	0.7796	0.0689
	0.1194	1.0084	0.0519	0.1012	0.9731	0.0575
	0.1556	1.0210	0.0436	0.1324	1.0076	0.0495
	0.121	1.0134	0.0516	0.0966	0.9602	0.0587
	0.0808	0.9395	0.0626	0.0524	0.7360	0.0704
0.0402	0.6442	15.7036	0.0126	0.2234	0.0778	
0.0075	<b>W11</b>			<b>W16</b>		
	<b>H<sub>d</sub></b>	<b>β</b>	<b>Fr</b>	<b>H<sub>d</sub></b>	<b>β</b>	<b>Fr</b>
	0.482323	0.4823	0.0902	0.0246	0.3195	0.0900
	0.798755	0.7988	0.0819	0.0680	0.7343	0.0825
	0.955056	0.9551	0.0709	0.1108	0.9218	0.0714
	0.996193	0.9962	0.0608	0.1500	0.9843	0.0613
	0.955414	0.9554	0.0705	0.1864	1.0054	0.0532
	0.816495	0.8165	0.0817	0.1586	0.9925	0.0593
	0.482234	0.4822	0.0904	0.1194	0.9461	0.0693
			0.0768	0.7918	0.0805	
			0.0322	0.4076	0.0890	
0.0125	<b>W17</b>			<b>W23</b>		
	<b>H<sub>d</sub></b>	<b>B</b>	<b>Fr</b>	<b>H<sub>d</sub></b>	<b>β</b>	<b>Fr</b>
	0.0422	0.4027	0.1490	0.0410	0.3741	0.1463
	0.075	0.6545	0.1410	0.0922	0.7170	0.1352
	0.1122	0.8336	0.1267	0.1280	0.8672	0.1198
	0.1546	0.9450	0.1099	0.1666	0.9381	0.1040
	0.1904	0.9784	0.0957	0.2036	0.9760	0.0911
	0.226	0.9982	0.0841	0.2376	0.9900	0.0805
	0.1924	0.9786	0.0949	0.2698	1.0015	0.0723
	0.1556	0.9453	0.1094	0.2386	0.9917	0.0803
	0.1144	0.8474	0.1265	0.2064	0.9773	0.0901
	0.0746	0.6544	0.1414	0.1704	0.9467	0.1029
	0.0312	0.3053	0.1512	0.1286	0.8596	0.1186
			0.0916	0.7123	0.1347	
			0.0466	0.4260	0.1465	

**Table 5.3.2-1(a) Approach Froude Numbers: WINTEC Data**

Discharge m <sup>3</sup> /s	W17			W23		
	H <sub>d</sub>	β	Fr	H <sub>d</sub>	β	Fr
0.0178	0.0264	0.2105	0.1893	0.0164	0.1275	0.1864
	0.0666	0.4993	0.1816	0.0674	0.4835	0.1763
	0.1132	0.7628	0.1684	0.1526	0.8487	0.1455
	0.1516	0.8814	0.1506	0.1900	0.9152	0.1292
	0.1866	0.9330	0.1332	0.2276	0.9571	0.1146
	0.2230	0.9696	0.1180	0.2612	0.9761	0.1028
	0.2564	0.9831	0.1052	0.2282	0.9572	0.1144
	0.2244	0.9706	0.1175	0.1926	0.9189	0.1281
	0.1886	0.9411	0.1330	0.156	0.8638	0.1450
	0.1516	0.8763	0.1499	0.0682	0.4899	0.1764
	0.1102	0.7416	0.1682	0.0196	0.1526	0.1866
	0.0676	0.5045	0.1810			
	0.0226	0.1805	0.1895			
0.0231/4	W17			W23		
	H <sub>d</sub>	β	Fr	H <sub>d</sub>	β	Fr
	0.0666	0.4330	0.2128	0.0304	0.1992	0.2168
	0.111	0.6687	0.2009	0.1006	0.6454	0.2031
	0.1918	0.9125	0.1657	0.1766	0.8042	0.1691
	0.22600	0.9440	0.1478	0.2122	0.9022	0.1521
	0.2596	0.9665	0.1328	0.2494	0.9383	0.1359
	0.2280	0.9492	0.1473	0.2146	0.9070	0.1513
	0.1930	0.9138	0.1651	0.1726	0.8250	0.1686
	0.1126	0.6783	0.2009	0.1096	0.6563	0.2026
0.0666	0.4359	0.2139	0.0444	0.2861	0.2141	
0.029	W11			W16		
	H <sub>d</sub>	β	Fr	H <sub>d</sub>	β	Fr
	0.0624	0.3546	0.21704	0.0310	0.09778	0.1930
	0.1058	0.5652	0.20721	0.0930	0.40736	0.1850
	0.1572	0.7736	0.19440	0.1790	0.85135	0.1459
	0.2220	0.8817	0.16259	0.2144	0.91968	0.1324
	0.2612	0.9355	0.14829	0.2544	0.95118	0.1198
	0.2232	0.8836	0.16214	0.2170	0.91866	0.1316
	0.1600	0.7874	0.19440	0.0716	0.85135	0.1459
	0.1068	0.5669	0.20620	0.0420	0.50988	0.1858
0.0612	0.3501	0.21813	0.0010	0.10485	0.1937	

Table 5.3.2-1(b) Approach Froude Numbers: WINTEC Data (cont)

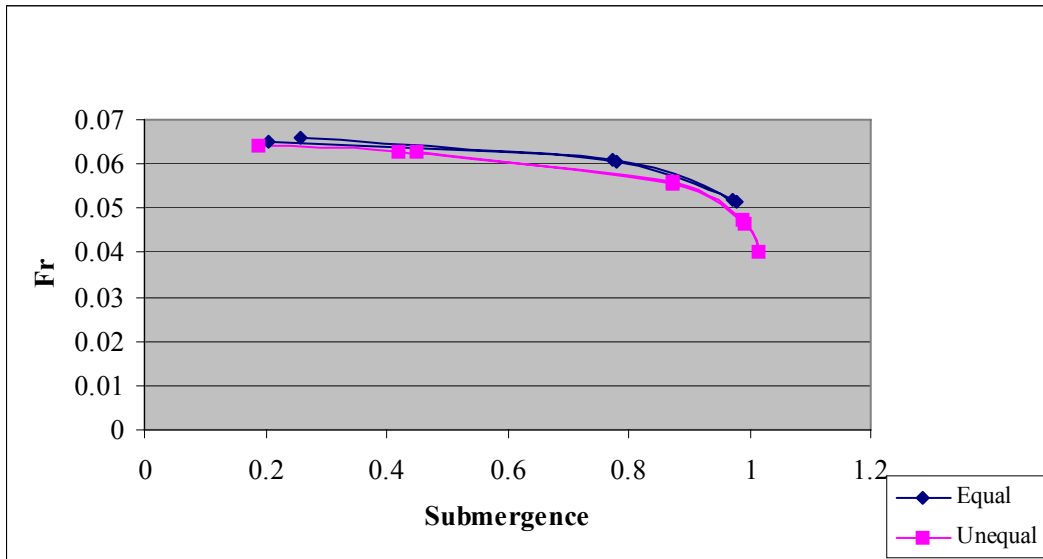


**Figure 5.3.2-1 Approach Froude Number for Models W11 and W16**  
**Discharge 0.0048 m<sup>3</sup>/s**

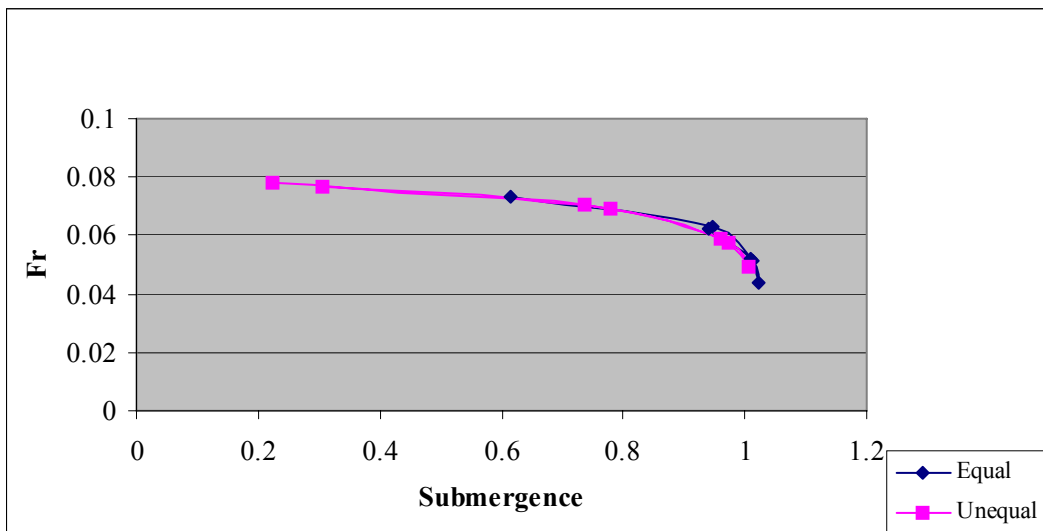


**Figure 5.3.2-2 Approach Froude Number for Models W17 and W23**  
**Discharge 0.0047 m<sup>3</sup>/s**

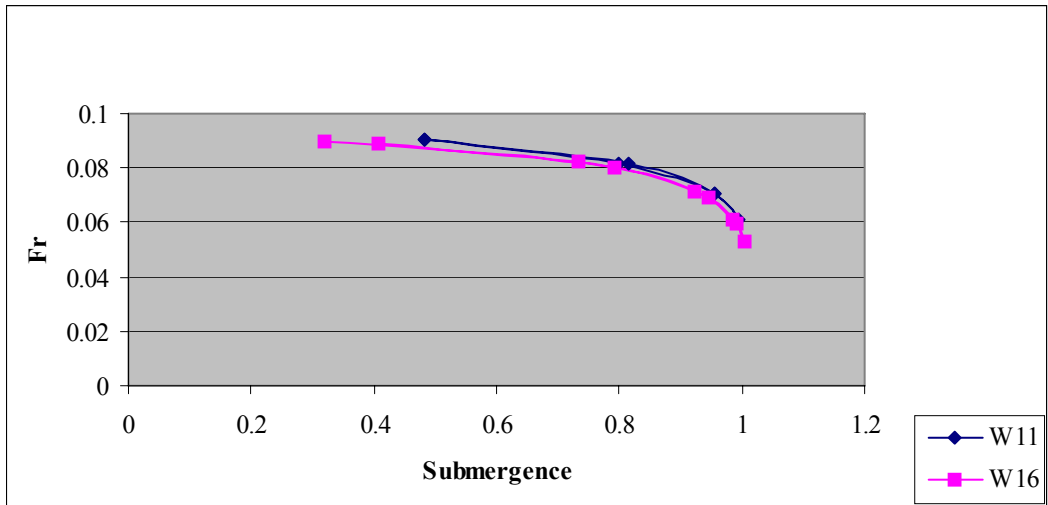


**Figure 5.3.2-3 Approach Froude Number for Models W11 and W16**  
**Discharge 0.0075 m<sup>3</sup>/s**

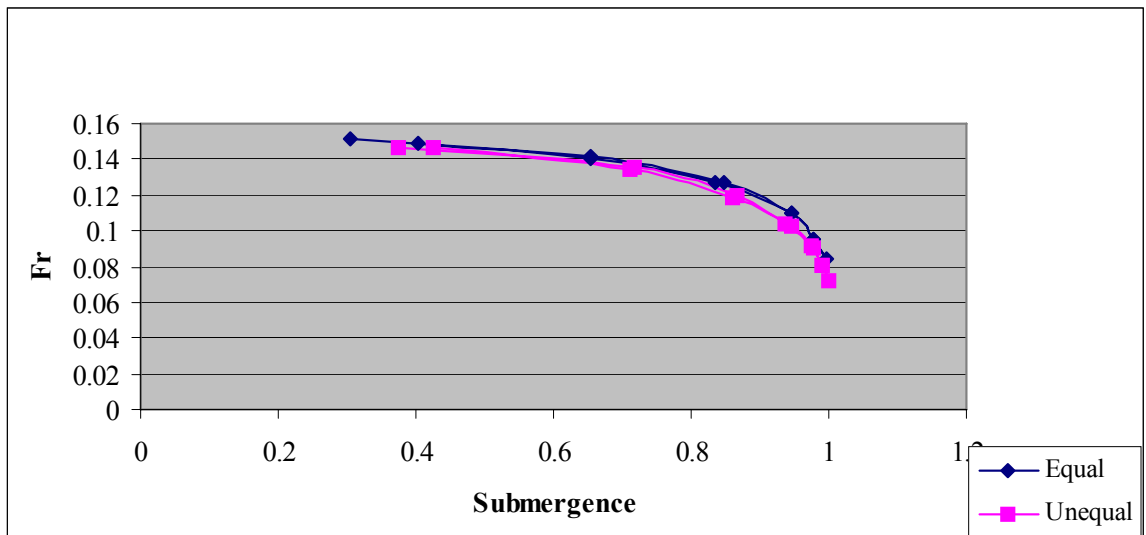


**Figure 5.3.2-4 Approach Froude Number for Models W17 and W23**  
**Discharge 0.0125 m<sup>3</sup>/s**

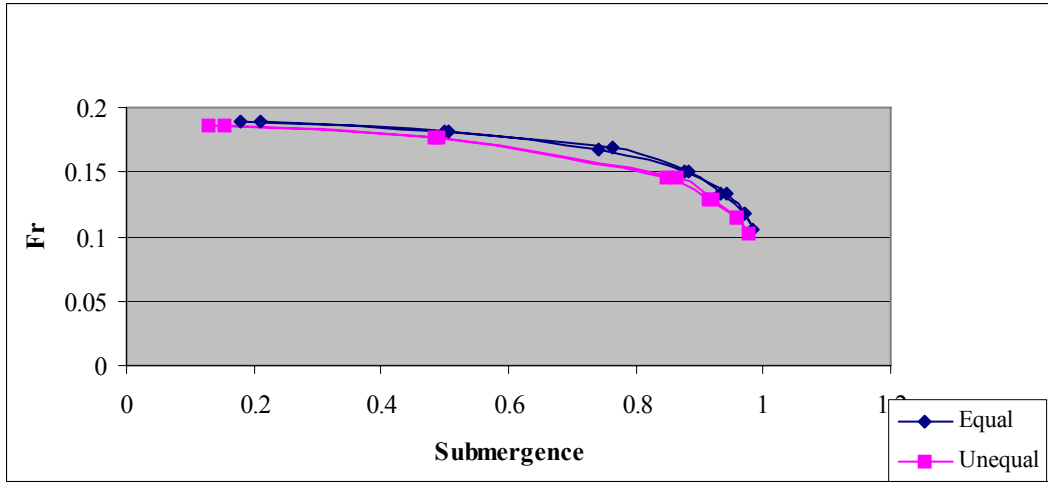


**Figure 5.3.2-5 Approach Froude Number for Models W17 and W23**  
**Discharge 0.0178 m<sup>3</sup>/s**

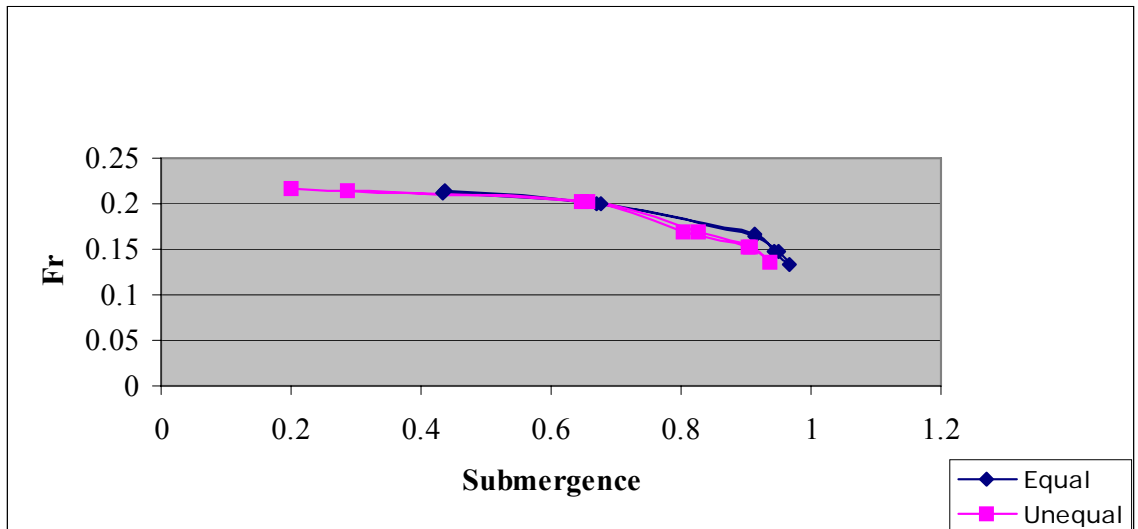


**Figure 5.3.2-6 Approach Froude Number for Models W17 and W23**  
**Discharge 0.0231/4 m<sup>3</sup>/s**

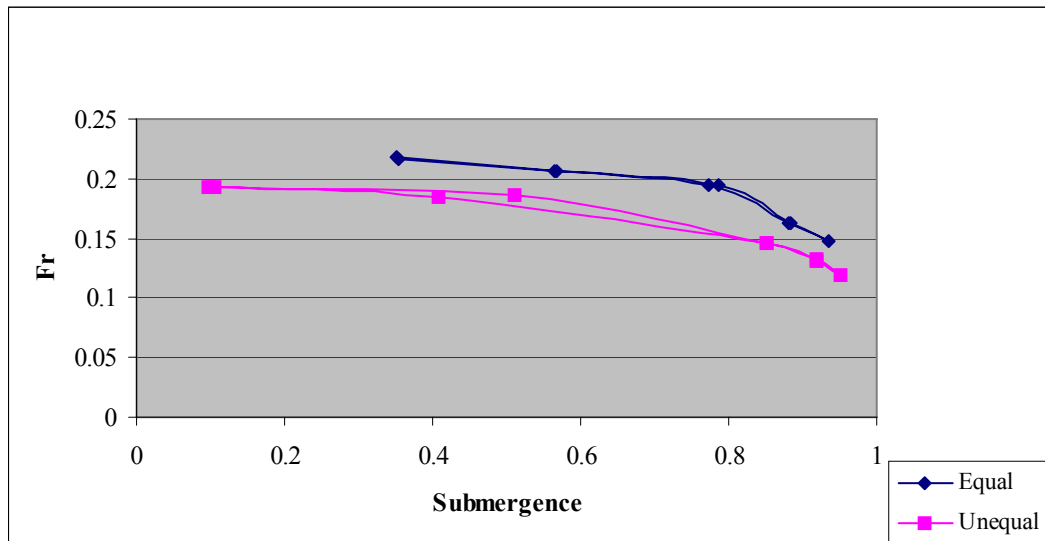


**Figure 5.3.2-7 Approach Froude Number for Models W17 and W23  
Discharge 0.029 m<sup>3</sup>/s**

#### 5.4 Calculation of Discharge with Conventional Formulas

##### 5.4.1 Method of Comparison

The results presented in the previous two sections indicate that there is an effect due to unequal beds. However, comparison of calculations of discharge is more difficult as the error due to unequal beds may be less than the error inherent in the equal bed formula. The plots in Chapter 3 indicate that there is not a simple relationship between error in calculation and submergence. Hence a simple comparison was made using the WINTEC data

##### 5.4.2 Waikato Institute of Technology Study Data

The attached Tables 5.4.2-1, 2, 3, 4, 5, 6 show typical sets of errors for each discharge. Comparing the errors for similar values of submergence, it can be seen that in general, the errors for the models with differing bed levels are greater than those with equal bed levels. However as the data range was limited this should be regarded as an indication only.

<b>0.5 l/s (0.0048, 0.0047)</b>				<b>0.5 l/s (0.0047, 0.0048)</b>			
<b>Equal (W11)</b>		<b>Unequal (W16)</b>		<b>Equal (W17)</b>		<b>Unequal (W23)</b>	
<b>β</b>	<b>% Error</b>	<b>β</b>	<b>% Error</b>	<b>β</b>	<b>% Error</b>	<b>β</b>	<b>% Error</b>
0.20	8.67	0.19	10.18	0.62	6.53	0.30	8.16
0.77	5.11	0.42	14.97	0.95	5.29	0.78	14.73
0.78	3.34	0.87	13.03	0.94	9.79	0.74	13.42
0.26	1.92	0.87	16.12	0.64	4.02	0.22	3.73
		0.45	12.61				

**Table 5.4.2-1 Comparison Errors, WINTEC Data, Approx. Scaled Discharge 0.0047 m<sup>3</sup>/s**

<b>1 l/s (0.0074, 0.0074)</b>			
<b>Equal (W11)</b>		<b>Unequal (W16)</b>	
<b><math>\beta</math></b>	<b>% Error</b>	<b><math>\beta</math></b>	<b>% Error</b>
0.48	3.40	0.32	5.93
0.80	5.51	0.73	9.53
0.82	7.75	0.79	71.89
0.48	4.14	0.41	69.55

**Table 5.4.2-2 Comparison Errors, WINTEC Data, Approx. Scaled Discharge 0.0074 m<sup>3</sup>/s**

<b>2 l/s (0.0125, 0.0128)</b>			
<b>Equal (W17)</b>		<b>Unequal (W23)</b>	
<b><math>\beta</math></b>	<b>% Error</b>	<b><math>\beta</math></b>	<b>% Error</b>
0.40	0.23	0.37	6.24
0.65	0.81	0.72	9.94
0.83	2.37	0.86	12.47
0.85	0.50	0.86	14.04
0.65	1.62	0.71	10.51
0.31	1.75	0.43	4.22

**Table 5.4.2-3 Comparison Errors, WINTEC Data Approx. Scaled Discharge 0.0125 m<sup>3</sup>/s**

<b>3l/s (0.0178)</b>			
<b>Equal (W17)</b>		<b>Unequal (W23)</b>	
<b><math>\beta</math></b>	<b>% Error</b>	<b><math>\beta</math></b>	<b>% Error</b>
0.21	3.70	0.13	0.70
0.50	1.51	0.48	6.44
0.76	6.87	0.85	11.43
0.88	2.27	0.86	9.29
0.88	0.39	0.49	5.88
0.74	4.14	0.15	0.36
0.50	1.07		
0.18	3.73		

**Table 5.4.2-4 Comparison Errors, WINTEC Data  
Approx. Scaled Discharge 0.0178 m<sup>3</sup>/s**

<b>4 l/s ( 0.0231 ,0.0234)</b>			
<b>Equal (W17)</b>		<b>Unequal (W23)</b>	
<b><math>\beta</math></b>	<b>% Error</b>	<b><math>\beta</math></b>	<b>% Error</b>
0.43	2.05	0.20	0.65
0.67	4.59	0.65	2.89
0.79	1.07	0.80	16.45
0.68	5.47	0.83	13.48
0.44	3.17	0.66	3.27
		0.29	2.39

**Table 5.4.2-5 Comparison Shapes, WINTEC Data  
Approx. Scaled Discharge 0.0231 m<sup>3</sup>/s**

<b>5 l/s (0.0287, 0.0287)</b>			
<b>Equal (W11)</b>		<b>Unequal (W16)</b>	
<b><math>\beta</math></b>	<b>% Error</b>	<b><math>\beta</math></b>	<b>% Error</b>
0.35	4.35	0.18	0.29
0.57	3.53	0.49	5.00
0.77	10.04	0.79	6.07
0.79	9.91	0.86	12.65
0.57	0.63	0.86	14.00
0.35	3.33	0.53	16.10
		0.38	8.73
		0.24	0.51
		0.01	4.96

**Table 5.4.2-6 Comparison Errors, WINTEC Data  
Approx. Scaled Discharge 0.0287 m<sup>3</sup>/s**

## Chapter 6 Possible New Discharge Formula for Thin Plate Weir

### 6.1 Existing Equations

It has already been commented that equations for discharge over submerged thin plate weirs are developed either empirically or by assuming some theoretical basis.

Empirical formulas are, strictly speaking, only applicable to the range of weir parameters ( $P_u$ ,  $H_u$ , discharge etc.) for which they were developed. Hence it was of interest to discover that the modified BVGJ, which was developed for weirs with  $P_u$  values of 0.260 m to 0.511 m is also a good description of flow over weirs with a range  $P_u$  values of 0.067 m – 0.1m (actual) /0.2 m (modelled).

Equations based on theoretical derivations are only strictly applicable as long as the underlying model is realistic. While the models underlying the Abou-Seida and Quraishi and Villemonte formulas could be considered reasonable, at low submergences, this is much less true at high submergences. The work in this thesis has shown that the errors in calculating the actual discharge become quite high at high submergences.

The theory based equations also reflect a modular flow mindset – submerged weir flow is interpreted in terms of modular flow, not a different flow pattern. The losses in the modular range are bundled into the  $C_d$  factor and the defining relationship for modular flow is

$$Q_m = f(H_u).$$

Treating submerged flow as a variation of modular flow assumes that the same pattern of losses occur when water passes over the weir. This is unlikely to be true, especially with

high submergences. It also ignores the fact that submerged flow has a second defining relationship, i.e.

$$H_u = g(H_d).$$

One advantage of the empirical approach is that it does allow for the distinctive pattern of submerged flow, although in a black box manner.

A better approach to developing a discharge formula for submerged flow might be to start with the  $H_u$  vs  $H_d$  curve and extrapolated backwards to get the values of  $H_0$  the value of  $H_u$  corresponding to  $H_d = 0$ . A value for discharge can then be calculated by inserting this value into an appropriate modular flow equation.

## **6.2 $H_u$ vs $H_d$ Graph: General Shape**

### **6.2.1 Introduction**

The initial step in developing this approach was to estimate the approximate relationship. The plots already presented suggested that the shape of the  $H_u$  vs  $H_d$  curves is a log or exponential relation. An Excel spreadsheet was used to calculate values, plot equations and do basic data analysis.

Using the data from the lowest flow for model C1 ( $Q_{mi} = 0.015 \text{ m}^3/\text{s}$ ), three options were calculated and plotted and the resulting linear regression equation and  $R^2$  values calculated. The options compared were

$$H_u = f(\ln H_d)$$

$$H_u = f(\exp H_d)$$

$$H_u = f(\exp H_d^2).$$

It was found that the third option had  $R^2 = 0.99$  which was the highest of the three. This gave a proposed relation of

$$H_u = A \exp(H_d^2) + B. \quad (6)$$

Where, A and B are both expected to be functions of Q

This relationship was checked for the remaining data.

### 6.2.2 University of Canterbury Study Data.

This analysis was repeated for the remaining sets of interpolated data. As a check, values for  $H_o'$ , (the last  $H_u$  reading before  $H_d$  reached the weir crest), and  $H_o$  (the value of  $H_u$  corresponding to  $H_d = 0$ ) were compared. In all cases  $R^2 > 0.99$  and the values of  $H_o$  and  $H_o'$  were in good agreement. Figure 6.2.2 is a typical example.

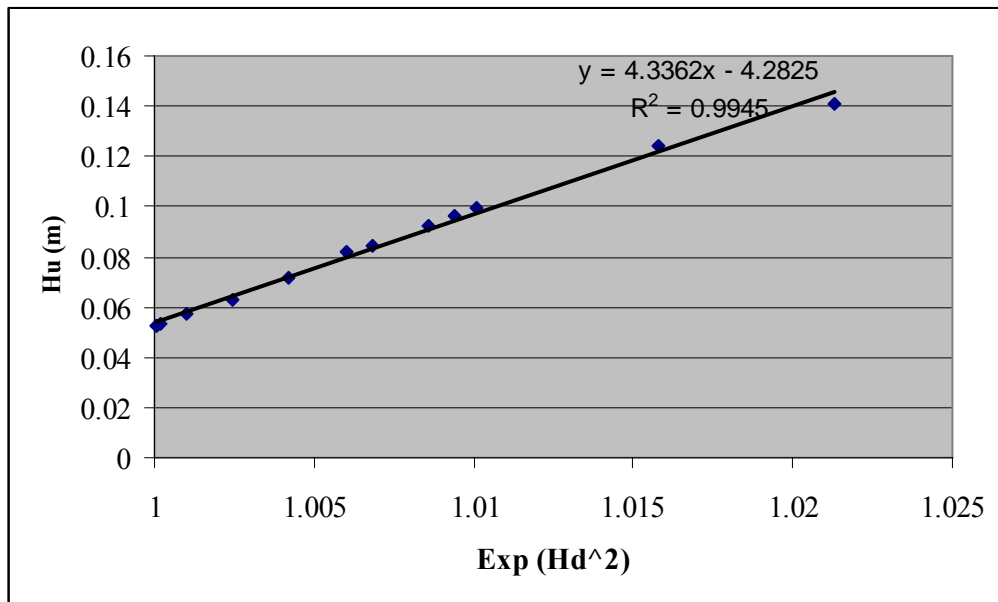


**Figure 6.2.2 Plot of  $H_u$  vs Exp ( $H_d^2$ ) for Model C1, Discharge 15 l/s**

### 6.2.3 Waikato Institute of Technology Study Data

The analysis was repeated for all 138 data sets of the WINTEC study i.e. (23 models x 6 discharges). Again the calculated values were plotted and a linear trendline superimposed and it was demonstrated that Equation 6 was a reasonable description of the relation between  $H_u$  and  $H_d$ . Figure 6.2.3 is a typical example.

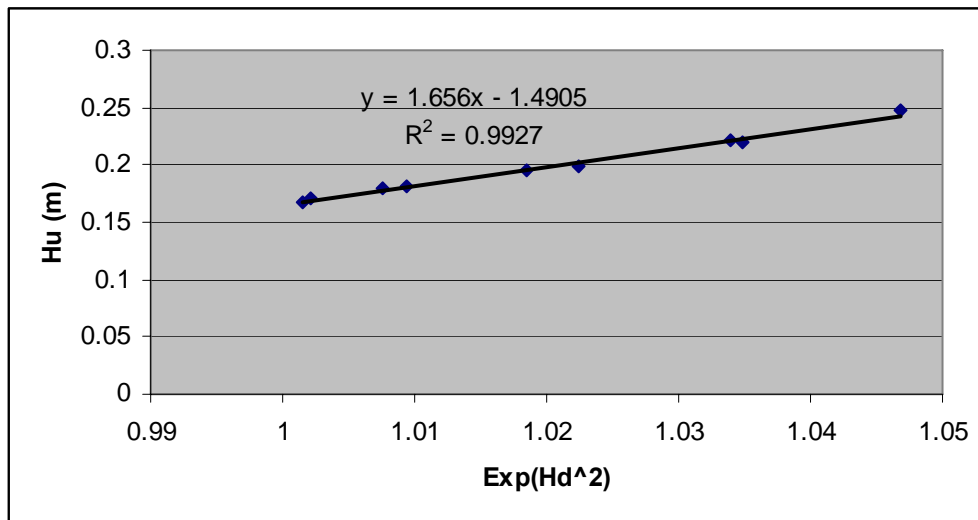


Figure 6.2.3 Plot of  $H_u$  vs  $\text{Exp}(H_d^2)$  for Model W1, Discharge  $0.0258 \text{ m}^3/\text{s}$

## 6.3 $H_u$ vs $H_d$ Dimensioned Expression

### 6.3.1 Non-Dimensional Factors

Although it has been established that Equation (6). is a good description of the relationship between the *values* of  $H_u$  and  $H_d$ , it is not dimensionally consistent. It is only possible to take the exponential of a number. Hence for a realistic description of the submerged flow behaviour it is necessary to non-dimensionalise the  $H_d$  factor.

$P_u$  and  $P_d$ , the upstream and downstream depths, were possible candidates for non-dimensionalising. As this study has demonstrated that flow over a submerged thin plate weir is influenced by the relative bed levels upstream and downstream it was decided to non-dimensionalise using  $P_d$ .

### 6.3.2 University of Canterbury Study Data

Table 6.3.2 contains the equations developed along with values of  $R^2$  and  $H_o$ . Figure 6.3.2 is a typical plot. In all cases, the  $R^2$  value was greater than 0.93

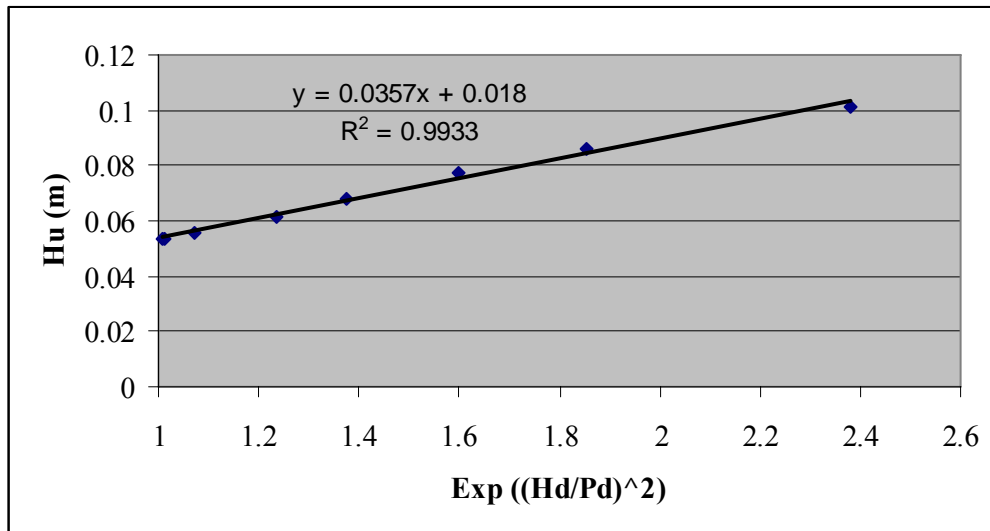


**Figure 6.3.2** Plot of  $H_u$  vs  $\text{Exp}((H_d/P_d)^2)$  for Model C5, Discharge 15 l/s

Model	Pd	L	Discharge	Ho	Equation	R*R	Ho'
C1	0.202	0.33	10 l/s	0.0424	$H_u = 0.201 * \text{Exp}(H_d/P_d^2) - 0.1565$	1	0.0445
			15 l/s	0.0524	$H_u = 0.2484 * \text{Exp}(H_d/P_d^2) - 0.2118$	0.9911	0.0366
			20 l/s	0.0628	$H_u = 0.1821 * \text{Exp}(H_d/P_d^2) - 0.135$	0.9843	0.0471
			25 l/s	0.0722	$H_u = 0.1364 * \text{Exp}(H_d/P_d^2) - 0.0784$	0.9747	0.058
C2	0.18	0.37	10 l/s	0.041	$H_u = 0.1629 * \text{Exp}(H_d/P_d^2) - 0.12$	0.9946	0.0429
			15 l/s	0.0534	$H_u = 0.1279 * \text{Exp}(H_d/P_d^2) - 0.0732$	0.9965	0.0547
			20 l/s	0.0638	$H_u = 0.099 * \text{Exp}(H_d/P_d^2) - 0.0335$	0.9947	0.0655
			25 l/s	0.0734	$H_u = 0.0521 * \text{Exp}(H_d/P_d^2) + 0.0302$	0.9493	0.0823
C3	0.156	0.42	10 l/s	0.0426	$H_u = 0.0892 * \text{Exp}(H_d/P_d^2) - 0.0433$	0.9752	0.0459
			15 l/s	0.0536	$H_u = 0.0863 * \text{Exp}(H_d/P_d^2) - 0.0315$	0.9893	0.0548
			20 l/s	0.0642	$H_u = 0.0636 * \text{Exp}(H_d/P_d^2) + 0.0029$	0.9858	0.0665
			25 l/s	0.074	$H_u = 0.0482 * \text{Exp}(H_d/P_d^2) + 0.0292$	0.981	0.0774
C4	0.133	0.49	10 l/s	0.0406	$H_u = 0.0762 * \text{Exp}(H_d/P_d^2) - 0.0318$	0.9907	0.044
			15 l/s	0.0534	$H_u = 0.0569 * \text{Exp}(H_d/P_d^2) - 0.0023$	0.9884	0.0546
			20 l/s	0.0636	$H_u = 0.0371 * \text{Exp}(H_d/P_d^2) + 0.0299$	0.9858	0.067
			25 l/s	0.0742	$H_u = 0.0314 * \text{Exp}(H_d/P_d^2) + 0.046$	0.9704	0.0774
C5	0.108	0.49	10 l/s	0.0408	$H_u = 0.0563 * \text{Exp}(H_d/P_d^2) - 0.0157$	0.9983	0.0406
			15 l/s	0.0564	$H_u = 0.0357 * \text{Exp}(H_d/P_d^2) + 0.018$	0.9933	0.0537
			20 l/s	0.0656	$H_u = 0.0231 * \text{Exp}(H_d/P_d^2) + 0.0441$	0.9551	0.0672
			25 l/s	0.0742	$H_u = 0.0139 * \text{Exp}(H_d/P_d^2) + 0.068$	0.9623	0.0819
C6	0.087	0.75	10 l/s	0.0418	$H_u = 0.0336 * \text{Exp}(H_d/P_d^2) + 0.0072$	0.9976	0.0408
			15 l/s	0.0528	$H_u = 0.0237 * \text{Exp}(H_d/P_d^2) + 0.0292$	0.9963	0.0529
			20 l/s	0.065	$H_u = 0.011 * \text{Exp}(H_d/P_d^2) + 0.0559$	0.9705	0.0669
			25 l/s	0.0732	$H_u = 0.006 * \text{Exp}(H_d/P_d^2) + 0.0735$	0.909	0.0741
C7	0.064	1	10 l/s	0.0412	$H_u = 0.0151 * \text{Exp}(H_d/P_d^2) + 0.0253$	0.9949	0.0404
			15 l/s	0.0524	$H_u = 0.008 * \text{Exp}(H_d/P_d^2) + 0.0457$	0.9852	0.0537
			20 l/s	0.0638	$H_u = 0.0063 * \text{Exp}(H_d/P_d^2) + 0.0578$	0.9808	0.052
			25 l/s	0.0752	$H_u = 0.003 * \text{Exp}(H_d/P_d^2) + 0.0792$	0.959	0.0822
C8	0.088	1	10 l/s	0.0408	$H_u = 0.0285 * \text{Exp}(H_d/P_d^2) + 0.0153$	0.9912	0.0438
			15 l/s	0.0564	$H_u = 0.0121 * \text{Exp}(H_d/P_d^2) + 0.0512$	0.9535	0.0633
			20 l/s	0.0656	$H_u = 0.0087 * \text{Exp}(H_d/P_d^2) + 0.0631$	0.9411	0.0718
			25 l/s	0.0742	$H_u = 0.0076 * \text{Exp}(H_d/P_d^2) + 0.0738$	0.9411	0.0814

**Table 6.3.2 Proposed Discharge Equation for University of Canterbury Models**

### 6.3.3 Waikato Institute of Technology Study Data

The analysis was repeated for all data sets of the WINTEC study where  $L < 1$  i.e. for uneven bed case. Tables 6.3.3-1,-2, -3 contains the equations developed along with values of  $R^2$  and  $H_0$ . Figure 6.3.3 is a typical plot. Although the lowest value of  $R^2$  was 0.8841, the other 107 expressions have  $R^2 > 0.9$  and 81 have  $R^2 > 0.96$ .

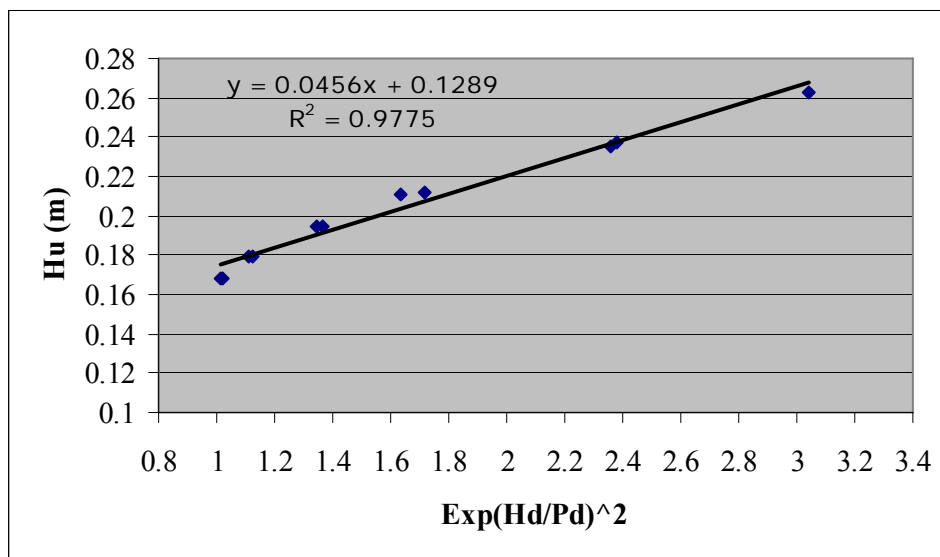


**Figure 6.3.3 Plot of  $H_u$  vs  $\text{Exp}((H_d/P_d)^2)$  for Model W 20, Discharge  $0.208 \text{ m}^3/\text{s}$**

Model	Pd	L	Discharge	Ho	Equation	R*R	Ho'
W2	0.255	0.93	0.0047	0.051	$Hu = 0.3318 * \text{Exp}(Hd/Pd)^2 - 0.2745$	0.9968	0.0573
			0.0071	0.074	$Hu = 0.2593 * \text{Exp}(Hd/Pd)^2 - 0.1834$	0.993	0.0759
			0.0152	0.1188	$Hu = 0.1276 * \text{Exp}(Hd/Pd)^2 - 0.0028$	0.9825	0.1248
			0.0203	0.14	$Hu = 0.0924 * \text{Exp}(Hd/Pd^2) + 0.0602$	0.9814	0.1526
			0.0206	0.163	$Hu = 0.0879 * \text{Exp}(Hd/Pd^2) + 0.081$	0.9814	0.1689
			0.031	0.1846	$Hu = 0.0955 * \text{Exp}(Hd/Pd^2) + 0.0913$	0.9886	0.1868
W4	0.249	0.93	0.0046	0.0566	$Hu = 0.2782 * \text{Exp}(Hd/Pd^2) - 0.2218$	0.9828	0.0564
			0.0071	0.074	$Hu = 0.18889 * \text{Exp}(Hd/Pd^2) - 0.1109$	0.9922	0.078
			0.0126	0.1026	$Hu = 0.1365 * \text{Exp}(Hd/Pd^2) - 0.0309$	0.9696	0.1056
			0.0176	0.1232	$Hu = 0.0814 * \text{Exp}(Hd/Pd^2) + 0.0587$	0.9666	0.1401
			0.0227	0.155	$Hu = 0.0792 * \text{Exp}(Hd/Pd^2) + 0.0759$	0.9802	0.1551
			0.0291	0.1694	$Hu = 0.0605 * \text{Exp}(Hd/Pd^2) + 0.1223$	0.9693	0.1828
W5	0.275	0.84	0.0045	0.0576	$Hu = 0.3049 * \text{Exp}(Hd/Pd^2) - 0.2455$	0.9936	0.0594
			0.0069	0.075	$Hu = 0.2513 * \text{Exp}(Hd/Pd^2) - 0.175$	0.9972	0.0763
			0.0121	0.105	$Hu = 0.1391 * \text{Exp}(Hd/Pd^2) - 0.0286$	0.9766	0.1105
			0.0167	0.1236	$Hu = 0.1166 * \text{Exp}(Hd/Ps^2) + 0.0205$	0.9705	0.1452
			0.0224	0.1538	$Hu = 0.0938 * \text{Exp}(Hd/Pd^2) + 0.0638$	0.9729	0.1576
			0.0274	0.175	$Hu = 0.0855 * \text{Exp}(Hd/Pd^2) + 0.0899$	0.9868	0.1754
W7	0.224	0.92	0.0049	0.0576	$Hu = 0.1953 * \text{Exp}(H/Pd^2) - 0.1358$	0.9858	0.0595
			0.0072	0.0742	$Hu = 0.1379 * \text{Exp}(Hd/Pd^2) - 0.0597$	0.9879	0.0782
			0.0125	0.1042	$Hu = 0.0908 * \text{Exp}(Hd/Pd^2) + 0.0183$	0.9751	0.1091
			0.0175	0.1236	$Hu = 0.0519 * \text{Exp}(Hd/Pd^2) + 0.0904$	0.9445	0.1423
			0.0215	0.1476	$Hu = 0.0513 * \text{Exp}(Hd/Pd^2) + 0.1063$	0.9601	0.1576
			0.0275	0.1696	$Hu = 0.0495 * \text{Exp}(Hd/Pd^2) + 0.127$	0.9722	0.1765
W8	0.25	0.82	0.0047	0.0568	$Hu = 0.2422 * \text{Exp}(H/Pd^2) - 0.1839$	0.99	0.0583
			0.0072	0.0736	$Hu = 0.1865 * \text{Exp}(Hd/Pd^2) - 0.1092$	0.9888	0.0773
			0.0126	0.1046	$Hu = 0.1199 * \text{Exp}(Hd/Pd^2) - 0.0101$	0.9775	0.1098
			0.0178	0.1244	$Hu = 0.0768 * \text{Exp}(Hd/Pd^2) + 0.0646$	0.9581	0.1414
			0.228	0.1504	$Hu = 0.0739 * \text{Exp}(Hd/Pd^2) + 0.0835$	0.9812	0.1574
			0.0296	0.1776	$Hu = 0.0683 * \text{Exp}(Hd/Pd^2) + 0.1107$	0.9737	0.179
W9	0.275	0.75	0.0048	0.0572	$Hu = 0.2732 * \text{Exp}(H/Pd^2) - 0.2122$	0.9875	0.061
			0.0072	0.0762	$Hu = 0.2188 * \text{Exp}(Hd/Pd^2) - 0.1409$	0.9901	0.0779
			0.0123	0.1046	$Hu = 0.154 * \text{Exp}(Hd/Pd^2) - 0.0454$	0.98	0.1086
			0.0171	0.1246	$Hu = 0.1016 * \text{Exp}(Hd/Pd^2) + 0.036$	0.9758	0.1376
			0.022	0.1442	$Hu = 0.0909 * \text{Exp}(Hd/Pd^2) + 0.0663$	0.9725	0.1572
			0.026	0.1666	$Hu = 0.0843 * \text{Exp}(Hd/Pd^2) + 0.1009$	0.9911	0.1852

Table 6.3.3-1 Proposed Basic Discharge Equation for WINTEC Models W2-W9

Model	Pd	L	Discharge	Ho	Equation	R*R	Ho'
W10	0.303	0.68	0.0044	0.0554	$H_u = 0.3555 \cdot \exp(H/Pd^2) - 0.2964$	0.9904	0.0591
			0.0071	0.074	$H_u = 0.2732 \cdot \exp(Hd/Pd^2) - 0.1948$	0.9944	0.784
			0.0121	0.1036	$H_u = 0.1782 \cdot \exp(Hd/Pd^2) - 0.0675$	0.9786	0.1107
			0.0165	0.1268	$H_u = 0.1347 \cdot \exp(Hd/Pd^2) + 0.0055$	0.9741	0.1402
			0.021	0.1444	$H_u = 0.1367 \cdot \exp(Hd/Pd^2) + 0.0169$	0.9764	0.1536
			0.028	0.176	$H_u = 0.1076 \cdot \exp(Hd/Pd^2) + 0.072$	0.9826	0.1796
W12	0.198	0.92	0.0048	0.0564	$H_u = 0.1538 \cdot \exp(H/Pd^2) - 0.0963$	0.9953	0.0575
			0.0073	0.0742	$H_u = 0.1177 \cdot \exp(Hd/Pd^2) - 0.0423$	0.9913	0.0754
			0.0127	0.1028	$H_u = 0.0582 \cdot \exp(Hd/Pd^2) + 0.0518$	0.9664	0.11
			0.0165	0.1234	$H_u = 0.0364 \cdot \exp(Hd/Pd^2) + 0.1054$	0.9396	0.1418
			0.0226	0.1484	$H_u = 0.0244 \cdot \exp(Hd/Pd^2) + 0.1423$	0.9184	0.1667
			0.0296	0.1762	$H_u = 0.0281 \cdot \exp(Hd/Pd^2) + 0.1523$	0.9865	0.1804
W13	0.225	0.81	0.0047	0.058	$H_u = 0.1927 \cdot \exp(H/Pd^2) - 0.1335$	0.995	0.0592
			0.0075	0.0758	$H_u = 0.1196 \cdot \exp(Hd/Pd^2) - 0.0366$	0.9848	0.083
			0.0131	0.1062	$H_u = 0.0859 \cdot \exp(Hd/Pd^2) + 0.0228$	0.9772	0.1087
			0.0176	0.128	$H_u = 0.0572 \cdot \exp(Hd/Pd^2) + 0.0822$	0.9564	0.1394
			0.212	0.1434	$H_u = 0.0485 \cdot \exp(Hd/Pd^2) + 0.1085$	0.9539	0.157
			0.0271	0.169	$H_u = 0.0416 \cdot \exp(Hd/Pd^2) + 0.1366$	0.9656	0.1782
W14	0.25	0.73	0.0048	0.0568	$H_u = 0.2415 \cdot \exp(H/Pd^2) - 0.1822$	0.9939	0.0593
			0.0072	0.0734	$H_u = 0.1797 \cdot \exp(Hd/Pd^2) - 0.1018$	0.9873	0.0779
			0.0126	0.103	$H_u = 0.1304 \cdot \exp(Hd/Pd^2) - 0.0258$	0.9779	0.1046
			0.0172	0.125	$H_u = 0.082 \cdot \exp(Hd/Pd^2) + 0.0534$	0.9729	0.1354
			0.0217	0.145	$H_u = 0.0721 \cdot \exp(Hd/Pd^2) + 0.0811$	0.9648	0.1532
			0.0246	0.161	$H_u = 0.0566 \cdot \exp(Hd/Pd^2) + 0.1169$	0.9687	0.1735
W15	0.276	0.66	0.0049	0.0568	$H_u = 0.3302 \cdot \exp(H/Pd^2) - 0.2723$	0.9961	0.0579
			0.0073	0.075	$H_u = 0.2174 \cdot \exp(Hd/Pd^2) - 0.1393$	0.9879	0.0781
			0.012	0.1008	$H_u = 0.1391 \cdot \exp(Hd/Pd^2) - 0.0286$	0.9766	0.1105
			0.0174	0.123	$H_u = 0.0981 \cdot \exp(Hd/Pd^2) + 0.0413$	0.9722	0.1394
			0.0222	0.143	$H_u = 0.0923 \cdot \exp(Hd/Pd^2) + 0.0625$	0.9736	0.1548
			0.029	0.175	$H_u = 0.0783 \cdot \exp(Hd/Pd^2) + 0.1034$	0.9705	0.1817
W16	0.303	0.59802	0.0047	0.0562	$H_u = 0.3325 \cdot \exp(H/Pd^2) - 0.2719$	0.9892	0.0606
			0.0074	0.075	$H_u = 0.2443 \cdot \exp(Hd/Pd^2) - 0.164$	0.9858	0.0803
			0.0127	0.104	$H_u = 0.1657 \cdot \exp(Hd/Pd^2) - 0.053$	0.9808	0.1127
			0.0176	0.128	$H_u = 0.1339 \cdot \exp(Hd/Pd^2) + 0.0055$	0.9729	0.1394
			0.0234	0.1522	$H_u = 0.1162 \cdot \exp(Hd/Pd^2) + 0.0407$	0.979	0.1569
			0.029	0.1746	$H_u = 0.1047 \cdot \exp(Hd/Pd^2) + 0.0728$	0.9829	0.1775
W18	0.172	0.91	0.0048	0.0626	$H_u = 0.081 \cdot \exp(H/Pd^2) - 0.0184$	0.9692	0.0626
			0.00725	0.0854	$H_u = 0.0472 \cdot \exp(Hd/Pd^2) + 0.0382$	0.9377	0.0854
			0.0127	0.115	$H_u = 0.0283 \cdot \exp(Hd/Pd^2) + 0.0867$	0.9179	0.115
			0.0182	0.1475	$H_u = 0.0155 \cdot \exp(Hd/Pd^2) + 0.132$	0.8751	0.1475
			0.0229	0.173	$H_u = 0.0112 \cdot \exp(Hd/Pd^2) + 0.1618$	0.8882	0.173
			0.0284	0.1861	$H_u = 0.0111 \cdot \exp(Hd/Pd^2) + 0.175$	0.913	0.1861
W19	0.199	0.79	0.0046	0.0589	$H_u = 0.1301 \cdot \exp(H/Pd^2) - 0.0712$	0.9821	0.0589
			0.0074	0.0797	$H_u = 0.0898 \cdot \exp(Hd/Pd^2) - 0.0101$	0.9723	0.0797
			0.0125	0.121	$H_u = 0.0346 \cdot \exp(Hd/Pd^2) + 0.0864$	0.8991	0.121
			0.0181	0.1427	$H_u = 0.0313 \cdot \exp(Hd/Pd^2) + 0.1114$	0.9246	0.1427
			0.23	0.1603	$H_u = 0.0274 \cdot \exp(Hd/Pd^2) + 0.1329$	0.9232	0.1603
			0.0281	0.1736	$H_u = 0.0292 \cdot \exp(Hd/Pd^2) + 0.1444$	0.9789	0.1736

Table 6.3.3-2 Proposed Basic Discharge Equation for WINTEC Models W10-W19

Model	Pd	L	Discharge	Ho	Equation	R*R	Ho'
W20	0.225	0.70	0.0048	0.0587	$H_u = 0.1824 * \text{Exp}(H/Pd^2) - 0.1237$	0.9862	0.0587
			0.0073	0.0762	$H_u = 0.148 * \text{Exp}(Hd/Pd^2) - 0.0718$	0.9917	0.0762
			0.0124	0.1215	$H_u = 0.0583 * \text{Exp}(Hd/Pd^2) + 0.0632$	0.9323	0.1215
			0.178	0.135	$H_u = 0.0544 * \text{Exp}(Hd/Pd^2) + 0.0806$	0.9586	0.135
			0.0231	0.1595	$H_u = 0.0431 * \text{Exp}(Hd/Pd^2) + 0.1164$	0.9452	0.1595
			0.028	0.1745	$H_u = 0.0456 * \text{Exp}(Hd/Pd^2) + 0.1289$	0.9775	0.1745
W21	0.25	0.63	0.0048	0.0608	$H_u = 0.2194 * \text{Exp}(H/Pd^2) - 0.1586$	0.9831	0.0608
			0.0075	0.0839	$H_u = 0.142 * \text{Exp}(Hd/Pd^2) - 0.0581$	0.9688	0.0839
			0.0128	0.1135	$H_u = 0.0981 * \text{Exp}(Hd/Pd^2) + 0.0154$	0.966	0.1135
			0.0178	0.1429	$H_u = 0.0663 * \text{Exp}(Hd/Pd^2) + 0.0766$	0.9525	0.1429
			0.0232	0.1586	$H_u = 0.0619 * \text{Exp}(Hd/Pd^2) + 0.0967$	0.9583	0.1586
			0.0283	0.1789	$H_u = 0.0597 * \text{Exp}(Hd/Pd^2) + 0.1201$	0.9609	0.1789
W22	0.276	0.57	0.0047	0.0642	$H_u = 0.1982 * \text{Exp}(H/Pd^2) - 0.134$	0.9822	0.0642
			0.0073	0.0756	$H_u = 0.142 * \text{Exp}(Hd/Pd^2) - 0.0664$	0.9797	0.0756
			0.0125	0.1207	$H_u = 0.0783 * \text{Exp}(Hd/Pd^2) + 0.0424$	0.9477	0.1207
			0.0179	0.1457	$H_u = 0.0663 * \text{Exp}(Hd/Pd^2) + 0.0794$	0.9442	0.1457
			0.0234	0.1545	$H_u = 0.0703 * \text{Exp}(Hd/Pd^2) + 0.0842$	0.968	0.1545
			0.0282	0.1818	$H_u = 0.0542 * \text{Exp}(Hd/Pd^2) + 0.1276$	0.9611	0.1818
W23	0.303	0.52	0.0048	0.0591	$H_u = 0.3598 * \text{Exp}(H/Pd^2) - 0.3007$	0.9899	0.0591
			0.0075	0.0828	$H_u = 0.2335 * \text{Exp}(Hd/Pd^2) - 0.1507$	0.985	0.0828
			0.0126	0.1186	$H_u = 0.1399 * \text{Exp}(Hd/Pd^2) - 0.0213$	0.9687	0.1186
			0.0178	0.1356	$H_u = 0.1319 * \text{Exp}(Hd/Pd^2) + 0.0037$	0.98	0.1356
			0.0234	0.154	$H_u = 0.1233 * \text{Exp}(Hd/Pd^2) + 0.0307$	0.9865	0.154
			0.0286	0.1777	$H_u = 0.1015 * \text{Exp}(Hd/Pd^2) + 0.0762$	0.9705	0.1777

**Table 6.3.3-3 Proposed Basic Discharge Equation for WINTEC Models W20-W23**

## 6.4 Coefficient and Constant

### 6.4.1 Introduction

Having established that the relationship between  $H_u$  and  $H_d$  can be described by the equation

$$H_u = A \exp((H_d/P_d)^2) + B,$$

it is necessary to establish expressions for  $A$  and  $B$ .

The equations in Tables 6.3.2 and 6.3.3 –1,-2,-3 indicate that the coefficient  $A$  decreases with increasing discharge and  $B$  increases with increasing discharge, i.e both the coefficient and constant are functions of  $H_o$ , the factor to be found . Here,

$$\text{Coefficient} = f(1/H_o),$$

And

$$\text{Constant} = g(H_o)$$

To check this, simple regression analyses of coefficient against  $H_o$ , and constant against  $H_o$  were done using the Excel This was done for the data sets from Models C1 – C7 and W17 – W23. These were chosen as these models had constant  $P_u$  values.

### 6.4.2 Constant

As the constant was expected to be a function of  $H_o$  , a linear analysis was done. For each model, the constant was plotted against  $H_o$  and a linear trendline plotted. The resulting equations are shown in Table 6.4.2 along with  $R^2$  and  $L$  ( $=P_u/P_d$ ) values.

The lowest  $R^2$  value was 0.93 (2 dp). Comparison with the  $L$  values shows that both the coefficients and the constants of the constant regression equation have values which increase with decreasing  $L$  and the constant increases with decreasing  $L$  values. This suggests that the expression for the constant also includes the  $L$  factor, although the relationship is not immediately obvious.

<b>Canterbury</b>			
<b>Model</b>	<b>L</b>	<b>Equation</b>	<b>R<sup>2</sup></b>
C1	0.33	Constant = 6.2073*H <sub>0</sub> - 0.4344	0.998
C2	0.37	Constant = 3.7995*H <sub>0</sub> - 0.2882	0.9982
C3	0.42	Constant = 2.3876*H <sub>0</sub> - 0.1567	0.9977
C4	0.49	Constant = 2.3628*H <sub>0</sub> - 0.1331	1
C5	0.6	Constant = 2.1347*H <sub>0</sub> - 0.1053	1
C6	0.75	Constant = 1.9685*H <sub>0</sub> - 0.0741	0.9998
<b>Waikato Institute of Technology</b>			
<b>Model</b>	<b>L</b>	<b>Equations</b>	<b>R*R</b>
M18	0.91	Constant = 1.5213*H <sub>0</sub> - 0.0992	0.9898
M19	0.79	Constant = 1.8791*H <sub>0</sub> - 0.1649	0.9894
M20	0.7	Constant = 2.2514*H <sub>0</sub> - 0.2399	0.9761
M21	0.63	Constant = 2.036*H <sub>0</sub> - 0.2681	0.985
M22	0.57	Constant = 2.1354*H <sub>0</sub> - 0.2421	0.9883
M23	0.52	Constant = 3.0487*H <sub>0</sub> - 0.4302	0.9746

**Table 6.4.2 Constant as Function of H<sub>0</sub>.**

### 6.4.3 Coefficient

As the coefficient was expected to be a function of  $H_o^{-1}$  a power trendline was plotted on each graph of coefficient vs  $H_o$ . The resulting equations and  $R^2$  values are listed in Table 6.4.3-2.

None of the derived equations had a power of exactly  $-1$ . However, except for Model C6 all had powers in the range  $(-1.1, -2)$ .

For the WINTEC data, the value of the power clearly increased numerically as the value of  $L$  decreased i.e as the difference between upstream and downstream bed levels increased. The University of Canterbury data did not show a similar monotonic increase.

As a brief check on the dependence on  $L$ , the value of the power in each of the WINTEC equations was divided by the value of  $L$ . The resulting values were

Model	Power	Power/ $L$
18	-1.9077	-2.0964
19	-1.5338	-1.9415
20	-1.435	-2.0757
21	-1.2704	-2.016
22	-1.1879	-2.084
23	-1.1379	-2.188

**Table 6.4.3-1 Coefficient as Function of  $L$**

These values suggest that the coefficient is a function of  $H_o^{-2L}$  although the small amount of data precludes a definite statement especially as this was not confirmed by the University of Canterbury data.

<b>Canterbury</b>			
<b>Model</b>	<b>L</b>	<b>Equation</b>	<b>R*R</b>
C1	0.33	Coefficient = 0.0033*H <sub>o</sub> <sup>^(-1.3104)</sup>	0.998
C2	0.37	Coefficient = 0.0008*H <sub>o</sub> <sup>^(-1.7196)</sup>	0.9981
C3	0.42	Coefficient = 0.0023*H <sub>o</sub> <sup>^(-1.2149)</sup>	0.9976
C4	0.49	Coefficient = 0.0005*H <sub>o</sub> <sup>^(-1.6309)</sup>	1
C5	0.6	Coefficient = 0.0001*H <sub>o</sub> <sup>^(-1.9724)</sup>	1
C6	0.75	Coefficient = 0.000005*H <sub>o</sub> <sup>^(-2.8044)</sup>	0.9999
<b>Waikato Institute of Technology</b>			
<b>Model</b>	<b>L</b>	<b>Equations</b>	<b>R*R</b>
M18	0.91	Coefficient = 0.0004*H <sub>o</sub> <sup>^(-1.9077)</sup>	0.9891
M19	0.79	Coefficient = 0.0017*H <sub>o</sub> <sup>^(-1.5338)</sup>	0.9887
M20	0.7	Coefficient = 0.0032*H <sub>o</sub> <sup>^(-1.435)</sup>	0.9745
M21	0.63	Coefficient = 0.0061*H <sub>o</sub> <sup>^(-1.2704)</sup>	0.984
M22	0.57	Coefficient = 0.007*H <sub>o</sub> <sup>^(-1.1879)</sup>	0.9878
M23	0.52	Coefficient = 0.0138*H <sub>o</sub> <sup>^(-1.1379)</sup>	0.9731

**Table 6.4.3-2 Coefficient as Function of H<sub>o</sub>**

The coefficient of the power term increases as  $L$  decreases. This is to be expected as it has been demonstrated that as  $L$  decreases, the graph of  $H_u$  vs  $H_d$  becomes steeper initially. However, the relationship between the power of the coefficient and  $L$  is not obvious at present.

The modular flow equation includes the  $C_d$  factor to allow for losses as flow goes over the weir. In the submerged case losses will still occur. However, these are the losses due to turbulence around a submerged body and there is no reason to assume that they will be the same as in the modular case.

It is anticipated that a value for these losses would have to be obtained empirically and incorporated into the coefficient of Equation 6 in a similar manner to the modular case.

## 6.5 Summary

This section of the study has indicated that discharge over a submerged weir can be described by an equation of the form

$$H_u = Ae^{\left(\frac{H_d}{P_d}\right)^2} + B$$

The coefficient and the constant have been demonstrated to be function of  $H_0$  for this data and probably are also functions of  $L$ . A will also allow for losses due to flow over the weir.

## **Chapter 7 Summary and Possible Further Work**

### **7.1 Unequal Bed Effect $L$**

The work described in this thesis has demonstrated that differing bed levels upstream and downstream of the thin plate weir have an effect on the pattern of discharge over the weir. The purpose of the study was to examine whether an effect existed and so considered the widest contrast in  $L$  values available. It was not intended to be an exhaustive study.

The study indicates that an effect exists. The expected effects on the shape of the  $H_u$  vs  $H_d$  plot and the approach Froude number were also demonstrated. The study has also indicated that using conventional formulas for discharge will result in even bigger errors.

### **7.2 Further Work Unequal Bed Effect $L$**

As this study was primarily qualitative, there is scope for further quantitative investigation. For example, at what stage does the unequal bed effect become sufficiently big to matter in practical engineering. Work to date indicates that it may be a function of the discharge.

There is scope for further work to understand the behaviour of submerged weirs. Two aspects of this are an estimation of the losses as flow passes over a submerged weir and the behaviour at very high submergence where the flow acts as a jet resulting in a downstream water level that is higher than upstream, and a submergence that is greater than 1.

## 7.2 Alternative Discharge Equation

This study has also introduced an outline for a new discharge calculation method for flow over a submerged weir. The study has demonstrated that the  $H_u$  vs  $H_d$  relation for submerging thin plate weir can be described by an equation of the form

$$H_u = Ae^{\left(\frac{H_d}{P_d}\right)^2} + B$$

The coefficient and the intercept are both functions of  $H_o$ , the upstream head corresponding to zero submergence (i.e.  $H_d = 0$ ). This value of  $H_o$  can then be entered into a modular flow equation. The coefficient and the constant also appear to be functions of  $L$  although the exact relationship is not yet defined.

Further work needs to be done to develop expressions for the coefficient and intercept of the equation including a study of the losses mentioned above. This would be a large undertaking requiring further laboratory work and more sophisticated statistical analysis and is unfortunately beyond the level of this M.Phil. study.

## References

Abou-Seida M. M. and Quraishi A. A. (1979) *A Flow Equation for Submerged Rectangular Weirs* Proceedings Institution of Civil Engineers, part 2, 1976 **61**, Dec 685 – 696

Borghei S.M., Z Vatannia, M Ghodsian and M R Jalili *Oblique Rectangular Sharp-Crested Weir*, paper 12967, Proceedings Institution of Civil Engineers, Water and Maritime Engineering 156, June 2003, Issue WM2, pgs 185-191

Kindsvater C.E. and R.W. Carter *Discharge Characteristics of Rectangular Thin Plate Weirs*, paper No. 3001, Transactions, American Society of Civil Engineers, vol 124, 1959.

Rajaratnam N. and Muralidhar D. (1969) *Flow Below Deeply Submerged Rectangular Weirs* Journal of Hydraulic Research **7** (1969), no.3 pp 355-373

Villemonte J. (1947) *Submerged-Weir Discharge Studies* Engineering News Record Dec 25 1947, pp 55-57.

Wu S, and Rajaratnam N (1996) *Submerged Flow Regimes of Rectangular Sharp-Crested Weirs*, Journal of hydraulic Engineering, Vol. 122, No.7, July 1996